Angiotensin converting enzyme 2 (ACE2) oxidative stress and vasmotor dysfunction interactions enhanced by air pollution and smoking with (SARS-CoV-2) 2019 spike protein effects regards infection ADE and vaccine development issues

D Lumsden

Abstract

As reported by government and News agencies the outbreak occurred in December 2019 and the epicentre being Wuhan in China. Widely reported are the lock downs in China while we can assume that they slow human interaction, we can't be sure of the percentage effectiveness of the lock down and asymptomatic people **who either left prior to the lock down or have breached lock down protocol.**

As we see WHO and various governments seemingly play down the risks as similar to the flu to avoid economic and societal shocks- this paper seeks to rationalise why the infection shows different behaviour in different groups and countries.

The author of this paper aims to bring together the information available and to combine it into a multi source explanation of the data at hand, without excluding parts of reports I have chosen to highlight the parts that seem greatly important and to reduce the text size of parts you may wish to look at yourself.

Goal

To show that there is an angiotensin-converting enzyme 2 (ACE2) interaction with Essential hypertension (EH) and evidence proves that Estrogen participates in the upregulate of ACE2 expression and activity level, Therefore, normal Estrogen level can protect pre-menopausal female from being harmed by high blood pressure and lessen effects of Sars-CoV-2.

ACE2 deficiency impaired function and level of activity of ACE2 affects cerebral arteries, and exaggerates cerebrovascular dysfunction with ageing and smoking and plays a critical part in Sars-Cov-2 sticky receptor causing major health problems from what may have otherwise been mild symptoms.

It is known that angiotensin II impairs neurovascular coupling, induces oxidative stress and produces vasomotor dysfunction in cerebral arteries and plays an important role in cerebrovascular dysfunction with ageing.
Therefore it is possible that by modulating effects of angiotensin II, ACE2 plays an important role in the maintenance of vascular function and prevention of cerebrovascular disease.
Increase ACE2 levels and controlling activity may be beneficial in the management and prevention of cerebrovascular disease and combat Sars-CoV-2 provided the activity of the ACE2 receptors remains within normal healthy limits.

A Mild Case recovered should not be seen as a clean bill of health for the following reasons
14 days the person may appear no longer contagious but questions remain incubation period and over accuracy of testing.
Lets say the case is mild and detected ,Antibody-dependent enhancement (ADE) is a mechanism through which dengue viruses, feline coronaviruses, and HIV viruses take advantage of anti-viral humoral immune responses to infect host target cells- ***this can provide a fatal outcome to population who otherwise either showed no symptoms or recovered from mild symptoms Previously***

Association of angiotensin-converting enzyme 2 gene polymorphism and enzymatic activity with essential hypertension in different gender

A case–control study

Qi Zhang, PhD,a Mingyu Cong, PhD,a Ningning Wang, MS,a Xueyan Li, MS,a Hao Zhang, MS,a Keyong Zhang, MS,a Ming Jin, MS,a Nan Wu, MS,a Changchun Qiu, PhD,a,b and Jingping Li, PhDa,∗

Monitoring Editor: Erika I. Boesen.

Abstract

Angiotensin-converting enzyme 2 (ACE2) plays an important role in the development of essential hypertension (EH). The aim of this study was to investigate the relationship of ACE2 gene polymorphisms and enzymatic activity with EH in the northeastern Chinese Han population. 34 single-nucleotide polymorphism (SNP) loci of ACE2 were detected in 1024 EH patients and 956 normotensive (NT) controls by Sequenom Mass-ARRAY RS1000. Five SNPs (rs1514283, rs4646155, rs4646176, rs2285666, and rs879922) in ACE2 gene were determined to significantly associate with EH in female participants, while no SNP locus was linked to male group. Specifically, it was the first time to report that rs4646155 was significantly associated with EH in females. Furthermore, the correlation between ACE2 activity and clinical parameters were performed by Pearson correlation analysis in EH patients. **We found that the ACE2 activity level was negatively correlated with body mass index (BMI), DBP, and pulse pressure, and significantly positively with ACE2 concentration, blood glucose and estrogen level in female EH patients. These results demonstrated that the genetic variants of ACE2 played vital roles in the development of EH. And the serum ACE2 activity can predict the development of cardiac dysfunction in EH patients.**

Keywords: ACE2, enzymatic activity, essential hypertension, gender, single nucleotide polymorphisms

Go to:

1. Introduction

Essential hypertension (EH) is a major risk factor for myocardial infarction, stroke and renal failure.[1] The prevalence of EH is increasing rapidly and it is estimated that the morbidity of EH will reach 29% of the global population by 2025.[2] As a major threat to human health worldwide, the incidence of EH in China has been an upward trend in the past several years. EH is a polygenetic and complex disease, caused by the interactions of genetic and environmental factors. Around 30% of the individual variability is considered to be genetically determined. A lot of studies have been performed to investigate the genetic variation in genes of renin–angiotensin system (RAS), especially the angiotensin-converting enzyme 2 (ACE2).

The RAS plays a vital role in the occurrence and development of EH. ACE2 is a key regulator in the RAS, which could convert Ang I to Ang 1 to 9 and degrade Ang II to the Ang 1 to 7.[3] ACE2 locates on the X chromosome in human genome. It encodes a protein of 805 amino acids, including 18 exons. In humans, ACE2 mainly expresses in the cardiovascular, renal and

gastrointestinal tissues.[4] Moreover, ACE2 also has been found in the brain, lung and testis.[5] It has been mapped to a defined quantitative trait locus (QTL) on the X chromosome in human.[1]

The single nucleotide polymorphisms (SNPs) of ACE2 play an important role in cardiovascular diseases. Up to now, several studies focused on the association of ACE2 SNPs with EH.[6–10] But some of these results were inconsistent or even contradictory. For example, Fan et al reported that the TT genotype frequency of rs2106809 was significantly higher in female hypertensive patients than age- and gender-matched normotensive subjects.[6] Nevertheless, other results showed the rs2106809 was no significant deviation in either hypertensive or normotensive women in Chinese Han population.[11,12] The possible reasons may be attributed to that the observed population have different ethnicity and race, and come from regions with different natural environment. Therefore, to more precisely elucidate the role of ACE2 SNPs in EH, further research is necessary to determine a wider range of ACE2 polymorphic loci associated with EH in population who come from different regions and ethnic groups. In addition, few studies reported the serum ACE2 activity level between EH patients and healthy individuals, and the relation between the serum ACE2 activity and EH also need to be uncovered. In this study, the association between ACE2 polymorphism and EH was investigated in a large number of Han population of the northeast Chinese. The serum ACE2 activity was also determined to analyze its relation with clinical baseline characteristics and biochemical parameters in EH patients.

Go to:

2. Methods

2.1. Study population

The studied cohort included 1024 (male, 510; female, 514) EH patients and 956 (male, 296; female, 660) NT controls. A case-control study was performed, in which all of the participants were Han Chinese from the Lan Xi of Heilongjiang Province in China. The EH patients were recruited from 2012 to 2015, in accordance with the Guidelines for Prevention and Treatment of Hypertension in China, and needed to meet the following criteria:

- (1) all subjects had no consanguinity at enrolment;
- (2) aged < 60;
- (3) systolic blood pressure (SBP) ≥ 140 mmHg and/or diastolic blood pressure (DBP) ≥ 100 mmHg;
- (4) absence of secondary causes of hypertension based on extensive biochemical and clinical examinations; and
- (5) absence of pharmacological treatment for hypertension.

The NT subjects were screened from a physical examination and matched for age and ethnicity with the EH patients from the same area. The inclusion criteria for the NT subjects were as follows: age ≥ 40 and mean SBP<120 mmHg and mean DBP<80 mmHg. The study was approved by the Ethics Committee of Qiqihar Medical University, China. Written informed consent was obtained from each participant or their legal guardian. Blood pressure was measured 3 times using a mercury sphygmomanometer with patient in a seated position by a standard auscultatory method. The average measured value of blood pressure including systolic and diastolic pressure levels was used for quantitative analyses. Body mass index (BMI) was calculated as follows: BMI=Weight (kg)/[Height (m)×Height (m)].

2.2. DNA extraction

Four millilitres of peripheral blood was collected in an EDTA tube from each subject for DNA extraction. Then genomic DNA was extracted from leukocytes using CWBIO blood genomic DNA mini kit (CWBIO, Beijing China). Finally, the DNA specimens were stored at −20°C.

2.3. SNP selection and genotyping assay

The SNPs were selected based on the SNP genotype information from the GenBank database. Equidistant SNPs in the ACE2 gene regions were identified as common SNPs in our study. These SNPs were chosen based on a minor allele frequency (MAF) of at least 1%. Multiplexed SNP Mass EXTEND assay was designed using the Sequenom Mass ARRAY Assay Design 4.0 software (Agena Bioscience, San Diego, CA).[13] SNP genotyping was performed using the Sequenom Mass ARRAY RS1000 platform following the manufacturer's protocols. The corresponding primers included in this project are listed in Supplementary table S1. Sequenom Typer 4.0 software was used for data analyses.[13]

2.4. Plasma ACE2 measurement

The plasma ACE2 concentration was determined by Human Angiotensin Converting Enzyme 2 (ACE2) Enzyme Immunoassay Kit (MLBIO, Shanghai China) according to the manufacturer's instructions. ACE2 enzymatic activity was determined by a spectrophotometric mono-reagent assay. The serum (50 μL) and the substrate solution (50 μL) were reacted at 37°C for 60 minutes in ACE2 activity enzyme-linked immunosorbent assay (ELISA) specific plate reader (MLBIO, Shanghai China) and the optical density value was monitored at 450 nm. The serum ACE2 activity was expressed as unit/L.

2.5. Statistical analysis

All of the database management and statistical calculations were performed with SPSS v.20.0 software (PASW Statistics, SPSS Inc., Chicago, IL). Continuous variables were shown as mean± SD. Anthropometric indices and genotype/allele frequencies were compared between the EH and NT subjects using chi-squared ($\chi 2$) tests. Hardy–Weinberg equilibrium was tested by Fisher's exact test ($P>.05$) using gene frequencies of the healthy individuals. For each odds ratio (OR), we calculated the 2-tailed probability value and 95% confidence interval (CI). A 2-tailed $P<.05$ was accepted as statistically significant. Haplotype distribution was analysed using the SHEsis software (http://analysis.bio-x.cn/SHEsisMain.htm).[14,15] Pearson correlation analysis was used to calculate the correlation between ACE2 concentration and enzymatic activity and the clinic data in all subjects.

Go to:

3. Results

3.1. Baseline characteristics

The clinical characteristics in formation of the EH patients and NT controls are presented in Table Table1.1. The significantly higher levels of SBP, DBP, pulse pressure, and total cholesterol were found in EH patients, as compared to controls in both male and female groups (all $P<.001$). As for BMI and triglycerides levels, the significant deviations between the 2 groups were determined only in females. Hardy–Weinberg equilibrium for ACE2 gene was tested only in control group, and was consistent with the expected result.

Table 1

Clinical characteristics of the study population (mean±SD).

Factors	Males		Females	
	EH	NT	EH	NT
Age (year)	56.67±10.23	54.84±11.99	56.67±10.23	50.00±8.57*
BMI (kg/m^2)	26.54±12.79	24.12±3.57	26.54±12.79	23.77±3.34*
SBP (mmHg)	148.68±18.76	111.49±11.88*	148.68±18.76	118.84±11.89*
DBP (mmHg)	91.61±10.00	74.19±7.75*	91.61±10.00	76.19±7.16*
PP (mmHg)	57.07±16.16	37.29±7.68*	57.07±16.16	42.63±9.79*
TC (mmol/L)	5.88±4.20	4.71±0.77*	5.88±4.20	4.77±1.05*
HDL (mmol/L)	1.51±0.66	1.30±0.49	1.51±0.66	1.54±0.71
TG (mmol/L)	1.88±1.25	1.25±0.72	1.88±1.25	1.40±0.89*
GLU (mmol/L)	4.91±1.18	5.01±0.66	4.91±1.18	4.46±0.86
ACE2 conc (ng/ml)	2.34±0.52	—	2.13±0.52	—
ACE2 activity (U/L)	6.89±1.65	—	6.53±1.98	—

Continuous variables are expressed in Mean±Standard Deviation.
ACE2 conc=ACE2 concentration, BMI=body mass index, DBP=diastolic blood pressure, GLU=blood glucose, HDL=High Density Lipoprotein, NT=normotensive, PP=pulse pressure, SBP=systolic blood pressure, TC=total cholesterol, TG=triglycerides.
* $P<.001$.

3.2. ACE2 gene polymorphisms

The genotype and allele frequencies at SNP loci rs1514283, rs4646155, rs4646176, and rs879922 in ACE2 are shown in Table Table2.2. At the rs1514283 locus, the frequencies of the CC genotype and C allele were significantly higher in the EH patients than in the NT controls (CC: 2.2% vs 0.7%, P <.05, OR=4.209, 95% CI 1.633–10.851; C: 3.7% vs 2.2%, P=.01). A significant association was found between the rs1514283 variant and EH risk under the dominant genetic model (TT vs CC+CT: OR=1.724, 95% CI 1.087–2.733, P=.02). For rs879922, there were also significant differences in the frequencies of the CC genotype and the C allele between EH patients and the NT controls (CC: 2.5% vs 0.6%, P<.01, OR=4.707, 95% CI 1.854–11.951; C: 4.4% vs 2.7%, P=.01). The dominant (GG vs CC+GC) distribution of C allele of rs879922 revealed a significant association (OR=1.520, 95% CI 1.002–2.307, P=.05) with EH risk. At the rs4646155 locus, the frequencies of the TT genotype and the T allele were significantly higher in the EH patients than the NT controls (TT: 1.9% vs 0.7%, P=.01, OR=3.492, 95% CI 1.324–9.212; T: 3.4% vs 2.2%, P=.02). A logistic regression analysis shown that the dominant effect (CC vs TT+TC) was associated with EH risk (OR=1.573 95% CI 0.985–2.511), but it did not reach statistical significance (P=.06). At the rs4646176 locus, the rates of the GG genotype and the G allele were significantly higher in the EH patients than in the NT participants (GG: 2.1% vs 0.6%, P<.01, OR=3.902, 95% CI 1.503–10.128; G: 3.7% vs 2.2%, P=.01). The association between rs4646176 and the risk of EH was investigated under both the dominant and recessive genetic model. The dominant (CC vs GG+GC) genetic model of G allele showed a significantly association with EH risk (OR=1.684, 95% CI 1.062–2.671, P=.03) in the Chinese Han population.

Table 2

Distribution of genotypes and alleles for each of the ACE2 gene polymorphisms in all subjects.

At the same time, the gene polymorphisms of ACE2 were analysed according to different groups of male and female in all the participants. None of the SNPs was significantly associated with EH in the male group. In the female group, the statistical results demonstrated that the genotype and allele distributions frequencies of 5 SNP loci (rs1514283, rs2285666, rs4646155, rs4646176, and rs879922) located in the introns of the ACE2 gene were significantly different between the EH and NT groups (Fig. (Fig.1).1). The distribution frequencies of genotype and allele for ACE2 SNPs in the female group are shown in Table Table3.3. At the rs1514283 locus, the frequency of the CC genotype was significantly higher in the EH patients than in the NT subjects (CC: 2% vs 0.3%, P=.02, OR=6.501, 95% CI 1.375–30.740). And

at the rs879922 locus, there was also a significant difference between the EH patients and the NT controls regarding to the CC genotype (CC: 2.3% vs 0.3%, P=.01, OR=7.442, 95% CI 1.609–34.426). These findings indicated that CC genotype of rs1514283 and rs879922 were high-risk factors for the progression of EH in females. Interestingly, a frequency of heterozygous genotype TC was significantly higher in NT group as compared with EH group for the rs2285666 locus (TC: 32.0% vs 44.8%, P<.001, OR=0.572, 95% CI 0.428–0.765). The data implicated that the TC genotype of rs2285666 carriers had a reduced risk of EH, and it was a potential genetic resistance factor in the development of EH in Chinese female Han population. As for the rs4646176, the frequencies of the GG genotype in the EH patients were significantly higher than that in the NT controls (GG: 1.8% vs 0.3%, P=.03, OR=5.615, 95% CI 1.163–27.101). The GG genotype of rs4646176 was a risk factor for EH in women. Moreover, the TT genotype frequencies of rs4646155 in the EH group were also higher than in the NT group (TT: 1.6% vs 0.3%, OR=4.793, 95% CI 0.967–23.765), and no significant difference was observed between the locus and EH (P =.06). This was a limitation of our study, which the sample size was still relatively small and not provide sufficient information to precisely estimate the association between rs4646155 and EH in the Chinese female Han population.

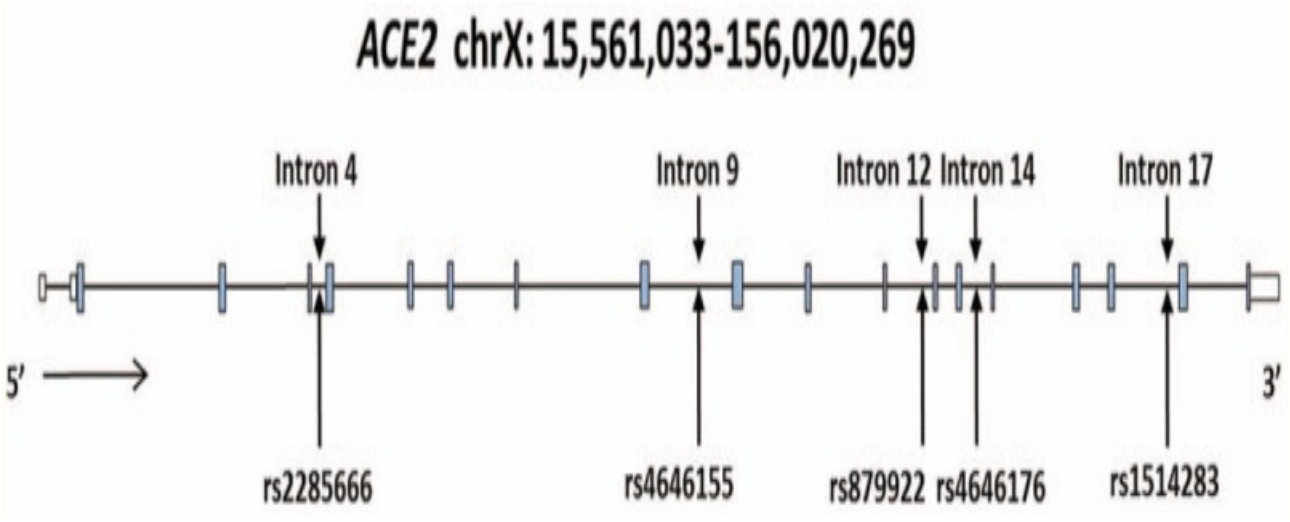

Figure 1

Schematic representation of ACE2 gene structure. Introns are shown as horizontal black line, exons are shown as blue boxes and white boxes represent the 5′ and 3′-UTRs.

Table 3

Distribution of genotypes and alleles for each of the ACE2 gene polymorphisms in females.

3.3. Linkage disequilibrium (LD) and haplotype analysis

LD analysis showed that the 4 ACE2 gene polymorphism loci (rs1514283, rs4646155, rs4646176 and rs879922) were in strong LD. rs1514283 and rs4646155: D'=0.992, r2=0.924; rs1514283 and rs4646176: D'=0.992, r2=0.977; rs1514283 and rs879922: D'=1.000, r2=0.812; rs4646155 and rs4646176: D'=1.000, r2=0.932; rs4646155 and rs879922: D'=1.000, r2=0.86; rs4646176 and rs879922: D'=1.00, r2=0.819. Unfortunately, the SHEsis haplotype analysis demonstrated that no haplotype associated with EH was found in the 5 ACE2 SNPs in this cohort.

3.4. ACE2 concentration and enzymatic activity assay

In order to further elucidate the relationship between ACE2 activity level and EH, we examined the concentration and activity of ACE2 for all subjects. The Pearson correlation analysis between ACE2 activity and clinical characters results are shown in Table Table4.4. **A strong positive correlation was found between ACE2 activity and concentration level in both male and female EH patients** (males: r=0.997, P<.001, females: r=0.966, P<.001). Meanwhile, serum ACE2 activity had a negative correlation with BMI in the male and female groups (male: r=−0.363, P<.001, female: r=−0.003, P<.001). Interestingly, in female EH patients, ACE2 activity level were significant negatively correlated with DBP and pulse pressure (DBP: r=−0.485, P<.001; PP: r=−0.100, P<.001), and positively correlated with blood glucose (GLU: r=0.537, P<.001). By contrast, no statistical correlations of these clinical parameters with ACE2 activity were found in male group, which further documented the specificity of our assay for ACE2. **However, ACE2 activity levels were extremely low or even undetectable in the plasma from normotensive subjects** (data not shown). **Some previous reports also showed that the ACE2 activity levels were very low in normal healthy persons, and increased in patients with cardiovascular disease**.[16,17]

Table 4

The result of Pearson correlation analysis between ACE2 level and clinical characters.

	Male			Female		
Factors	***r***	***p***	**FDR**	***R***	***p***	**FDR**
ACE2 conc (ng/ml)	0.997	<.001	.024	0.966	<.001	.006
Age (years)	−0.155	.17	.371	0.452	.12	.288
BMI (kg/m^2)	−0.363	<.001	.012	−0.003	<.001	.005
SBP (mm Hg)	0.116	.29	.497	0.499	.98	1.069
DBP (mm Hg)	−0.023	.83	1.048	−0.485	<.001	.004
SBP-DBP (mm Hg)	0.144	.19	.380	−0.100	<.001	.003
TC (mmol/L)	0.020	.85	1.020	−0.176	.49	.653
HDL (mmol/L)	−0.118	.29	.464	0.100	.22	.406
TR (mmol/L)	−0.093	.40	.565	0.018	.90	1.028
GLU (mmol/L)	−0.108	.33	.495	0.537	<.001	.003
E2 (ng/ml)	—	—	—	0.352	.01	.027
T (ng/ml)	0.408	<.001	.008	—	—	—

FDR = false discovery rate, *P* = *P* value, *r* = Pearson's Correlation coefficient.
ACE2 conc = ACE2 concentration, BMI = body mass index, DBP = diastolic blood pressure, E2 = oestrogen, GLU = blood glucose, HDL = High Density Lipoprotein, SBP = systolic blood pressure, T = testosterone, TC = total cholesterol, TG = triglycerides.

Go to:

4. Discussion

At present, EH is 1 of the most common cardiovascular diseases, and it is also a major public health problem around the world. At least 970 million people worldwide are suffering from elevated blood pressure (hypertension), and about 66% of them live in developing countries. EH is a complex disease, which is considered to the result of the genetic and environmental interaction. The RAS plays a vital role in the occurrence and development of EH. As an important member of the RAS, ACE2 is a dipeptidyl carboxydipeptidase, which counterbalances the action of angiotensin-converting enzyme. The over-expression of ACE2

may decrease RAS activation. The significant associations between ACE2 gene polymorphisms and EH have been reported for people of different race and ethnicity.[6,18–20]

In the present study, we found that the 4 SNPs of ACE2 (rs1514283, rs4646155, rs4646176, and rs879922) were associated with EH in northeastern Han populations of China. As a tag SNP in the CHB (Han Chinese in Beijing) SNP database for HapMap project, rs4646155 can capture the information of 4 ACE2 SNPs (rs4646140, rs4646144, rs4646155, and rs61433707) with minor allele frequencies equal to or greater than 3% in the HapMap CHB database. Up to now, only a few studies focused on the correlation between rs4646155 and hypertension, but these results showed that no significant difference in the rs4646155 genotypes/alleles frequencies between hypertensive patients and normotensive health volunteers.[6,17] In this study, it was the first time to report that the TT genotype of rs4646155 was a significant association with EH (OR=3.492), especially in females (OR=4.793). Prolonged exposure to low temperature may be the main cause of this inconsistency. Low temperature was a well-known risk factor for high blood pressure.[21] Under the condition of low temperature, the body maintains normal body temperature by sympathetic activity and vasoconstriction, which prevents heat loss and increases blood pressure.[22] The cold pressor test (CPT), which is a standard test for characterization of sympathetic function, also make certain that the blood pressure variations in the response to cold stimulation.[23,24] And CPT has been documented to predict the subsequent risk of hypertension in normotensive persons.[25] In this study, all the participants came from the northeastern Han Chinese within 3 generations reside in Lan Xi (46° 20′0″ N, 126° 16′0″ E) of Heilongjiang Province. The annual average temperature in this area is about 5°C and the mean temperature is below 0°C about 6 months of 1 year. The subjects of previous studies were resident in Henan[6] (the annual average temperature 14.3 °C) and Guangdong province[17] (the annual average temperature 21.8°C). The prevalence of hypertension was consistently higher in northern than in southern residents (32.4% in Heilongjiang, 26.1% in Henan, 15.8% in Guangdong).[26] Therefore, the cold environmental and genetic factors may be the risk factors associated with EH for the population of the cold region. We will further confirm the relationship between the ACE2 SNP locus and ACE2 protein activity in subsequent experiments.

In addition, we observed that the TC genotype of rs2285666 conferred a protective effect on EH in female group of all participants. Rs2285666 was 1 of the most frequently investigated loci in the studies of ACE2 gene polymorphism. Thus far, some prior studies have reported the relation between rs2285666 and blood pressure change, but these results were inconsistent.[11,18–20] Two studies reported that the T allele of rs2285666 were significant associations with hypertension or SBP or DBP in female groups of Chinese population.[18,19] And Zhong et al found that the C allele of the SNP associated with higher blood pressure.[20] However, another orthostatic blood pressure study including 3630 Chinese Han subjects indicated that the hypertension had no association with the rs2285666 locus.[11] In 2 meta-analyses, the results of rs2285666 polymorphism were also conflicting. One study combined 2528 hypertension patients and 2024 normotensive controls from Chinese Han population and reported no association between the locus polymorphism and hypertension.[27] The other study, which included 7251 hypertension patients comprising of Chinese Han, Chinese Dongxiang, Anglo-Celtic population, showed that the TT genotype of rs2285666 was a significant association with hypertension in Chinese Dongxiang and Anglo-Celtic females.[28]

In the present study, we observed that the TC heterozygous genotype of rs2285666 was a protective factor for EH in females of Chinese Han subjects. The heterogeneity of the association between rs2285666 gene polymorphism and hypertension may be caused by the following reasons. First, several reports have shown that hormonal and sex chromosomes contributed to the blood pressure variations between the sexes.[29,30] Second, there was a much great difference in the frequency of distribution of ACE2 variants among different racial and ethnic lines.[19,28] For instance, the T allele frequencies of rs2285666 were 40.1% in Chinese Han, 32.4% in Chinese Dongxiang, 22.0% in Anglo Celtic.[19,31] At last, it is possible that the rs2285666 has characteristic of QTL for hypertension. A quantitative trait locus (QTL) is a region of DNA which is associated with a particular phenotypic trait, which varies in degree and which can be attributed to polygenic effects, that is, the product of 2 or more genes, and their environment.[26] Phenotypic variation for quantitative traits is the result of the segregation of alleles at quantitative trait loci (QTL). Environmental factors and other external influences can also play a role in phenotypic variation.[26] **The previous study has reported that ACE2 gene maps to a QTL on the X chromosome in 3 different rat models of hypertension**.[1]

Furthermore, we found that rs2285666 was a protein truncating variant (PTV) locus through checking GTEx database, which the type was splice disruption model. PTVs are genetic variants predicted to shorten the coding sequence of genes,[32] also commonly referred to as loss-of-function variants as they often result in a non-functional or unstable gene product.[33] PTVs are generally the strongest acting genetic variants in medical genetics and, as 1 functional copy of the gene is removed, may often provide insight into what is achievable pharmacologically via inhibition of the product of the gene.[32] Thus, the homozygous variants of rs2285666 may result in the product inhibition for ACE2 gene.

The National Center for Biotechnology Information (NCBI) Genotype-Tissue Expression (GTEx) database aims to evaluate the relationship between genetic variation and gene expression in normal human tissues to understand how this relationship contributes to disease susceptibility and development.[34,35] Expression quantitative trait locus (eQTL) browser in the GTEx database is a central resource that archives and displays results of a national research project for determining association between genetic variations and high-throughput molecular-level expression phenotypes, and this information can provide insight into the biological relevance of data from genome-wide association studies.[35] To characterize the functional relevance of the 5 SNP loci found in this study, we utilized this database resource to evaluate the relationship of these variants with the expression levels of ACE2 in human different tissues. The GTEx database indicated that the rs879922 polymorphism was a significant eQTL for ACE2. A significant association was observed between the expression level of ACE2 and different genotypes of rs879922 in 361 normal tibial nerve ($P=7.4\times10-5$), whereas the relative expression of ACE2 was significantly lower in subjects with the CC genotype of rs879922 compared with those carrying the GG/CG genotype (Fig. (Fig.22).

Figure 2

The genotype of rs879922 was correlated with expression of ACE2 in the tibial nerve on GTEx Portal.

The LD analysis showed that rs1514283, rs4646155, rs4646176, and rs879922 were in strong LD. And in haplotype analysis, 3 haplotypes were found in these 4 SNPs. But all the 3 haplotypes were not significantly different between EH patients and controls (all P>.05) (LFT=0.01, data not shown). Only when lowest frequency threshold (LFT) was set at 0.001, the frequency of the T-C-C-G haplotype was significantly higher in controls than in EH patients (OR 0.733, 95% CI 0.544–0.988, P=.04). Yet haplotype with frequency less than LFT will not be considered in analysis. Therefore, it is necessary to further confirm the correlation between the haplotype and EH in large sample size. **To sum up, only when more ACE2 SNP locus associated with EH were revealed, we can fully understand the role of ACE2 in EH. The rich SNPs information can predict the risk of hypertension, and provide a theoretical basis for the prevention and treatment of hypertension. And abundant gene polymorphism information can also lay a solid foundation for personalized medicine. Personalized medicine is becoming a medical reality, as important phenotype-genotype relationships are uncovered. In addition, the discovery of a large number of SNP loci associated with hypertension could provide new targets for the research of anti-hypertensive drugs and the possibility of obtaining more effective anti-hypertensive drugs. Thus, new SNP locus associated with hypertension are important for the prevention, diagnosis, treatment of EH and the development of new drugs, and also a key element of individualized care.**

ACE2 undergoes "shedding" from endothelial cells, which result in the release of the ectodomain with catalytic active into the circulation.[36] The activity of ACE2 can be measured in serum by ELISA. In reviewing the literature, a number of studies focused on the association between ACE2 activity and EH in animal models.[37–39] **However, only few reports noted that the serum activity level of ACE2 was associated with cardiovascular disease,**[40] specifically EH. Thus, in **this study, we evaluated the correlation of ACE2 activity with clinical characters between the different genders in Chinese Han EH patients. The results indicated that ACE2 activity was inversely related to DBP in females EH patients. Previously, only 1 research reported the association between ACE2 activity and DBP response to cold pressor test in women.[24] And a study in animal model showed that the elevated diastolic pressure in the spontaneously hypertensive rat was associated with the reduction in ACE2 activity.[37] Moreover, a research about ACE2 activity in human atrial fibrillation (AF) demonstrated that elevated plasma ACE2 activity level was associated with impaired left ventricular (LV) diastolic function.[41] In addition, the association between pulse pressure and ACE2 activity was found in female EH patient for the first time in this study. The pulse pressure is an important parameter represented heart function, and a high pulse pressure tends to accelerate the normal aging of heart. The increased pulse pressure has been considered as a marker of arterial stiffness and an important predictor of new-onset AF.[42] These results suggested that ACE2 activity could be a potential biomarker for the variations of blood pressure, providing the useful information for the prediction and prevention of cardiac dysfunction in EH patients.**

Accumulated evidence proves that estrogen participates in the upregulates of ACE2 expression and activity level.[43] Our results showed the positive association between ACE2 activity and estrogen level in EH patients. Estrogen can regulate the components of the renin-angiotensin-aldosterone system, which increases synthesis of angiotensinogen, ACE2 and AT2R and decreases the expression of renin, ACE and AT1R.[17] Moreover, estrogen can impair the increment of aldosterone. Therefore, normal estrogen level can protect female from being harmed by high blood pressure caused by renin-angiotensin-aldosterone system. These

results provided evidence that genetic variant of ACE2 plays a vital role in the development of EH. And the serum ACE2 activity can be used as a potential biomarker for the identification of blood pressure variation, providing the useful information for the prediction and prevention of cardiac dysfunction in EH patients.

In summary, here we observed that 5 SNPs (rs1514283, rs4646155, rs4646176, rs2285666, and rs879922) of ACE2 gene were significantly associated with EH in women of Chinese Han population. It is the first time to report that the susceptibility of rs4646155 for EH in female group. In addition, we found the ACE2 activities were significantly correlated with DBP, pulse pressure and blood glucose in female EH patients. The finding may provide a novel insight into the clinical diagnosis of EH and the development of antihypertensive drugs.

Go to:

Acknowledgment

We thank the subjects for participating in this study. We gratefully acknowledge the assistance of clinical, field and laboratory staff that made this work possible.

Go to:

Author contributions

Conceptualization: Qi Zhang, Changchun Qiu.

Formal analysis: Jingping Li.

Investigation: Keyong Zhang.

Methodology: Hao Zhang.

Resources: Mingyu Cong.

Software: Ningning Wang.

Validation: Xueyan Li, Ming Jin, Nan Wu.

Writing – original draft: Qi Zhang.

Web link https://www.ncbi.nlm.nih.gov/pmc/articles/PMC6211892/

IMPACT OF ACE2 DEFICIENCY AND OXIDATIVE STRESS ON CEREBROVASCULAR FUNCTION WITH AGING

Ricardo A. Peña Silva, MD,1,3 Yi Chu, PhD,2 Jordan D. Miller, PhD,2 Ian J. Mitchell, BSc,2 Josef M. Penninger, MD, PhD,4 Frank M. Faraci, PhD,1,2 and Donald D. Heistad, MD1,2

Go to:

Abstract

Background and Purpose

Angiotensin II produces oxidative stress and endothelial dysfunction in cerebral arteries, and angiotensin II type I receptors may play a role in longevity and vascular aging. **Angiotensin converting enzyme type 2 (ACE2) converts angiotensin II to**

angiotensin (1–7) and thus may protect against effects of angiotensin II. We hypothesized that ACE2 deficiency increases oxidative stress and endothelial dysfunction in cerebral arteries, and examined the role of ACE2 in age-related cerebrovascular dysfunction.

Methods

Endothelial function, expression of angiotensin system components, NADPH oxidase subunits, and proinflammatory cytokines were examined in cerebral arteries from adult [12 mo old] and old [24 mo old] ACE2 knockout (KO) and wild type (WT) mice. The superoxide scavenger tempol was used to examine the role of oxidative stress on endothelial function.

Results

Vasodilatation to acetylcholine was impaired in adult ACE2 KO [24±6% (mean +/− SE)] compared to WT mice [52±7%, $p<0.05$]. In old mice, vasodilatation to acetylcholine was impaired in WT mice [29±6%] and severely impaired in ACE2 KO mice [7±5%]. Tempol improved endothelial function in adult and old ACE2 KO and WT mice. Aging increased mRNA for TNFα in WT mice, and significantly increased mRNA levels of Nox2, p47phox, and Rcan1 in both ACE2 KO and WT mice. mRNA levels of angiotensin system components did not change during aging.

Conclusions

ACE2 deficiency impaired endothelial function in cerebral arteries from adult mice and augmented endothelial dysfunction during aging. Oxidative stress plays a critical role in cerebrovascular dysfunction induced by ACE2 deficiency and aging.

Keywords: Endothelium, angiotensin converting enzyme 2, aging, cerebral arteries, oxidative stress

Go to:

INTRODUCTION

Stroke is the second most frequent cause of death from cardiovascular events in the US[1]. Hypertension and endothelial dysfunction increase with age and are risk factors for stroke[2–5]. Aging is associated with endothelial dysfunction and oxidative stress in cerebral arteries[6–8]. In people without coronary artery disease, endothelial dysfunction is associated with a four-fold increase in the risk of cerebrovascular events[4]. Cerebral endothelial dysfunction may also have a role in the pathophysiology of vascular cognitive impairment and Alzheimer's disease[9–11, 2].

Angiotensin II increases reactive oxygen species (ROS) and superoxide levels via increases in expression and activation of NADPH oxidases, a major source of superoxide anion in the vasculature[12]. Superoxide reacts with the vasodilator nitric oxide (NO.) to produce peroxynitrite, resulting in decreased NO bioavailability and endothelial dysfunction[13, 14, 4]. Angiotensin II impairs endothelial function in cerebral arteries and the microcirculation[14–16].

Interestingly, genetic deletion of angiotensin II type 1 (AT1) receptors markedly attenuates cerebrovascular dysfunction during aging[8, 6]. Pharmacological modulation of angiotensin signaling in patients with stroke is associated with decreased inflammation, better functional outcome, and decreased risk for future cardiovascular events[17].

Angiotensin converting enzyme type 2 (ACE2), a homolog of ACE with different substrate specificity, metabolizes angiotensin II into angiotensin 1–7[18, 19]. Binding of angiotensin (1–7) to the Mas receptor[20] attenuates signaling cascades activated by angiotensin II, decreases activity of NAPDH oxidase [21], and produces vasodilatation[20, 22]. Several studies suggest that ACE2 levels may be reduced with aging[23, 24], which should result in magnification of effects of angiotensin II. However, little is known about the function of ACE2 in cerebral arteries or in endothelial dysfunction during aging. In this study, we tested the hypothesis that ACE2 deficiency increases oxidative stress and vasomotor dysfunction in cerebral arteries, and examined effects of ACE2 on endothelial function in adult animals and during aging.

Go to:

METHODS

Experimental animals

Studies were performed in adult [12±0.2 mo old (mean±SE)] and old [24±0.4 mo old] male ACE2 deficient (knockout or KO) and wild type (WT) mice (n=54). The ACE2 gene is located in the X chromosome, and ACE2 KO mice and WT littermates were derived from breeding heterozygous females with WT or KO males[25]. The mice were bred onto a C57 background for eight generations. All experimental protocols and procedures conform to the National Institutes of Health guidelines and were approved by the Institutional Animal Care and Use Committee of the University of Iowa.

Studies of endothelial function

Mice were euthanized with an overdose of sodium pentobarbital (150 mg/kg ip). The brain was rapidly removed and placed in ice-cold Krebs solution. The basilar artery was carefully isolated, removed, cannulated and pressurized to 60 mmHg in an organ bath. After an equilibration period of 30 minutes, baseline diameter was measured and contraction was examined in response to KCl (50 mmol/L). The arteries were submaximally constricted with the thromboxane A2 analog U46619 before assessment of dilator responses. Endothelium-dependent vasodilatation was tested with acetylcholine (ACh). Endothelium-independent vasodilatation was tested with sodium nitroprusside (SNP) and papaverine. To test the role of ROS, arteries were preincubated (30 min) with Tempol (1 mmol/L), a superoxide scavenger, before treatment with acetylcholine.

Cerebral arteries were also used for analysis of gene expression and immunohistochemical studies. Plasma was collected for measurement of angiotensin levels. Detailed methods are available in the Online-only Data Supplement (http://stroke.ahajournals.org).

Statistics

Results are expressed as mean±SEM. Statistical significance in assays of endothelial function was determined by repeated measures two-way ANOVA on the complete data set. Then, the significance of comparisons within the adult or old data set was evaluated using Tukey post hoc test, and the highest (10−4 M) concentration of acetylcholine. Comparison between adult and old mice was performed with ANOVA followed by Newman-Keuls multiple comparison test. Statistical significance for gene expression and peptide measurement assays was determined by two way ANOVA and Bonferroni post hoc test. Significant differences were identified when $P<0.05$. The analysis was performed using Prism 5 (Graphpad, La Jolla, CA) and was validated in SAS (SAS Institute Inc, Cary, NC).

Go to:

RESULTS

Expression of components of the ACE2/Angiotensin 1–7/Mas axis and the renin angiotensin system

ACE2 deficiency was confirmed in ACE2 KO mice using real time-qPCR in samples from kidneys and brain arteries (Table 1 and Table S1.). ACE2 mRNA levels in cerebral arteries and kidneys were not significantly different between adult and old WT mice. ACE2 mRNA levels in brain cortex from adult and old WT mice did not change during aging (data not shown).

Table 1

Gene expression in cerebral arteries from adult and old ACE2 KO and WT mice

	Adult		Old	
	WT	**ACE2 KO**	**WT**	**ACE2 KO**
ACE2	1.00 (±0.25)	0.05 (±0.03)*	1.39 (±0.17)	0.06 (±0.06)*
Mas	1.00 (±0.14)	0.86 (±0.08)	1.05 (±0.32)	0.73 (±0.05)
AT1	1.00 (±0.14)	0.88 (±0.27)	1.09 (±0.14)	1.07 (±0.21)
EcSOD #	1.00 (±0.09)	1.08 (±0.11)	1.40 (±0.18)*	1.42 (±0.10)
Catalase #	1.00 (±0.09)	1.13 (±0.11)	1.44 (±0.14)*	1.78 (±0.18) †
Nrf2	1.00 (±0.05)	0.93 (±0.07)	1.11 (±0.09)	1.16 (±0.10)
IL-6	1.00 (±0.21)	0.57 (±0.21)	1.27 (±0.41)	1.76 (±0.70)
TNFα #	1.00 (±0.23)	0.99 (±0.31)	2.03 (±0.39)*	1.64 (±0.28)
Rcan1 #	1.00 (±0.07)	0.98 (±0.09)	1.42 (±0.10)*	1.41 (±0.09) †
iNOS	1.00 (±0.17)	0.65 (±0.11)	1.16 (±0.24)	1.12 (±0.12)

Data expressed as mean ±SEM

n= 6–7 mice / value

*P<0.05 vs adult WT

†P=<0.05 vs adult KO

#P<0.05 Overall effect of aging (two-way ANOVA)

The presence of ACE2 protein was assessed using western blotting and immunostaining. ACE2 expression was confirmed in kidney homogenates from WT mice, but was absent in kidney homogenates from an ACE2 KO mouse (Fig 1B). ACE2 protein was not detected by Western blotting in homogenates from cerebral arteries (Fig 1B). ACE2 expression by immunofluorescence was abundantly localized in epithelium of renal tubules (Fig 1A). Weak positive staining for ACE2 was detected in sections from cerebral arteries, but it was difficult to differentiate from weak background staining in ACE2 KO mice (Fig 1A).

Figure 1

ACE2 expression in basilar arteries and kidneys. Panel A: ACE2 staining in basilar artery, especially in the smooth muscle layer of adult WT mice. ACE staining was also seen in the epithelium of renal tubules in adult and old WT mice. Staining was absent in sections from ACE2 KO mice. Similar findings were observed in 3 mice from each group. Panel B: Western blots showing ACE2 expression in kidney homogenates from WT mice, and absence of protein in the ACE2 KO mouse. ACE2 staining was not detected by western blotting in brain arteries.

In cerebral arteries and kidneys, mRNA levels of the angiotensin 1–7 receptor Mas and the angiotensin II type 1 receptor (AT1R) were similar in all groups (Table 1 and Table S1).

Effect of ACE2 deficiency on blood pressure

Systolic blood pressure was comparable (P>0.05) between adult ACE2 KO (104±3) and WT mice (106±4 mmHg). Similar results were found in old ACE2 KO (113±12) vs WT mice (109±6 mmHg).

Vascular function in adult ACE2 KO and WT mice

Baseline diameter of the basilar artery under resting conditions (prior to precontraction) was similar in ACE2 KO (163±8 µm) and WT mice (172±6µm). Dilatation to acetylcholine was reduced by ~50% in the basilar artery from adult ACE2 KO mice [24±6%] compared to adult WT mice [52±7%, p<0.05]. Tempol improved responses to acetylcholine in both ACE2 KO (to 78±7%, p<0.05) and WT

mice (87±13%, p<0.05) (Fig 2A). Vasodilatation to the endothelium independent agonist, sodium nitroprusside, and papaverine was similar in both groups.

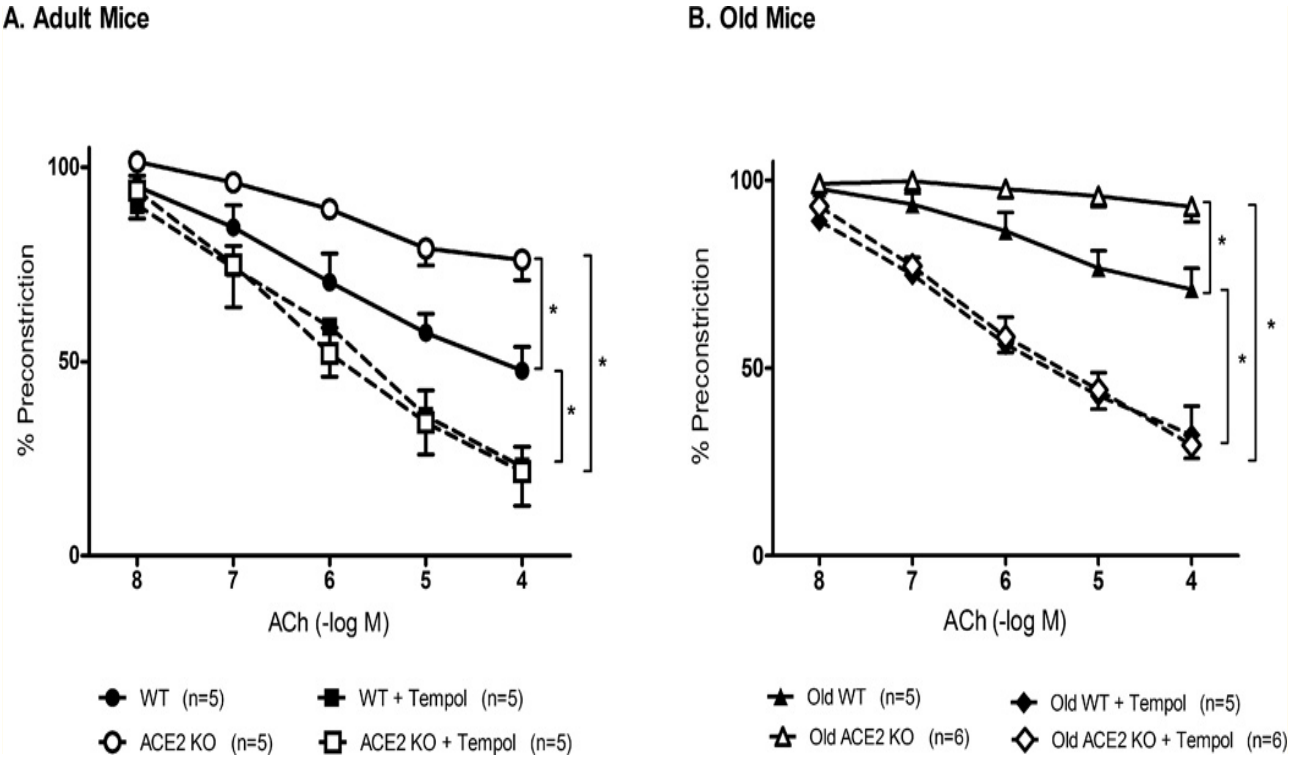

Figure 2

Effects of ACE2 deficiency and oxidative stress on vascular function. Panel A: Vasodilatation to acetylcholine (ACh) in adult ACE2 WT(●, n=5) and KO (○, n=5) mice. Role of oxidative stress was examined after incubation with tempol of basilar arteries from adult ACE2 WT (■) and KO (□) mice. Panel B: Vasodilatation to acetylcholine (ACh), was examined in old ACE2 WT(▲, n=5) and KO (△, n=6) mice. Tempol was also added to arteries from old ACE2 WT (◆) and KO (◇) mice. Values are mean ±SE, *p<0.05.

Vasoconstriction to KCl (50 mmol/L) was comparable between ACE2 KO (43±5%) and WT mice (48±3%). Vasoconstriction to U46619 was also similar in ACE2 KO (26±1%) and WT mice (25±3%).

Effect of ACE2 deficiency and aging in cerebral vascular function

Diameter of the basilar artery was similar in old ACE2 KO (166 ±5 µm) vs WT (182 ±7 µm) mice (p=0.07). Maximal vasodilatation to acetylcholine was significantly less in old WT mice than in adult WT mice (Fig S1). Similarly, maximal responses to acetylcholine were less in old ACE2 KO mice than in adult ACE2 KO mice (p<0.05). In old mice, vasodilatation to acetylcholine was

profoundly impaired in ACE2 KO mice, and was significantly less than in old WT mice (Fig 2B). Tempol improved responses to acetylcholine in both old ACE2 KO ($p<0.01$) and old WT mice ($p<0.01$). Vasodilatation to sodium nitroprusside and papaverine was similar in both groups.

Vasoconstriction to KCl was also preserved in ACE2 WT (43±4%) and KO mice (51±2%). Vasoconstriction in response to U46619 was similar in old ACE2 WT (28±4%)and KO mice (32±2%).

Oxidative stress and inflammation

mRNA transcript levels of NADPH oxidase subunits p47phox and Nox2 were higher in cerebral arteries from old vs adult mice (Fig 3). Expression of the subunits was not affected by genotype (Fig 3). Nrf2 levels were similar in the four groups. Expression of EcSOD was increased in old WT mice (Table 1). Catalase was increased significantly in old ACE2 KO and WT mice (Table 1). Nitrotyrosine immunostaining was relatively low in sections of basilar artery from adult WT mice. Quantification of these data was difficult, but the immunostaining appeared to be increased in adult ACE2 KO mice and old ACE2 KO and WT mice (Fig S2).

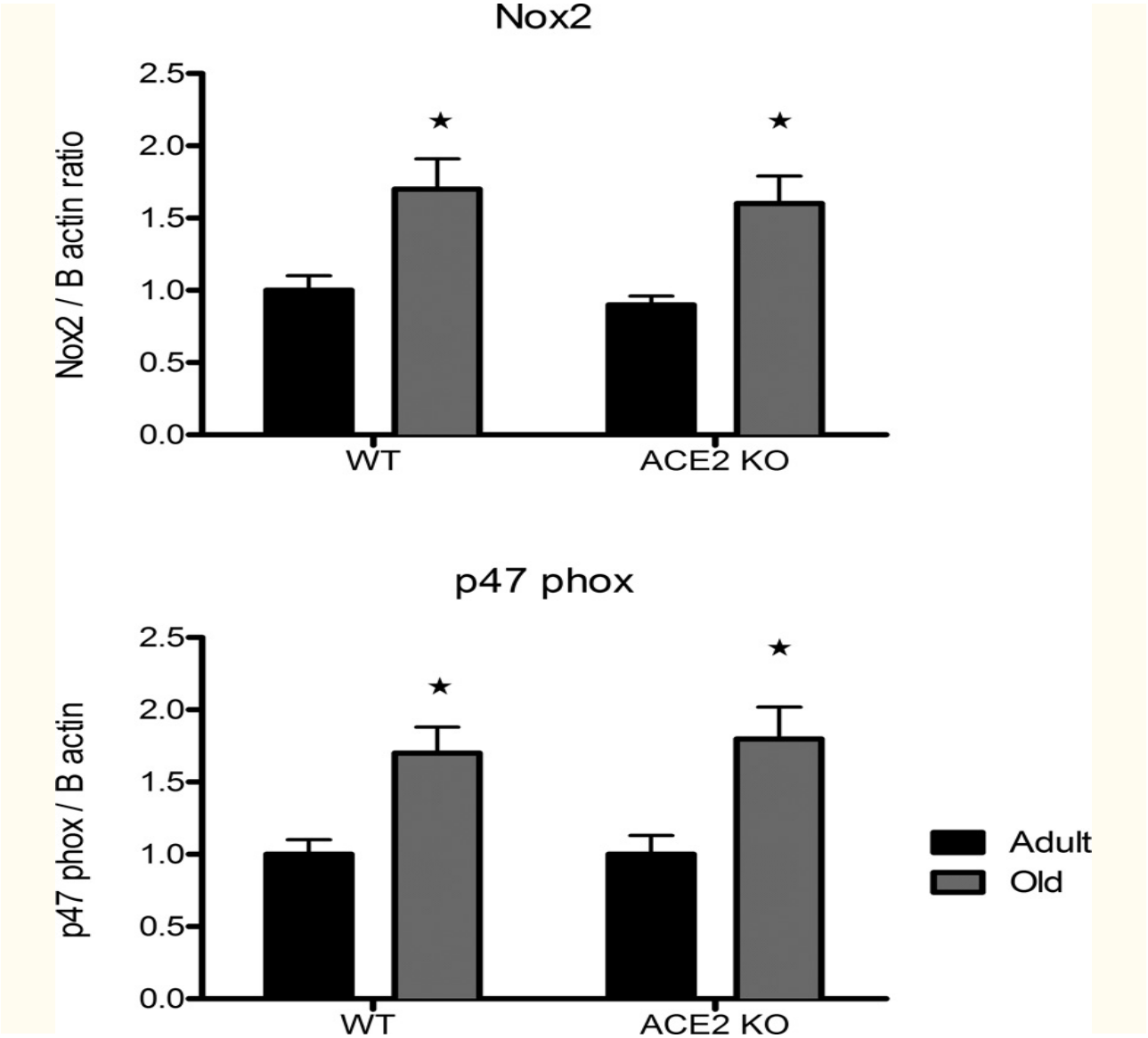

Open in a separate window

Figure 3

Effect of aging on expression of NADPH oxidase subunits. Relative expression levels of Nox2 and p47phox mRNA in cerebral arteries from adult (black bars) and old (gray bars) wild type or ACE2 KO mice. Values are mean ±SE (n=7/group), *p<0.05 vs adult mice.

Aging was associated with increased mRNA levels of TNFα in WT mice. Rcan1 mRNA levels were also significantly increased in cerebral arteries from both ACE2 KO and WT mice. IL-6 and iNOS mRNA levels were not significantly different between groups (Table 1).

Levels of angiotensins in plasma

Angiotensin II levels were not significantly different between adult ACE2 KO and WT mice (Fig 4A). Angiotensin II levels were not significantly affected by aging although they tended to be lower in old ACE2 KO and WT mice. Likewise, angiotensin 1–7 levels were not affected by aging or genotype (Fig 4B).

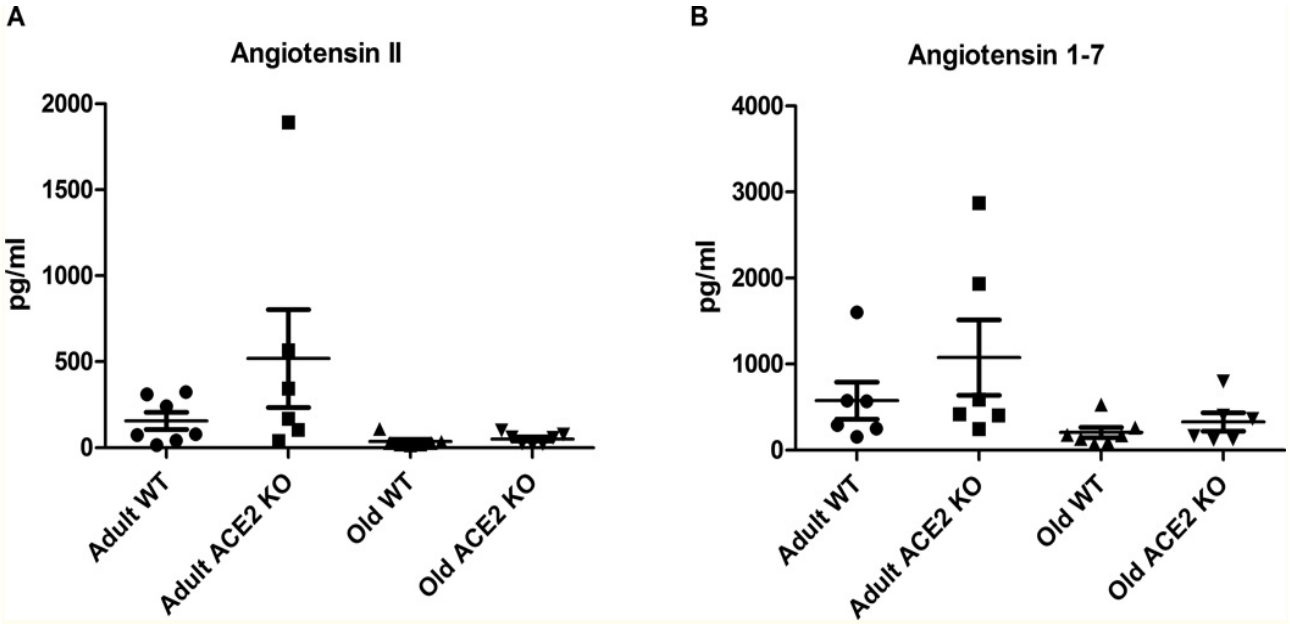

Figure 4

Plasma levels of angiotensin peptides. Panel A: Angiotensin II levels in plasma from adult WT (n=7), adult ACE2 KO (n=6), old WT (n=7) and old ACE2 KO (n=7) mice. Panel B: Angiotensin 1–7 levels in plasma from adult WT (n=6), adult ACE2 KO (n=6), old WT (n=6) and old ACE2 KO (n=7) mice. There were no significant differences in plasma peptide levels between groups. Values are mean ±SE.

Go to:

DISCUSSION

There are several major new findings in this study. First, genetic deficiency of ACE2 impaired endothelial function in the cerebral circulation. Second, cerebrovascular dysfunction during aging was greater in ACE2 KO mice than in WT mice. Third, oxidative stress plays a key role in cerebrovascular dysfunction with ACE2 deficiency and during aging. These findings provide evidence for an important role of ACE2 in the maintenance of endothelial function in cerebral arteries under normal conditions and support the overall concept that the renin angiotensin system has a major impact on the cerebrovasculature with aging. We chose to study cerebral vessels, because cerebral arteries are important resistance vessels in the brain[14] and play an important role in the

pathophysiology of stroke[33]. Previous data have shown that young ACE2 KO mice have endothelial dysfunction in conduit vessels such as aorta[26], but effects on the cerebral circulation and mechanisms responsible for impaired vascular function in ACE2 KO mice have not been explored.

There is a poor understanding of the role of ACE2 in cardiovascular disease or stroke. Studies of ACE2 polymorphisms in patients suggest a weak association of the ACE2 G9570A polymorphism with stroke [27]. Decreased expression of ACE2 has been found in kidneys of patients with diabetes and renal disease[28]. Hypertension is an important risk factor for stroke and one might expect that ACE2 deficiency would be associated with hypertension. ACE2 deficiency however has little or no effect on blood pressure[29], and hypertension does not appear to contribute to endothelial dysfunction in ACE2 deficient mice. We did not find any significant differences in blood pressure between WT and ACE2 KO mice in either age group. Our values for blood pressures are comparable to those reported previously for ACE2 KO mice[25]. These findings in mice are consistent with studies in humans, in which association of ACE2 polymorphisms with hypertension is variable[30–32].

We found that endothelial function was impaired in adult ACE2 KO mice. Moreover, we found that cerebrovascular dysfunction during aging was augmented in old ACE2 KO mice. Because a superoxide scavenger restored endothelial responses to acetylcholine, our data suggest that oxidative stress plays a primary role in dysfunction caused by ACE2 deficiency. Furthermore, nitrotyrosine staining appeared to be higher in basilar arteries from ACE2 KO mice which suggest that these vessels are exposed to relatively greater oxidative stress than wild type mice. Consistent with these findings, superoxide has been proposed to be a key mediator of cerebrovascular dysfunction in other models of aging and disease[6, 7, 12, 13, 33–35].

ACE2 may play an important role in regulation of oxidative stress in blood vessels. ACE2 overexpression prevents angiotensin II-induced increase in ROS and NADPH oxidase expression in endothelium[26]. On the other hand, ACE2 inhibition enhanced angiotensin-II-stimulated ROS formation[36]. We measured expression of antioxidant proteins, NADPH oxidase subunits, and proinflammatory genes to explore possible mechanisms that may contribute to increased dysfunction in ACE2 KO mice. Concordant with previous studies[6, 7], we found that aging increased expression of NADPH oxidase subunits in cerebral arteries. In addition, gene expression data indicated that aging had a significant effect on the expression of the proinflammatory molecules TNFα and Rcan 1. Rcan1 modulates vasomotor function[37] and its expression is increased

by angiotensin II[38]. We also found an increase in SOD and catalase mRNA levels in cerebral arteries from old mice, which presumably is a compensatory mechanism to limit increases in ROS. We did not find changes in Nrf2, which is thought to be a master regulator of antioxidant expression during aging. Our findings for antioxidant enzymes and Nrf2 in cerebral vessels differ from previous studies in which decreased activity and expression of antioxidant proteins was found in rat aorta [39] and carotid arteries from macaques[40].

We initially speculated that expression of ACE2 decreases with aging which, by loss of inhibitory effects on the renin angiotensin system, might lead to higher concentrations of angiotensin II and more angiotensin II-related cardiovascular pathology with aging. Multiple lines of evidence suggest an association between increased angiotensin II signaling and aging. First AT1 receptor deficient mice live longer than WT controls[41]. Second, cerebrovascular dysfunction with aging is attenuated in AT1 receptor deficient mice[8]. Third, long term administration of AT1 receptor blockers is associated with improved metabolic profiles during aging, which mimic some of the effects of caloric restriction[42]. We did not find, however, an effect of aging on expression of ACE2, Mas or AT1 receptors in cerebral arteries, kidney, or brain cortex. These results differ from findings in rat lung, in which expression of ACE2 protein decreases with aging[24].

We used mice in which ACE2 is knocked out in all tissues. Contrary to what could be expected, we did not find differences in plasma levels of angiotensin II or angiotensin 1–7 between ACE2 KO and WT mice. These results agree with previous studies that demonstrated that plasma angiotensin II or angiotensin 1–7 were not significantly different in plasma from ACE2 deficient and WT mice[43, 44]. It is possible that other enzymes including prolyl[45] or neutral endopeptidases[46] compensate for ACE2 deficiency and maintain normal angiotensin 1–7 levels. Moreover, ACE2 metabolizes several peptides including angiotensin II, apelin, des-Arg[9] bradykinin, ghrelin and neurotensins[18]. Some of these peptides modulate vasomotor function, so it is possible that the altered vascular phenotype in ACE2 KO mice can be explained by alterations in signaling pathways other than (or in addition to) the angiotensin II pathway.

In summary, this is the first study to show that ACE2 deficiency impaired function in cerebral arteries, and exaggerates cerebrovascular dysfunction with aging. It is known that angiotensin II impairs neurovascular coupling[12], induces oxidative stress and produces vasomotor dysfunction in cerebral arteries[15, 16], and plays an important role in cerebrovascular dysfunction with aging[8, 9, 22]. Therefore it is possible that by modulating effects of angiotensin II, ACE2 plays an important role in the maintenance of vascular function and prevention of cerebrovascular disease. Therapeutic approaches to increase ACE2 levels and activity might be beneficial in the management and prevention of cerebrovascular disease.

Go to:

ACKNOWLEDGEMENTS

We thank Dr Chantal Allamargot in the Central Microscopy Research Facility and Dr Ana Sierra in Internal Medicine for technical assistance with immunostaining, Dr Rhonda de Cook in the Department of Statistics (University of Iowa) for statistical advising. We also thank Dr Bridget Brosnihan at the Hypertension Core Laboratory at Wake Forest University for measurement of angiotensin peptides.

SOURCES OF FUNDING

This work was supported by NIH grants NS-24621, HL-62984, HL-38901 and HL-113863; a Carver Program of Excellence. R.P was supported by a Fulbright Scholarship and American Heart Association Predoctoral Fellowships (0815525G, 10PRE3780044).

Go to:

Footnotes

DISCLOSURES

None

Go to:

REFERENCES

1. Roger VL, Go AS, Lloyd-Jones DM, Benjamin EJ, Berry JD, Borden WB, et al. Heart disease and stroke statistics-2012 update: A report from the American Heart Association. Circulation. 2012;125:e2–e220. [PMC free article] [PubMed] [Google Scholar]

2. Yavuz BB, Yavuz B, Sener DD, Cankurtaran M, Halil M, Ulger Z, et al. Advanced age is associated with endothelial dysfunction in healthy elderly subjects. Gerontology. 2008;54:153–156. [PubMed] [Google Scholar]

3. Donato AJ, Magerko KA, Lawson BR, Durrant JR, Lesniewski LA, Seals DR. Sirt-1 and vascular endothelial dysfunction with ageing in mice and humans. J Physiol. 2011;589:4545–4554. [PMC free article] [PubMed] [Google Scholar]

4. Targonski PV, Bonetti PO, Pumper GM, Higano ST, Holmes DR, Jr, Lerman A. Coronary endothelial dysfunction is associated with an increased risk of cerebrovascular events. Circulation. 2003;107:2805–2809. [PubMed] [Google Scholar]

5. Lind L, Berglund L, Larsson A, Sundstrom J. Endothelial function in resistance and conduit arteries and 5-year risk of cardiovascular disease. Circulation. 2011;123:1545–1551. [PubMed] [Google Scholar]

6. Mayhan WG, Arrick DM, Sharpe GM, Sun H. Age-related alterations in reactivity of cerebral arterioles: Role of oxidative stress. Microcirculation. 2008;15:225–236. [PubMed] [Google Scholar]

7. Park L, Anrather J, Girouard H, Zhou P, Iadecola C. Nox2-derived reactive oxygen species mediate neurovascular dysregulation in the aging mouse brain. J Cereb Blood Flow Metab. 2007;27:1908–1918. [PubMed] [Google Scholar]

8. Modrick ML, Didion SP, Sigmund CD, Faraci FM. Role of oxidative stress and AT1 receptors in cerebral vascular dysfunction with aging. Am J Physiol Heart Circ Physiol. 2009;296:H1914–H1919. [PMC free article] [PubMed] [Google Scholar]

9. Zuliani G, Cavalieri M, Galvani M, Passaro A, Munari MR, Bosi C, et al. Markers of endothelial dysfunction in older subjects with late onset Alzheimer's disease or vascular dementia. J. Neurol. Sci. 2008;272:164–170. [PubMed] [Google Scholar]

10. Girouard H, Iadecola C. Neurovascular coupling in the normal brain and in hypertension, stroke, and Alzheimer disease. J Appl Physiol. 2006;100:328–335. [PubMed] [Google Scholar]

11. Benarroch EE. Neurovascular unit dysfunction: A vascular component of Alzheimer disease? Neurology. 2007;68:1730–1732. [PubMed] [Google Scholar]

12. Kazama K, Anrather J, Zhou P, Girouard H, Frys K, Milner TA, et al. Angiotensin II impairs neurovascular coupling in neocortex through NADPH oxidase-derived radicals. Circ. Res. 2004;95:1019–1026. [PubMed] [Google Scholar]

13. Girouard H, Park L, Anrather J, Zhou P, Iadecola C. Cerebrovascular nitrosative stress mediates neurovascular and endothelial dysfunction induced by angiotensin II. Arterioscler. Thromb. Vac. Biol. 2007;27:303–309. [PubMed] [Google Scholar]

14. Faraci FM. Protecting against vascular disease in brain. Am J Physiol Heart Circ Physiol. 2011;300:H1566–H1582. [PMC free article] [PubMed] [Google Scholar]

15. Chrissobolis S, Faraci FM. Sex differences in protection against angiotensin II-induced endothelial dysfunction by manganese superoxide dismutase in the cerebral circulation. Hypertension. 2010;55:905–910. [PMC free article] [PubMed] [Google Scholar]

16. Capone C, Faraco G, Park L, Cao X, Davisson RL, Iadecola C. The cerebrovascular dysfunction induced by slow pressor doses of angiotensin II precedes the development of hypertension. Am J Physiol Heart Circ Physiol. 2011;300:H397–H407. [PMC free article] [PubMed] [Google Scholar]

17. Di Napoli M, Papa F. Angiotensin-converting enzyme inhibitor use is associated with reduced plasma concentration of c-reactive protein in patients with first-ever ischemic stroke. Stroke. 2003;34:2922–2929. [PubMed] [Google Scholar]

18. Vickers C, Hales P, Kaushik V, Dick L, Gavin J, Tang J, et al. Hydrolysis of biological peptides by human angiotensin-converting enzyme-related carboxypeptidase. J. Biol. Chem. 2002;277:14838–14843. [PubMed] [Google Scholar]

19. Turner AJ, Tipnis SR, Guy JL, Rice GI, Hooper NM. Aceh / ACE2 is a novel mammalian metallocarboxypeptidase and a homologue of angiotensin-converting enzyme insensitive to ACE. Biochemistry (Mosc) 2002;353:346–353. [PubMed] [Google Scholar]

20. Santos RA, Simoes e Silva AC, Maric C, Silva DM, Machado RP, de Buhr I, et al. Angiotensin-(1–7) is an endogenous ligand for the G protein-coupled receptor mas. Proc. Natl. Acad. Sci. U.S.A. 2003;100:8258–8263. [PMC free article] [PubMed] [Google Scholar]

21. Sampaio WO, Henrique de Castro C, Santos RA, Schiffrin EL, Touyz RM. Angiotensin-(1–7) counterregulates angiotensin II signaling in human endothelial cells. Hypertension. 2007;50:1093–1098. [PubMed] [Google Scholar]

22. Feterik K, Smith L, Katusic ZS. Angiotensin-(1–7) causes endothelium-dependent relaxation in canine middle cerebral artery. Brain Res. 2000;873:75–82. [PubMed] [Google Scholar]

23. Liang W, Zhu Z, Guo J, Liu Z, Zhou W, Chin DP, et al. Severe acute respiratory syndrome, Beijing 2003. Emerg Infect Dis. 2004;10:25–31. [PMC free article] [PubMed] [Google Scholar]

24. Xie X, Chen J, Wang X, Zhang F, Liu Y. Age- and gender-related difference of ACE2 expression in rat lung. Life Sci. 2006;78:2166–2171. [PubMed] [Google Scholar]

25. Crackower MA, Sarao R, Oudit GY, Yagil C, Kozieradzki I, Scanga SE, et al. Angiotensin-converting enzyme 2 is an essential regulator of heart function. Nature. 2002;417:822–828. [PubMed] [Google Scholar]

26. Lovren F, Pan Y, Quan A, Teoh H, Wang G, Shukla PC, et al. Angiotensin converting enzyme-2 confers endothelial protection and attenuates atherosclerosis. Am J Physiol Heart Circ Physiol. 2008;295:H1377–H1384. [PubMed] [Google Scholar]

27. Mo YJ, Huang WH, Chen DL, Chen FR. Relationship of angiotensin-converting enzyme 2 gene polymorphism with the prognosis of hypertensive stroke patients. Nan Fang Yi Ke Da Xue Xue Bao. 2010;30:84–87. [PubMed] [Google Scholar]

28. Reich HN, Oudit GY, Penninger JM, Scholey JW, Herzenberg AM. Decreased glomerular and tubular expression of ACE2 in patients with type 2 diabetes and kidney disease. Kidney Int. 2008;74:1610–1616. [PubMed] [Google Scholar]

29. Gurley SB, Coffman TM. Angiotensin-converting enzyme 2 gene targeting studies in mice: Mixed messages. Experimental Physiology. 2008;93:538–542. [PubMed] [Google Scholar]

30. Fan X, Wang Y, Sun K, Zhang W, Yang X, Wang S, et al. Polymorphisms of ACE2 gene are associated with essential hypertension and antihypertensive effects of captopril in women. Clin Pharmacol Ther. 2007;82:187–196. [PubMed] [Google Scholar]

31. Benjafield AV, Wang WY, Morris BJ. No association of angiotensin-converting enzyme 2 gene (ACE2) polymorphisms with essential hypertension. Am J Hypertens. 2004;17:624–628. [PubMed] [Google Scholar]

32. Lu N, Yang Y, Wang Y, Liu Y, Fu G, Chen D, et al. ACE2 gene polymorphism and essential hypertension: An updated meta-analysis involving 11,051 subjects. Mol Biol Rep. 2012;39:6581–6589. [PubMed] [Google Scholar]

33. Kitayama J, Faraci FM, Lentz SR, Heistad DD. Cerebral vascular dysfunction during hypercholesterolemia. Stroke. 2007;38:2136–2141. [PubMed] [Google Scholar]

34. Kitayama J, Yi C, Faraci FM, Heistad DD. Modulation of dilator responses of cerebral arterioles by extracellular superoxide dismutase. Stroke. 2006;37:2802–2806. [PubMed] [Google Scholar]

35. Girouard H, Park L, Anrather J, Zhou P, Iadecola C. Angiotensin II attenuates endothelium-dependent responses in the cerebral microcirculation through nox-2-derived radicals. Arterioscler Thromb Vasc Biol. 2006;26:826–832. [PubMed] [Google Scholar]

36. Gwathmey TM, Pendergrass KD, Reid SD, Rose JC, Diz DI, Chappell MC. Angiotensin-(1–7)-angiotensin-converting enzyme 2 attenuates reactive oxygen species formation to angiotensin II within the cell nucleus. Hypertension. 2010;55:166–171. [PMC free article] [PubMed] [Google Scholar]

37. Riper DV, Jayakumar L, Latchana N, Bhoiwala D, Mitchell AN, Valenti JW, et al. Regulation of vascular function by RCAN1 (ADAPT78) Arch Biochem Biophys. 2008;472:43–50. [PubMed] [Google Scholar]

38. Esteban V, Mendez-Barbero N, Jimenez-Borreguero LJ, Roque M, Novensa L, Garcia-Redondo AB, et al. Regulator of calcineurin 1 mediates pathological vascular wall remodeling. J Exp Med. 2011;208:2125–2139. [PMC free article] [PubMed] [Google Scholar]

39. Demaree SR, Lawler JM, Linehan J, Delp MD. Ageing alters aortic antioxidant enzyme activities in Fischer-344 rats. Acta Physiol. Scand. 1999;166:203–208. [PubMed] [Google Scholar]

40. Ungvari Z, Bailey-Downs L, Gautam T, Sosnowska D, Wang M, Monticone RE, et al. Age-associated vascular oxidative stress, Nrf2 dysfunction, and NF-{kappa}B activation in the nonhuman primate Macaca mulatta. J. Gerontol. A. Biol. Sci. Med. Sci. 2011;66:866–875. [PMC free article] [PubMed] [Google Scholar]

41. Benigni A, Corna D, Zoja C, Sonzogni A, Latini R, Salio M, et al. Disruption of the Ang II type 1 receptor promotes longevity in mice. 2009:119. [PMC free article] [PubMed] [Google Scholar]

42. de Cavanagh EMV, Inserra F, Ferder L. Angiotensin II blockade: A strategy to slow ageing by protecting mitochondria? Cardiovasc. Res. 2010:31–40. [PubMed] [Google Scholar]

43. Bharadwaj MS, Strawn WB, Groban L, Yamaleyeva LM, Chappell MC, Horta C, et al. Angiotensin-converting enzyme 2 deficiency is associated with impaired gestational weight gain and fetal growth restriction. Hypertension. 2011;58:852–858. [PMC free article] [PubMed] [Google Scholar]

44. Patel VB, Bodiga S, Basu R, Das SK, Wang W, Wang Z, et al. Loss of angiotensin-converting enzyme-2 exacerbates diabetic cardiovascular complications and leads to systolic and vascular dysfunction: A critical role of the angiotensin II/AT1 receptor axis. Circ. Res. 2012;110:1322–1335. [PMC free article] [PubMed] [Google Scholar]

45. Welches WR, Santos RA, Chappell MC, Brosnihan KB, Greene LJ, Ferrario CM. Evidence that prolyl endopeptidase participates in the processing of brain angiotensin. J. Hypertens. 1991;9:631–638. [PubMed] [Google Scholar]

46. Yamamoto K, Chappell MC, Brosnihan KB, Ferrario CM. In vivo metabolism of angiotensin I by neutral endopeptidase (ec 3.4.24.11) in spontaneously hypertensive rats. Hypertension. 1992;19:692–696. [PubMed] [Google Scholar]

https://www.ncbi.nlm.nih.gov/pmc/articles/PMC3529166/

Adipocyte deficiency of ACE2 increases systolic blood pressures of obese female C57BL/6 mice

Robin Shoemaker,✉1 Lisa R. Tannock,2 Wen Su,3 Ming Gong,3 Susan B. Gurley,4 Sean E. Thatcher,5 Frederique Yiannikouris,5 Charles M. Ensor,5 and Lisa A. Cassis5

Associated Data

Supplementary Materials

Data Availability Statement

Go to:

Abstract

Background

Obesity increases the risk for hypertension in both sexes, but the prevalence of hypertension is lower in females than in males until menopause, despite a higher prevalence of obesity in females. **We previously demonstrated that angiotensin-converting enzyme 2 (ACE2), which cleaves the vasoconstrictor, angiotensin II (AngII), to generate the vasodilator, angiotensin-(1-7) (Ang-(1-7)), contributes to sex differences in obesity-hypertension. ACE2 expression in adipose tissue was influenced by obesity in a sex-specific manner, with elevated ACE2 expression in obese female mice. Moreover, estrogen stimulated adipose ACE2 expression and reduced obesity-hypertension in females. In this study, we hypothesized that deficiency of adipocyte ACE2 contributes to obesity-hypertension of females.**

Methods

We generated a mouse model of adipocyte ACE2 deficiency. Male and female mice with adipocyte ACE2 deficiency or littermate controls were fed a low (LF) or a high fat (HF) diet for 16 weeks and blood pressure was quantified by radiotelemetry. HF-fed mice of each sex and genotype were challenged by an acute AngII injection, and blood pressure response was quantified. To translate these findings to humans, we performed a proof-of-principle study in obese transwomen in which systemic angiotensin peptides and blood pressure were quantified prior to and after 12 weeks of gender-affirming 17β-estradiol hormone therapy.

Results

Adipocyte ACE2 deficiency had no effect on the development of obesity in either sex. HF feeding increased systolic blood pressures (SBP) of wild-type male and female mice compared to LF-fed controls. Adipocyte ACE2 deficiency augmented obesity-induced elevations in SBP in females, but not in males. Obese female, but not obese male mice with adipocyte ACE2 deficiency, had an augmented SBP response to acute AngII challenge. In humans, plasma 17β-estradiol concentrations increased in obese transwomen administered 17β-estradiol and correlated positively with plasma Ang-(1-7)/AngII balance, and negatively to SBP after 12 weeks of 17β-estradiol administration.

Conclusions

Adipocyte ACE2 protects female mice from obesity-hypertension, and reduces the blood pressure response to systemic AngII. In obese transwomen undergoing gender-affirming hormone therapy, 17β-estradiol administration may regulate blood pressure via the Ang-(1-7)/AngII balance.

Electronic supplementary material

The online version of this article (10.1186/s13293-019-0260-8) contains supplementary material, which is available to authorized users.

Keywords: Angiotensin-converting enzyme 2, Angiotensin-(1-7), Transgender, Obesity, Blood pressure

Go to:

Background

Obesity is a primary contributor to the development of hypertension in men and women [1, 2]. Although women have increased adiposity compared to men [3, 4], the prevalence of hypertension is greater in men versus women until menopause [5]. After menopause, the prevalence of obesity and hypertension increases in women [5], suggesting sex hormone-mediated mechanisms contribute to protection from obesity-associated hypertension in women.

The renin-angiotensin system (RAS) plays a primary role in regulating blood pressure. Activation of the RAS with obesity contributes to hypertension in experimental models [6, 7] and in humans [8, 9]. Adipose tissue expresses components of the RAS necessary for the production of the vasoconstrictor peptide, angiotensin II (AngII) [10]. Studies from our laboratory demonstrated that adipose tissue serves as a primary source of elevated plasma concentrations of AngII in obese male mice with hypertension [7]. **However, this finding may be specific to males, as other studies demonstrated that obese female mice with lower blood pressure than males displayed no increase in plasma AngII concentrations compared to low fat (LF)-fed controls [11]. Rather, obesity in female mice was associated with increased plasma concentrations of the vasodilator peptide, angiotensin-(1-7) (Ang-(1-7)) [11]. Further, compared to lean females, obese female mice had increased adipose tissue expression of angiotensin-converting enzyme 2 (ACE2), a monocarboxypeptidase that cleaves AngII to generate Ang-(1-7) [11]. Whole-body deficiency of ACE2 converted obese female mice to a hypertensive phenotype, elevating blood pressure to the level of obese males [11]. These results suggest that the balance of Ang-(1-7) to AngII, regulated by ACE2, is different in males versus females, contributing to sex differences in the development of obesity-hypertension.**

To define mechanisms for sex differences in obesity-hypertension, studies examined the effects of estrogens to regulate the balance of systemic and/or local concentrations of Ang-(1-7) to AngII. 17-β estradiol increased ACE2 mRNA abundance in 3T3-L1 adipocytes (a mouse embryonic fibroblast cell line that can be induced to differentiate into adipocyte-like cells) through an estrogen receptor alpha (ERα)-mediated mechanism [11]. Moreover, administration of 17-β estradiol to ovariectomized obese female mice increased adipose ACE2 mRNA abundance, lowered plasma AngII concentrations and decreased systolic blood pressure [12]. However, 17-β estradiol administration had no effect on these parameters in ovariectomized obese females that were ACE2 deficient, suggesting that protective effects of 17-β estradiol to prevent obesity-hypertension in females were ACE2-mediated. Taken

together, these data suggest that estradiol stimulates ACE2 expression in adipocytes to increase the balance of Ang-(1-7) to AngII and protect females from obesity-hypertension.

In this study, we hypothesized that ACE2 expression in adipocytes protects female mice from hypertension associated with obesity. To test this hypothesis, we developed a murine model of adipocyte ACE2 deficiency and used this model to examine effects of adipocyte ACE2 deficiency on the development of hypertension in female and male mice made obese by consumption of a high-fat (HF) diet. Further, to relate these findings to humans, we performed a proof-of-principle study examining the associations among blood pressure, systemic concentrations of estradiol, and the Ang-(1-7)/AngII balance in a patient population of transgendered women (biological males) receiving estradiol therapy.

Go to:

Methods

Experimental animals

All studies using mice were approved by an Institutional Animal Care and Use Committee at the University of Kentucky and were conducted in accordance with the National Institutes of Health (NIH) Guide for the Care and Use of Laboratory Animals. Female mice with loxP sites flanking exon 4 of the Ace2 gene on a C57BL/6 background (Ace2fl/fl) were bred to male Ace2fl/y hemizygous transgenic mice expressing Cre recombinase under the control of the adipocyte-specific promoter, adiponectin. The resulting offspring were either experimental animals with adipocyte-ACE2 deletion (Ace2Adipo) or littermate controls (females Ace2fl/fl; males Ace2fl/y). Mice were maintained on a standard murine diet (Harlan Laboratories, Indianapolis, IN) until 8 weeks of age.

Initial studies characterized the efficiency and specificity of adipocyte ACE2 deficiency using 8-week-old male and female mice (n = 7–8 mice per genotype). Kidney, heart, liver, subcutaneous (SubQ), and retroperitoneal fat (RPF) were dissected, frozen in liquid nitrogen, and stored at − 80 °C until use. For Cre expression studies, female mice carrying the transgene with the ROSA26-stop-lacZ reporter (Jackson Laboratory, Bar Harbor, ME, stock # 0003474) were bred to male Ace2Adipo mice.

For blood pressure studies, 8-week-old male and female mice of each genotype were randomly assigned to receive ad libitum either a low fat (LF, 10% kcal from fat; D12450B, Research Diets Inc, New Brunswick, NJ) or a high fat diet (HF, 60% kcal from fat; D12492, Research Diets, New Brunswick, NJ) for 4 months (n = 6–13 mice/genotype/diet group). Bodyweight was quantified weekly. Fat and lean mass were measured at week 14 of diet feeding by EchoMRI (EchoMRI-100TM, Echo Medical Systems, Houston, TX). Blood pressure was measured by radiotelemetry in a subset of mice (n = 5 mice per genotype/diet group) at week 16 of diet feeding for 5 consecutive days, and again following acute administration of AngII (subcutaneous, 20 μg/kg). The method for blood pressure measurement is described previously [13]. Briefly, anesthetized (isoflurane, to effect) mice were implanted with carotid artery catheters advanced to the aortic arch and radiotelemeter implants (model PA-C10) inserted in a subcutaneous pocket on the right flank. After 1 week of recovery, blood pressure was monitored continuously, with values reported every 5 s. Inclusion criteria for blood pressure measurements were (1) pulse pressures > 20 mmHg and (2) pulse pressures > 1 standard deviation of the mean. At study endpoint, mice were anesthetized with ketamine/xylazine (100/10 mg/kg, i.p.) for exsanguination and tissue harvest.

Acute administration of AngII

HF-fed female Ace2fl/fl and Ace2Adipo and male Ace2fl/y and Ace2Adipo mice (n = 4 mice per group) with radiotelemetry implants were subcutaneously (interscapular) administered 20 μg/kg of AngII (Sigma-Aldrich) in 0.9% sterile saline. Blood pressure was recorded via telemetry continuously for 60 min after administration of AngII. Baseline (time = 0 min) blood pressure reported is the average blood pressure over 15 min prior to administration of AngII. Blood pressure at time = 2, 5, 10, 15, 20, 30, 40, 50, and 60 min following AngII administration is the average value per minute. Data are reported as time course and as integrated area under the curve (AUC).

Detection of β-galactosidase activity in tissues

Whole organs were fixed in formalin at 4 °C for 1 h, then rinsed three times with buffer (100 mM sodium phosphate, 2 mM MgCl2, 0.01% sodium deoxycholate, 0.02% NP-40). Organs were incubated overnight in X-gal staining buffer (rinse buffer with 5 mM potassium ferricyanide, 5 mM potassium ferrocyanide, 1 mg/mL X-gal) and then visualized, where blue staining indicates expression of Cre recombinase.

Tissue DNA and RNA extraction and PCR

Adipose tissue genotyping was performed using DNA extracted from RPF (DNeasy, Qiagen, Alameda, CA). cDNA was generated using the forward primer: 5′–AGCTCATAGAGAAAGAGGGAGCACG and either the reverse primer: 5′–ACAGCCAGGGTGATACAGAGAAACC (generates products demonstrating the presence [912 bp] or the absence [723 bp] of the floxed ACE2 gene) or the reverse primer 5′–AAGGGTAATGTGTGAGCTGGAACCC (generates a 912 bp product demonstrating the deletion of exon 4 of the ACE2 gene).

Total RNA was extracted from tissues using the Maxwell RSC (Promega, Madison, WI). RNA concentrations were determined using a NanoDrop 2000 spectrophotometer (Thermo Scientific, Wilmington, DE); 400 ng of RNA was used for reverse transcription to make cDNA using qScript cDNA Supermix (Quanta, Gaithersburg, MD). The following mouse primers were used to probe gene products from cDNA amplified using SYBR Green PCR Master Mix (Quanta, Gaithersburg, MD): ACE2, forward 5′–TCCAGACTCCGATCATCAAGC, reverse 5′–

GCTCATGGTGTTCAGAATTGTGT; 18S, forward 5′–CGGCTACCACATCCAAGGAA, reverse 5′–GCTGGAATTACCGCGGCT. Data are expressed as ΔΔCt relative to 18S rRNA.

Studies in humans

This study was approved and work was completed in compliance with approval from the Institutional Review Board of the University of Kentucky. Study participants were transgender women (biological males) seeking gender-affirming hormone therapy recruited from the endocrine clinic at the University of Kentucky (n = 4 subjects). Inclusion criteria were biologic male subjects between the age of 21 and 60 with a body mass index (BMI) between 30 and 45 kg/m2 seeking initiation of estrogen therapy for the first time. Exclusion criteria were fasting blood sugar > 126 mg/dL, or use of diabetes medications, current use of angiotensin-converting enzyme (ACE) inhibitors or angiotensin I receptor blockers (ARBs), anti-inflammatory medications (e.g., steroids), prior estrogens, or any other medication or condition that may affect the RAS pathway. Note that subjects participating in this study delayed the use of spironolactone until after at least 12 weeks of estradiol therapy. Subjects were in overall good health and had no significant hepatic, cardiac, or renal impairment. Subjects were seen at baseline (prior to initiation of estrogen therapy) and 12 weeks after estradiol treatment (estradiol, 1–2 mg/day, orally, dose determined by the endocrinologist). Blood pressure and anthropometric measurements took place during office visits at the endocrine clinic. Blood pressure was measured by arm cuff in the seated and resting position. Blood collection took place at the outpatient Clinical Service Core (CSC) of the institutional Center for Clinical and Translational Science (CCTS). For blood collection, subjects were fasted overnight and arrived at the outpatient CSC at 8am. Plasma was collected after centrifugation and stored at − 80 °C until analysis.

Quantification of plasma parameters in humans

Estradiol concentrations were quantified using a commercial ELISA kit (Calbiotech, ES180S, Spring Valley, CA; analytical sensitivity of 3 pg/mL). Angiotensinogen concentrations were quantified using a commercial kit (IBL, 27412, Minneapolis, MN; analytical sensitivity of 0.03 ng/mL). Ang-(1-7) peptide concentrations were quantified using a commercial kit (Peninsula Labs, San Carlos, CA, S-1330; analytical sensitivity of 0.01 ng/mL). Plasma renin activity (IBL, IB59131; analytical sensitivity of 0.14 ng/mL) and AngII peptide concentrations were quantified by enzyme- and radioimmunoassay, respectively, as described previously [6, 13, 14].

Statistical analyses

Data are presented as mean ± SEM. Statistical analyses were performed using SigmaPlot version 12.3. All data passed normality or equal variance tests or logarithmic transformation was used to achieve normality. Two-tailed Student's t tests were used for the analysis of data between two groups. For two-factor analysis, a two-way ANOVA was used to analyze end-point measurements with between-group factors of genotype and diet, followed by Holm-Sidak for post hoc analyses. Response to acute AngII administration was analyzed as a time course using repeated measures (RM) two-way ANOVA, and as the integrated area under the curve (AUC). Correlation analyses were performed for plasma parameters and blood pressures of humans. Values of $p < 0.05$ were considered to be statistically significant.

Go to:

Results

Development of a mouse model of adipocyte ACE2 deficiency

The ACE2 gene was deleted from adipose tissue using the Cre-Lox system driven by the adipocyte-specific promoter, adiponectin (Fig. (Fig.1a).1a). ACE2 mRNA abundance was decreased by 47% in subcutaneous (SubQ) adipose tissue (p = 0.121), and by 51% in retroperitoneal fat (RPF, p < 0.05) from Ace2Adipo compared to Ace2fl/y mice (Fig. (Fig.1b).1b). In contrast, there was no difference in ACE2 mRNA abundance in the kidney, heart, or liver from Ace2fl/y compared to Ace2Adipo mice (Fig. (Fig.1b).1b). Deletion of ACE2 in Ace2Adipo but not Ace2fl/fl mice was confirmed by PCR in DNA extracted from RPF (Fig. (Fig.1c).1c). Positive β-galactosidase staining was present in adipose tissues (epididymal [EF], RPF, and SubQ) of Ace2Adipo, but not Ace2fl/y mice (Additional file 1: Figure S1). In contrast, no β-galactosidase staining was present in the liver, heart, or kidney of Ace2fl/fl or Ace2Adipo mice (Fig. (Fig.11d).

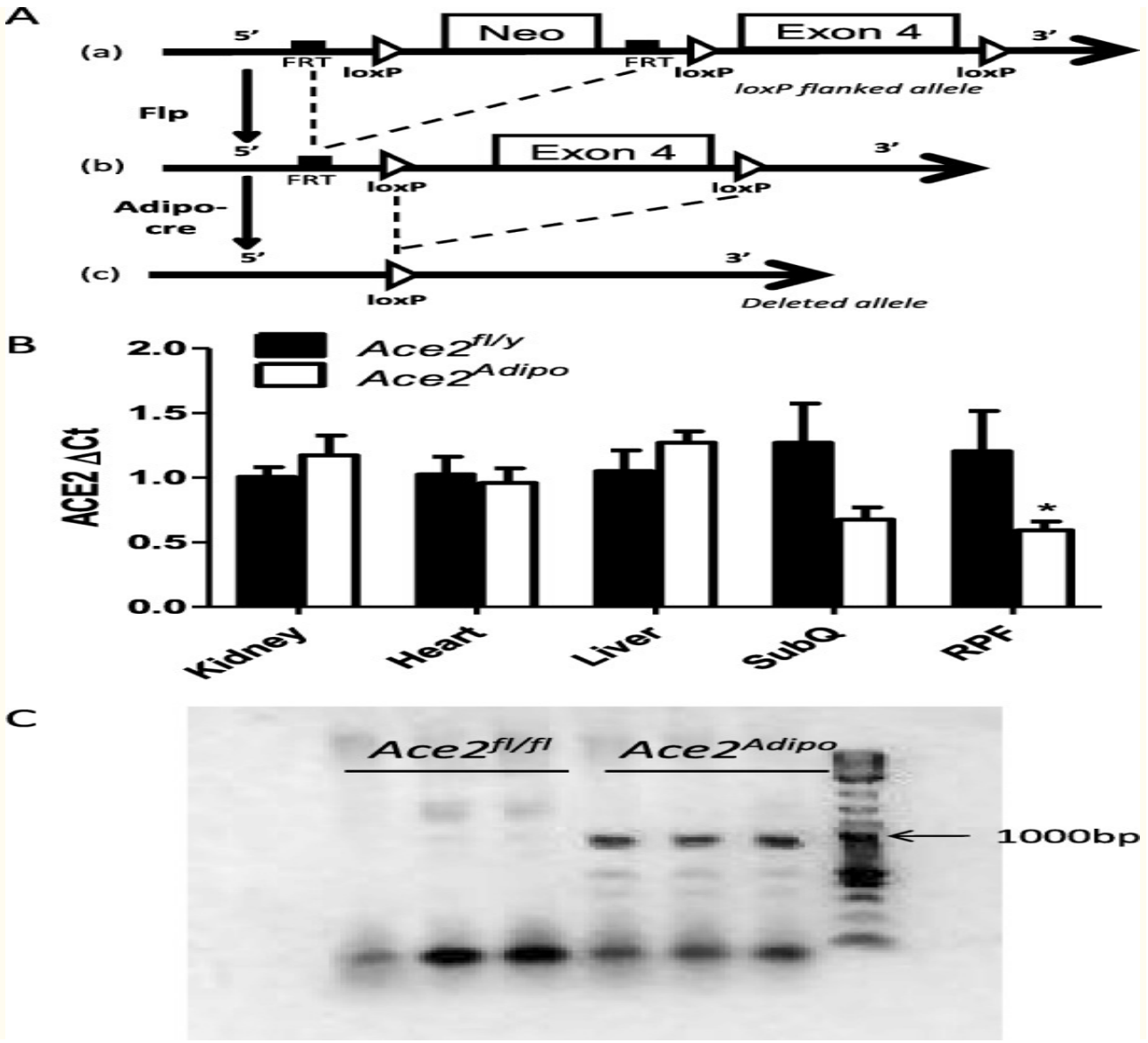

Open in a separate window

Fig. 1

Development of a mouse model of adipocyte ACE2 deficiency. **a** Schematic representation depicting the loxP-flanked ACE2 allele before (**a**) and after successive recombination with Flp (**b**) and transgenic adiponectin-driven Cre expression (**c**). The disrupted allele is shown in **c**, indicating deletion of exon 4 of the ACE2 gene. **b** Tissue characterization demonstrating reduced ACE2 mRNA abundance is specific to adipose tissues (subcutaneous, SubQ; retroperitoneal, RPF) (n = 4–8 male mice/genotype). Data are mean + SEM; $P < 0.05$ compared to Ace2fl/y using t test. **c** PCR reactions were performed with DNA extracted from RPF (n = 3 female mice/genotype). Primers amplify a 923 base pair product for the disrupted portion of the ACE2 gene

Deficiency of ACE2 had no effect on the development of obesity in male or female mice

Both LF- and HF-fed male mice (Fig. (Fig.2b)2b) had significantly greater body weights than female mice (Fig. (Fig.2a)2a) throughout the study, independent of ACE2 genotype. After 15 weeks of diet feeding, body weight was increased significantly in HF-fed compared to LF-fed female and male mice ($p < 0.001$), with no differences in body weight between genotypes (Fig. (Fig.2a,2a, b). In LF-fed mice of both genotypes, male mice had greater fat mass and less lean mass (as a percentage of body weight) compared to female mice (Fig. (Fig.2c,2c, d; $p < 0.001$). In HF-fed mice of both genotypes, female mice had greater fat mass (as a percentage of body weight) compared to male mice (Fig. (Fig.2d;2d; $p < 0.001$). While HF-feeding increased fat mass in both female and male mice ($p < 0.01$), the percent increase in fat mass was markedly higher in females (313% and 260% increase in Ace2fl/fl and Ace2Adipo, respectively) compared to males (55% and 47% increase in Ace2fl/y and Ace2Adipo, respectively), with no differences between genotypes. Lean mass percentage of body weight decreased in both female and male mice with HF-feeding (Fig. (Fig.2c;2c; $p < 0.01$). Within genotypes, lean mass was greater in HF-fed male Ace2fl/y ($p < 0.01$) but not Ace2Adipo male mice compared to female counterparts (Fig. (Fig.22c).

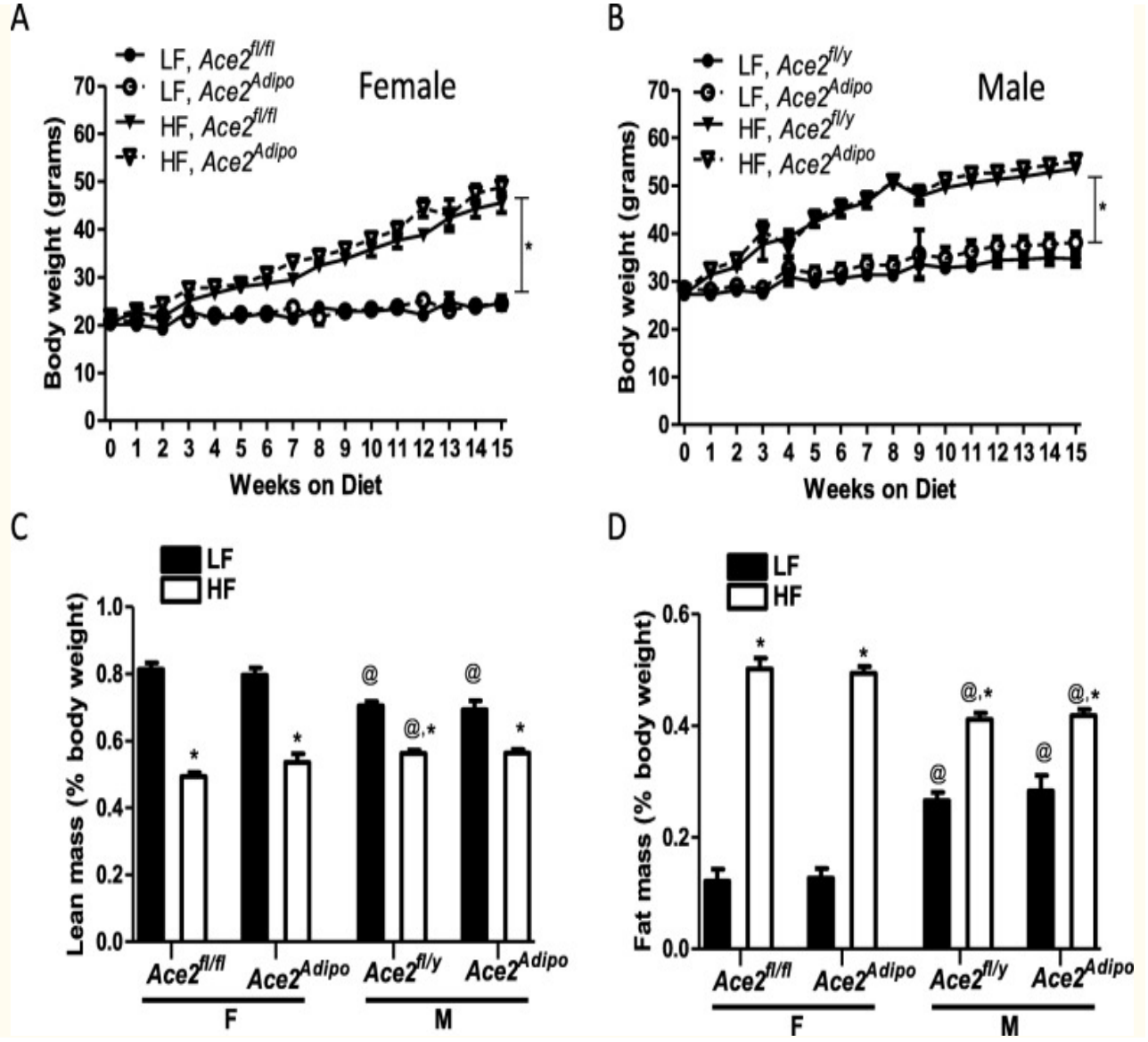

Fig. 2

Deficiency of ACE2 in adipocytes has no effect on the development of obesity in male or female mice. Body weights (weekly) of female Ace2fl/fl (**a**) or male Ace2fl/y (**b**) and Ace2Adipo mice fed a low fat (LF) or high fat (HF) diet. Lean mass (**c**) and fat mass (**d**) (as % body weight) of female or male mice from each genotype fed the LF or HF diet. Data are mean + SEM from n = 6–13 mice/genotype/diet. *p < 0.05 compared to LF within sex using two-way ANOVA followed by Holm-Sidak pairwise analysis; @p < 0.01 compared to female within diet group using two-way ANOVA followed by Holm-Sidak pairwise analysis

Ace2 deficiency in adipocytes increases SBP of HF-female mice to the level of wild-type HF-fed male mice

Male Ace2fl/y mice had elevated SBP compared to female Ace2fl/fl controls under both LF- and HF-fed conditions (24 h; Fig. Fig.3a;3a; p < 0.01). Similarly, DBP of LF-fed male Ace2fl/y mice was also higher than LF-fed Ace2fl/fl females (24 h; Fig. Fig.3b;3b; p < 0.001). In response to a HF diet, female Ace2fl/fl mice had increased SBP and DBP compared to LF-fed Ace2fl/fl female mice (Fig. (Fig.3a,3a, b; p < 0.001). Male HF-fed Ace2fl/y mice exhibited an increase in SBP, but not DBP, compared to male LF-fed Ace2fl/y controls (Fig. (Fig.3a,3a, b; p < 0.01).

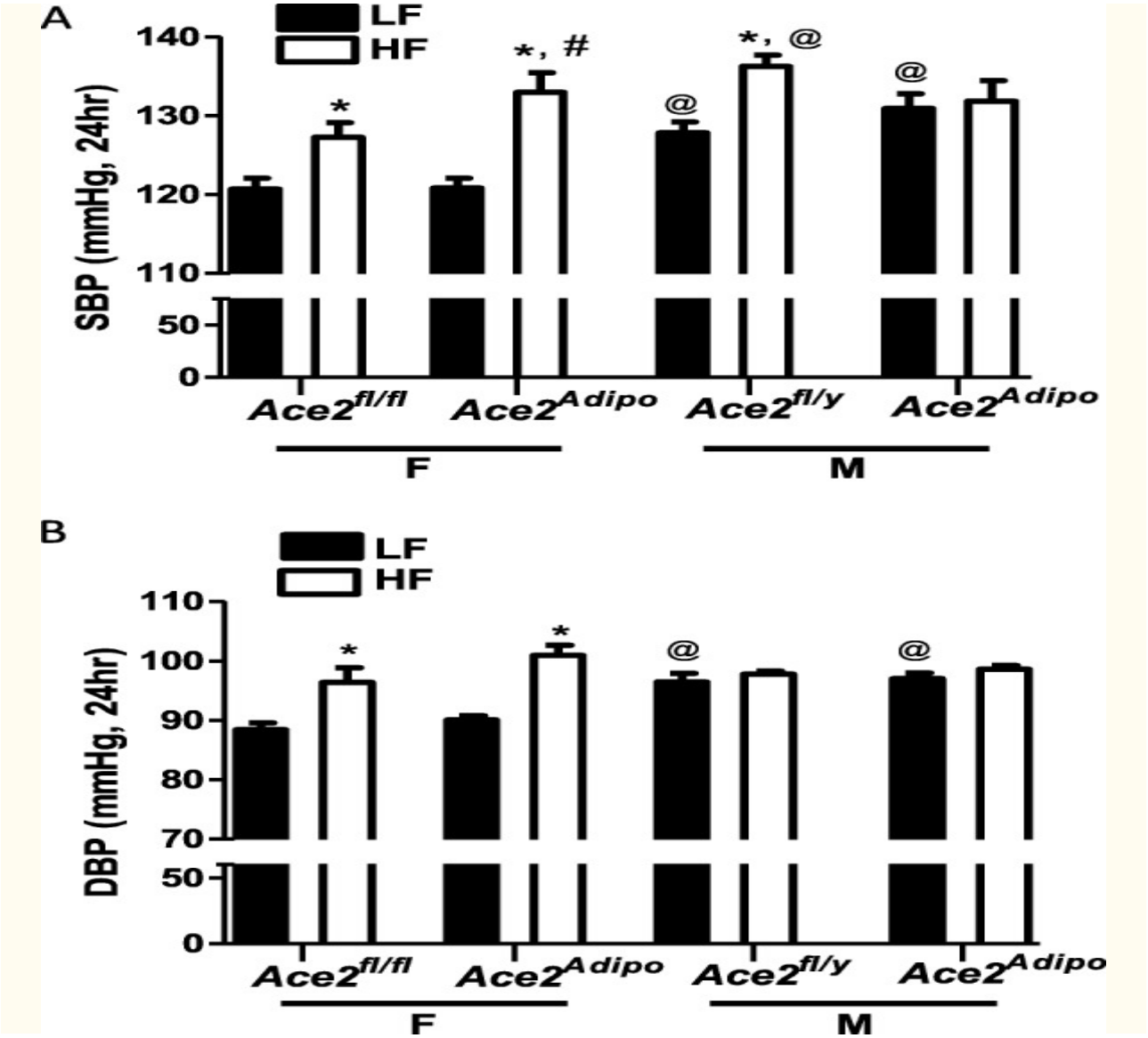

Open in a separate window

Fig. 3

ACE2 deficiency in adipocytes increases blood pressures of obese female, but not obese male mice. Systolic blood pressures (SBP, 24-h average) (**a**) of female Ace2fl/fl and male Ace2fl/y and Ace2Adipo mice fed a LF or HF diet for 4 months. Diastolic blood pressures (DBP) (**b**) of female and male mice of each genotype fed the LF or HF diet for 4 months. Data are mean + SEM from 4–5 mice/genotype/diet. *$p < 0.01$ compared to LF within sex using two-way ANOVA followed by Holm-Sidak pairwise analysis; #$p < 0.05$ compared to Ace2fl/fl within sex group using two-way ANOVA followed by Holm-Sidak pairwise analysis; @$p < 0.01$ compared to female within diet group using two-way ANOVA followed by Holm-Sidak pairwise analysis

Under LF feeding, male Ace2Adipo mice had elevated SBP and DBP compared to LF-fed female Ace2Adipo mice (Fig. (Fig.3a,3a, b; $p < 0.001$). In response to the HF diet, female Ace2Adipo mice exhibited an increase in SBP and DBP compared to LF-fed Ace2Adipo females (Fig. (Fig.3a,3a, b; $p < 0.01$). Moreover, SBP of HF-fed female Ace2Adipo mice were elevated significantly compared to HF-fed Ace2fl/fl females (Fig. (Fig.3a;3a; $p <$

0.05). In contrast, there was no effect of HF diet on SBP or DBP in Ace2Adipo male mice (Fig. (Fig.3a,3a, b; $p > 0.05$). Moreover, deficiency of ACE2 in adipocytes of HF-fed females resulted in blood pressure levels (SBP and DBP) that were similar to those of HF-fed Ace2fl/y male mice.

Female LF-fed mice, regardless of genotype, had significantly more physical activity than LF-fed males (Tables (Tables1;1 and and2;2; 24 h, $p < 0.01$). HF-feeding resulted in a significant reduction in physical activity in females of each genotype (Table (Table1;1; $p < 0.05$). In contrast, there was no significant effect of HF-feeding on physical activity of male mice of either genotype (Table (Table2;2; $p > 0.05$). Heart rates of female mice were higher than males regardless of diet or genotype (Tables (Tables1;1 and and2;2; $p < 0.05$). Moreover, HF feeding resulted in a significant increase in heart rate for each sex and genotype (Tables (Tables1;1 and and2;2; $p < 0.05$).

Table 1

Telemetry parameters of female mice

	Ace2 fl/fl		*Ace2* Adipo	
	LF	**HF**	**LF**	**HF**
24 h				
MAP (mmHg)	105.3 ± 1.1	112.4 ± 2.1*	106.1 ± 0.7	117.7 ± 2.1, #
Heart rate (bpm)	584 ± 8	617 ± 9*	563 ± 4#	622 ± 7*
Activity (counts/min)	12.8 ± 1.4	6.5 ± 0.6*	9.9 ± 1.5	6.4 ± 0.8*
PP (mmHg)	32.2 ± 1.2	30.8 ± 1.4	30.7 ± 1.5	32.0 ± 1.5
Light				
SBP (mmHg)	115.3 ± 1.1	122.3 ± 1.9*	114.9 ± 1.3	127.8 ± 2.5*
DBP (mmHg)	84.5 ± 0.8	92.7 ± 2.4*	85.2 ± 1.3	97.1 ± 1.0*
MAP (mmHg)	100.7 ± 0.7	100.8 ± 2.0*	100.8 ± 1.2	113.3 ± 2.1*, #
Heart rate (bpm)	576.6 ± 8.2	606.8 ± 9.3*	549.0 ± 4.5	610.8 ± 9.5*
Activity (counts/min)	7.1 ± 1.0	4.9 ± 0.4*	5.8 ± 0.7	4.3 ± 0.7
PP (mmHg)	30.8 ± 1.2	29.6 ± 1.3	29.7 ± 1.3	30.6 ± 1.3
Dark				
SBP (mmHg)	128.3 ± 0.4	134.3 ± 1.9	129.0 ± 1.7	139.7 ± 2.4*
DBP (mmHg)	94.0 ± 1.6	101.4 ± 2.8*	96.7 ± 0.6	105.3 ± 1.7*
MAP (mmHg)	111.8 ± 1.6	118.5 ± 2.2*	113.5 ± 0.9	123.6 ± 2.0*
Heart rate (bpm)	596.4 ± 8.1	634.0 ± 8.4*	578.9 ± 6.8	635.0 ± 7.0*
Activity (counts/min)	20.0 ± 1.8	8.9 ± 0.8*	15.1 ± 2.5	9.4 ± 1.2*
PP (mmHg)	34.4 ± 1.3	32.9 ± 1.5	32.2 ± 1.7	33.8 ± 1.4

PP pulse pressure, SBP systolic blood pressure, DBP diastolic blood pressure, MAP mean arterial pressure

Data are mean ± SEM (n = 4–5 mice/diet/genotype)

* $p < 0.05$ compared to LF within genotype following pairwise statistical analysis

# $p < 0.05$ compared to Ace2fl/fl within the diet group following pairwise statistical analysis

Table 2

Telemetry parameters of male mice

	Ace2 fl/y		*Ace2* Adipo	
	LF	**HF**	**LF**	**HF**
24 h				
MAP (mmHg)	112.5 ± 0.8	117.7 ± 0.7*	114.1 ± 0.9	115.3 ± 1.2
Heart rate (bpm)	556.7 ± 6.7	582.2 ± 7.5*	559.7 ± 6.5	581.1 ± 14.2*
Activity (counts/min)	5.9 ± 0.7	5.0 ± 0.5	5.6 ± 0.8	5.5 ± 0.7
PP (mmHg)	31.3 ± 2.1	38.2 ± 1.0	33.8 ± 2.0	33.18 ± 2.8
Light				
SBP (mmHg)	120.9 ± 1.3	130.0 ± 1.6*	123.88 ± 1.6	128.8 ± 2.5

	Ace2 fl/y		*Ace2* Adipo	
	LF	**HF**	**LF**	**HF**
DBP (mmHg)	91.6 ± 0.6	93.3 ± 1.1	91.9 ± 1.2	94.6 ± 1.6
MAP (mmHg)	106.3 ± 0.4	112.2 ± 1.2*	108.1 ± 0.8	110.9 ± 1.5
Heart rate (bpm)	524.3 ± 5.2	555.3 ± 10.1*	534.6 ± 11.1	561.4 ± 13.0
Activity (counts/min)	3.0 ± 0.3	3.3 ± 0.5	3.0 ± 0.4	3.5 ± 0.2
PP (mmHg)	29.2 ± 1.9	35.6 ± 0.8	31.9 ± 1.9	32.3 ± 2.5
Dark				
SBP (mmHg)	139.0 ± 1.3	142.1 ± 2.3	140.5 ± 2.5	134.5 ± 3.7
DBP (mmHg)	105.3 ± 2.1	104.3 ± 1.2	104.1 ± 1.0	102.5 ± 1.6
MAP (mmHg)	122.3 ± 1.3	125.4 ± 1.7	122.4 ± 1.4	120.4 ± 2.2
Heart rate (bpm)	598.6 ± 10.6	621.3 ± 7.7	595.3 ± 3.7	614.9 ± 15.0
Activity (counts/min)	10.8 ± 1.1	7.3 ± 0.7	9.2 ± 1.4	7.4 ± 1.7
PP (mmHg)	33.7 ± 2.5	40.9 ± 1.4	36.4 ± 2.2	35.1 ± 3.0

PP pulse pressure, SBP systolic blood pressure, DBP diastolic blood pressure, MAP mean arterial pressure

Data are mean ± SEM (n = 4–5 mice/diet/genotype)

* $p < 0.05$ compared to LF within genotype following pairwise statistical analysis

# $p < 0.05$ compared to Ace2fl/y within the diet group following pairwise statistical analysis

SBP response to acute AngII challenge is augmented in obese female mice with adipocyte-ACE2 deficiency

Previous studies demonstrated that adipocyte-derived AngII contributes to increased SBP of HF-fed male mice [7]. AngII is a substrate for ACE2. Therefore, we challenged HF-fed Ace2fl/fl and Ace2Adipo male and female mice with a single dose of the ACE2 substrate, AngII (20 µg/kg body weight, subcutaneous) and quantified blood pressure. In male and female mice of each genotype, SBP was increased by administration of AngII, with a rapid peak blood pressure effect within 2 minutes of AngII administration; Fig. Fig.4a,4a, b). Female HF-fed Ace2Adipo mice exhibited an increased maximal blood pressure response to AngII (Fig. (Fig.4a;4a; $p < 0.05$) that was extended in duration compared to HF-fed Ace2fl/fl females, as evidenced by an increased AUC (blood pressure response above baseline through 60 min; Fig. Fig.4c;4c; $p < 0.05$). In contrast, there was no significant effect of adipocyte ACE2 deficiency on the maximal response or duration of the blood pressure response to AngII between HF-fed male Ace2fl/y and Ace2Adipo mice (Fig. (Fig.4b,4b, d).

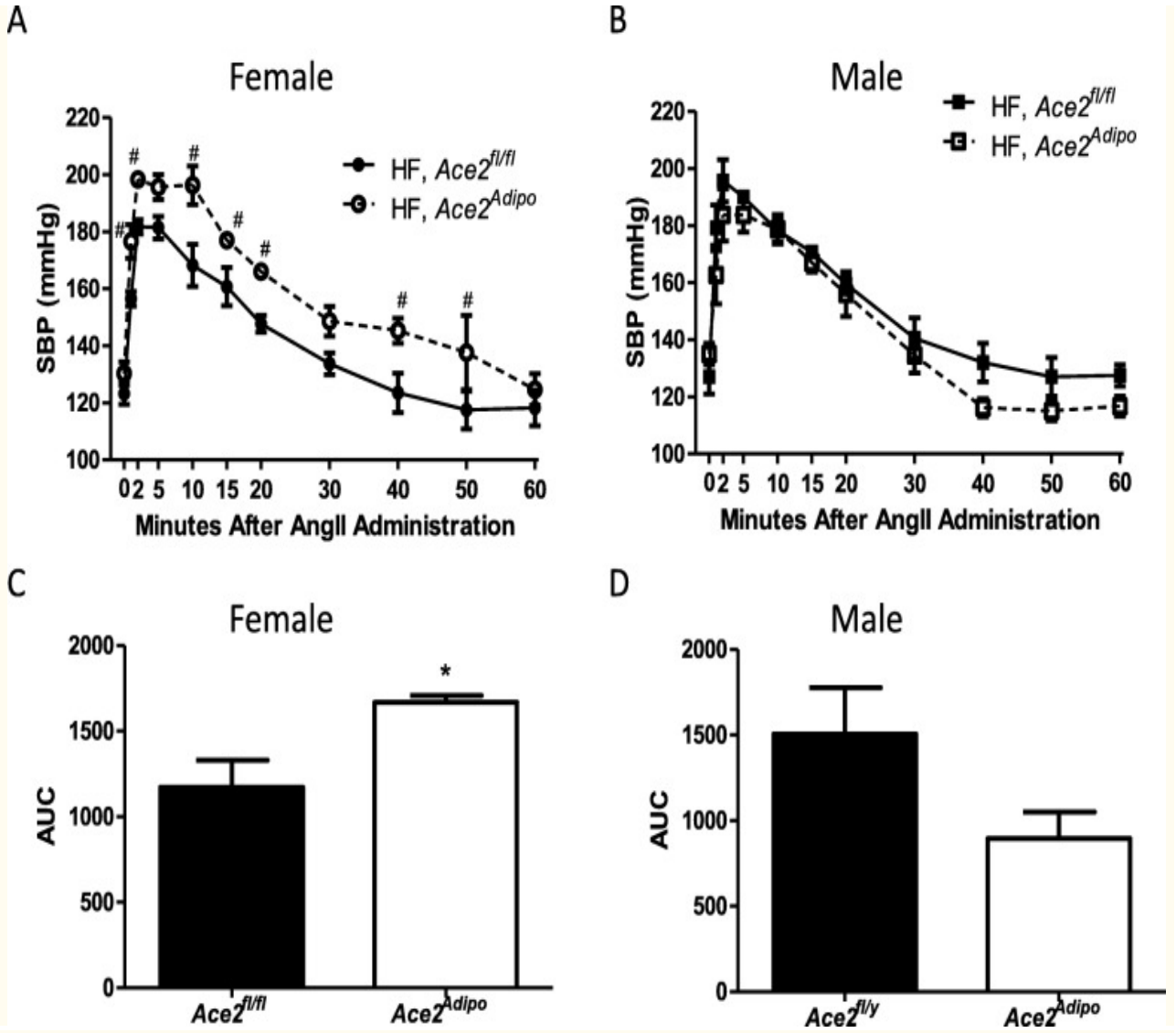

Fig. 4

Systolic blood pressure (SBP) response to acute AngII challenge is augmented in obese female, but not obese male mice with adipocyte-ACE2 deficiency. At 4 months of HF feeding, the time course of SBP following an acute injection (sc) of AngII (20 μg/kg) to female Ace2fl/fl (**a**) or male Ace2fl/y (**b**) and Ace2Adipo mice. Data are reported as the average blood pressure per minute at each time point. Integrated area under the curve (AUC) corresponding to the time course of SBP response to AngII for HF-fed female Ace2fl/fl (**c**) or HF-fed male Ace2fl/y (**d**) and Ace2Adipo mice. Data are mean + SEM for n = 4 mice/genotype. #$p < 0.05$ compared to Ace2fl/fl at each time point using repeated measures (RM) two-way ANOVA; *$p < 0.05$ compared to Ace2fl/fl using t test

In obese transwomen administered 17β-estradiol, increased plasma Ang-(1-7)/AngII balance is inversely correlated with changes in SBP

We sought to translate findings from experimental mice to humans and therefore examined effects of 12 weeks of estradiol therapy on plasma Ang-(1-7)/AngII balance and SBP in obese transwomen initiating gender-affirming hormone therapy (n = 4 subjects). Body mass index (BMI), as an index of obesity, was not significantly influenced by estradiol administration (Table (Table3;3; $p > 0.05$). As anticipated, plasma concentrations of estradiol were increased significantly with estradiol treatment compared to baseline estradiol concentrations (Fig. (Fig.5a;5a; $p < 0.05$), although estradiol levels in one subject did not reach the target estradiol levels for gender-affirming hormone therapy (81.3 pg/mL vs target range of 90–200 pg/mL). Plasma concentrations of individual components of the RAS (angiotensinogen, renin, AngII, Ang-(1-7)) were not significantly influenced by estradiol administration compared to baseline values (Table (Table3;3; $p > 0.05$). The ratio of plasma concentrations of Ang-(1-7) to AngII, a surrogate for ACE2 activity, was increased 2.57-fold with estradiol compared to baseline, but this effect was not statistically significant (Table (Table3;3; $p = 0.19$). Moreover, after 12 weeks of estradiol administration, the balance of Ang-(1-7)/AngII in plasma correlated positively to plasma estradiol concentrations, although the correlation was not statistically significant (Fig. (Fig.5b;5b; $r2 = 0.746$; $p = 0.136$). In addition, after 12 weeks of estradiol administration, the increase in plasma Ang-(1-7)/AngII balance correlated significantly to reductions of SBP (Fig. (Fig.5c;5c; $r2 = 0.967$; $p = 0.016$).

Table 3

Characteristics of obese, transgendered women at baseline, and 12 weeks following oral estradiol therapy.

Parameter	Baseline	12 weeks of estradiol
BMI (m/kg2)	37.5 ± 3.4	38.1 ± 3.4
Plasma renin activity (ng/mL*h)	0.85 ± 0.25	0.76 ± 0.25
Plasma angiotensinogen (μg/mL)	17.0 ± 3.9	20.8 ± 5.0
Plasma AngII (pg/mL)	42.3 ± 9.0	40.8 ± 14.6
Plasma Ang-(1-7) (ng/mL)	0.36 ± 0.05	0.42 ± 0.02
Ratio of Ang-(1-7)/AngII (pg/mL)	5.53 ± 1.74	14.13 ± 3.73

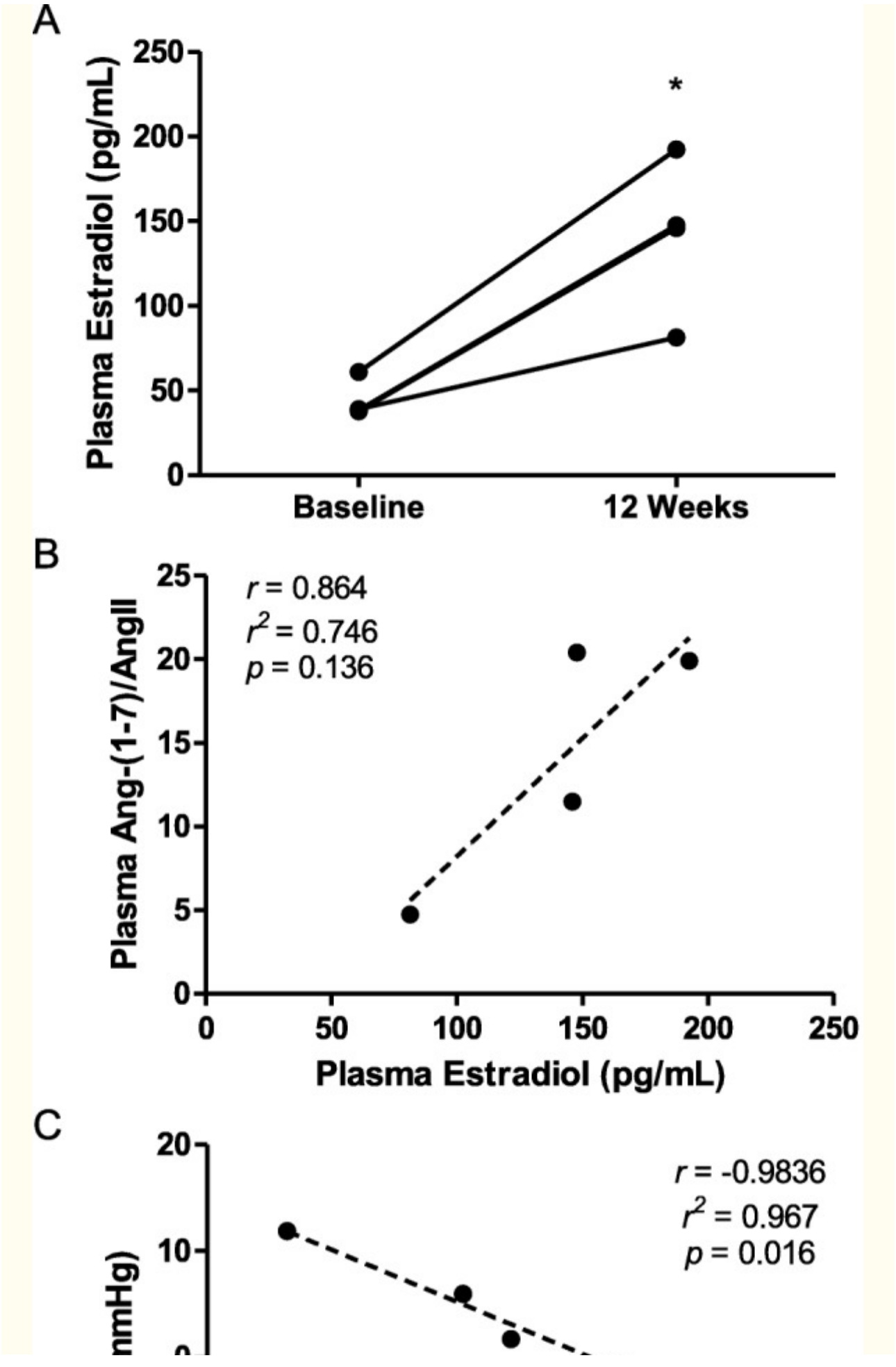
A
250
200
150
100
50
0
Plasma Estradiol (pg/mL)
*
Baseline
12 Weeks
B
25
20
15
10
5
0
Plasma Ang-(1-7)/AngII
r = 0.864
r2 = 0.746
p = 0.136
0
50
100
150
200
250
Plasma Estradiol (pg/mL)
C
20
10
mmHg)
r = -0.9836
r2 = 0.967
p = 0.016

Open in a separate window

Fig. 5

Administration of 17β-estradiol to obese transwomen initiating gender-affirming hormone therapy increases plasma concentrations of 17β-estradiol, which correlates positively to plasma Ang-(1-7)/AngII balance and negatively to systolic blood pressures (SBP). **a** Plasma 17β-estradiol concentrations before (baseline) and after administration of 17β-estradiol to obese transwomen for 12 weeks. **b** Scatterplot showing the correlation between the ratio of Ang-(1-7) to AngII concentrations in plasma to plasma 17β-estradiol concentrations after 12 weeks of 17β-estradiol administration. **c** Scatterplot showing correlation between change in SBP and the ratio of Ang-(1-7) to AngII in plasma following 12 weeks 17β-estradiol administration. N = 4 subjects. *p < 0.05 compared to baseline

Go to:

Discussion

This study investigated the role of adipocyte ACE2 in the differential regulation of blood pressure in female versus male mice with diet-induced obesity. We translated these experimental findings to humans by studying the effects of estradiol therapy in transwomen on the plasma Ang-(1-7)/AngII balance and blood pressure. The major findings of these studies are (1) deficiency of ACE2 in adipocytes increased SBP in obese female, but not male mice, (2) obese female, but not male mice with adipocyte ACE2 deficiency exhibit an augmented blood pressure response to the ACE2 substrate, AngII, (3) administration of estradiol as part of gender-affirming hormone therapy in a small, proof-of-principle study led to higher plasma Ang-(1-7)/AngII balance, which correlates inversely to change in systolic blood pressure in obese transwomen. These data demonstrate a role for adipocyte ACE2 in protection of female mice from obesity-hypertension. Moreover, since the human study demonstrated a correlation between serum estradiol concentrations and the systemic Ang-(1-7)/AngII balance and blood pressure, these results suggest that positive regulation of ACE2 by estrogen may serve as a potential protective mechanism against obesity-hypertension in females.

Obesity is a prominent risk factor for the development of hypertension. Despite the increased prevalence of obesity in women versus men, premenopausal women have a lower prevalence of hypertension, suggesting that the blood pressure-elevating effects of obesity are lower in women. Polymorphisms of ACE2 have been linked to essential hypertension in females [15]. A recent study demonstrated that systemic ACE2 activity levels were negatively correlated with BMI and blood pressure in female essential hypertension patients [16]. Previous studies from our laboratory demonstrated that plasma Ang-(1-7) concentrations were higher in obese normotensive female mice than obese hypertensive male mice and were associated with increased adipose tissue expression and activity of ACE2. In contrast, ACE2 expression and activity in the kidney, a site with considerable expression of the Ang-(1-7) peptide-forming enzyme, were not altered in obese male or obese female mice compared to lean controls.

Whole-body deficiency of ACE2 increased blood pressure in obese male mice and converted female obese mice to a hypertensive phenotype [11]. Moreover, obese hypertensive ACE2 deficient females exhibited reductions in plasma concentrations of Ang-(1-7) [11]. However, the cell type responsible for effects of whole-body ACE2 deficiency to promote obesity-hypertension in both sexes was not identified. Findings from the present study extend previous results by demonstrating that adipocyte ACE2 contributes to protection from obesity-hypertension in females, but not in obese males. Since previous findings demonstrated that whole body deficiency of ACE2 increased SBP in both obese female and male mice [11], these results suggest that effects of ACE2 deficiency to promote obesity-hypertension in males were not adipocyte-mediated. In contrast, our results suggest that in obese females, adipocytes are the predominant source of ACE2 for the development of obesity-hypertension.

We demonstrated previously that 17β-estradiol promoted ACE2 mRNA expression in 3T3-L1 adipocytes by eliciting ERα-binding to the ACE2 promoter [12]. Further, administration of 17β-estradiol to obese ovariectomized female mice reduced blood pressure and stimulated ACE2 activity and mRNA abundance in adipose tissue, while having no effect on blood pressures of obese ACE2-null females [12]. In this study, deletion of ACE2 in adipocytes increased blood pressures of obese female mice, but had no effect on blood pressures of obese male mice. These findings are consistent with published reports of estrogen regulation of the ACE2/Ang-(1-7) axis, which would support a sex-specific effect of adipocyte ACE2. For example, in ovariectomized hypertensive rats, administration of 17β-estradiol reduced blood pressure and promoted the production of Ang-(1-7) [17]. In a renal wrap model of hypertension in female rats, 17β-estradiol administration to ovariectomized female rats with renal wrap hypertension upregulated renal ACE2 expression and activity and reduced renal injury [18]. However, it is possible that testosterone also regulates ACE2 expression, since renal ACE2 activity was demonstrated to be higher in male compared to that in female mice [11, 19]. Moreover, since previous findings demonstrated that ACE2 activity was increased by obesity in adipose tissue of female, but not male mice [11], then these results suggest that obesity per se may introduce sex- and tissue-specific regulation of ACE2. Regardless, results from the present study indicate a primary role for adipocyte ACE2 in the development of obesity-hypertension in females.

An interesting finding of the present study was an augmented response to an acute blood pressure challenge with AngII in female, but not in male obese mice with adipocyte ACE2 deficiency. Since AngII is a substrate of ACE2, then these results suggest that adipocyte ACE2 deficiency either influences the systemic half-life of AngII and the balance of Ang-(1-7)/AngII, or that local conversion of systemic AngII to Ang-(1-7) by adipocyte ACE2 regulates blood pressure. In agreement, previous findings from our laboratory demonstrated that adipocyte expression of angiotensinogen, the precursor to AngII, influences systemic concentrations of AngII and the development of obesity-hypertension in male mice [7]. These results suggest that local expression of components of the RAS can influence systemic levels of these components and the circulating production of angiotensin peptides. In support, the liver was demonstrated as a primary source of renal AngII [20], and hepatic deficiency of angiotensinogen was demonstrated to influence adipose explant production of angiotensinogen in obese male mice [7]. It is unclear from the present study if adipocyte ACE2 influences the systemic half-life of AngII; however, results from this study demonstrate that adipocyte ACE2 regulates the blood pressure response to an acute systemic AngII challenge.

In normotensive humans, blood pressure is higher in males than in females [21]. This finding is consistent with studies in rodents, where normotensive male rats have higher blood pressures than female rats [22]. Our results extend these and other findings [11] by demonstrating that obese female wild type mice have lower blood pressures than obese males. Blood pressure is thought to be directly related to adiposity [9]. Thus, it is noteworthy that HF-fed females had more adiposity than HF-fed males, but yet had lower blood pressures than obese males. These findings suggest that the more expanded fat mass of HF-fed females results in the potential production of adipocyte-derived factors, such as ACE2, that protect against obesity-hypertension. Alternatively, the presence of estrogens in obese females augments the production of protective factors, such as adipocyte ACE2, to blunt the development of obesity-hypertension. Additional vasoprotective effects of estrogen include induction of nitric oxide to promote vasodilation [23] and blunting of vasoconstrictor effects mediated by the sympathetic nervous system [24]. Even with obesity, estrogen may have positive metabolic effects such as increased energy expenditure, regulation of food intake, and inhibition of adipogenesis [25]. Thus, declining estrogen levels resulting in both increasing body weight and loss of vascular protection may contribute to the rise in hypertension post-menopause.

To translate these findings from mice to humans, we performed a proof-of-principle study in obese transwomen initiating gender-affirming hormone therapy with 17β-estradiol. Approximately 1.4 million persons in the USA, or 0.6% of adults, identify as transgender [26, 27]. Unfortunately, the cardiovascular health of transgender persons taking cross-sex hormone therapies long-term is largely unknown. In this study, we focused on obese transgender women before and after initiation of 17β-estradiol administration for 3 months as part of standard transgender therapy. Notably, participation in this study required delaying the use of spironolactone for 12 weeks, which limited participation. Previous studies found that in 21 transgender women taking 17β-estradiol (2–6 mg/day) for 5 years, plasma estradiol levels rose from 108 to 237 pmol/L, and systolic blood pressure decreased from 119 to 112 mmHg [28]. We recently demonstrated a negative correlation between BMI and estradiol dose needed to achieve target estradiol levels of 90–200 pg/mL [29], likely due to higher estradiol levels found in obese males from aromatization of androgens to estrogens in adipose tissue [30–32]. In agreement, results from this study demonstrate mean plasma17-β estradiol concentrations reached the target estradiol levels despite use of a fairly low dose of 17β-estradiol (1–2 mg/day) in obese transwomen. In the current study, we report 12 weeks of estradiol therapy had no significant effect to modulate individual components of the RAS, which is at odds with published literature reporting significant systemic alterations of the RAS by estradiol [33]. However, studies of estrogen's influence on the RAS in humans are largely based on hormonal changes throughout the menstrual cycle [34], during pregnancy [35], or with estrogen-replacement therapy [36] in cisgender women. To our knowledge, these are the first studies examining effects of 17β-estradiol administration to obese transwomen on indices of the systemic RAS. Moreover, our results extend previous findings by demonstrating an association between 17β-estradiol levels, plasma Ang-(1-7)/AngII balance, and systolic blood pressures of transwomen.

There are several limitations to the clinical study. First, there were challenges in recruitment due to participation requiring a delay in use of spironolactone therapy for its anti-androgenic effects. Second, we do not have measures of testosterone levels in these transwomen; testosterone was not measured as the literature reports inconsistent effects of estradiol on testosterone levels [37, 38], and there is no evidence that testosterone levels affect desired body changes of gender-affirming

hormone therapy. Third, these measures were drawn only once after only 12 weeks of therapy, and although mean plasma 17β-estradiol levels achieved the target of 90–200 pg/mL, not all subjects achieved a plasma 17β-estradiol level in the target range on their initial prescribed dose of estradiol. Further changes in the RAS may occur over more prolonged therapy. Finally, we were unable to determine if adipose ACE2 contributes to the observed associations between systemic 17β-estradiol concentrations, plasma Ang-(1-7)/AngII balance, and blood pressure. However, taken together, the murine and clinical data support estrogen regulation of ACE2 as a contributor to blood pressure regulation in the development of obesity-hypertension.

Go to:

Conclusions

In conclusion, these results demonstrate that deficiency of ACE2 in adipocytes augments the development of hypertension and the pressor response to AngII in obese female, but not obese male mice. These results suggest that adipocyte ACE2 protects female mice from the development of obesity-hypertension. Moreover, translation of these findings to obese transwomen demonstrates a negative association among plasma Ang-(1-7)/AngII balance and systolic blood pressure with increased plasma 17β-estradiol concentrations. Taken together, these results suggest that adipocyte-derived ACE2 regulates the balance of vasodilator (Ang-(1-7) to vasoconstrictor (AngII) angiotensin peptides and contributes to sex differences in obesity-hypertension.

Go to:

Additional file

Additional file 1:(922K, pptx)

Figure S1. Positive β-galactosidase staining in adipose tissue of mice with adipocyte deficiency of ACE2. (PPTX 922 kb)

Go to:

Acknowledgements

The authors wish to acknowledge the excellent technical assistance from Victoria English in breeding the colony of adipocyte ACE2 deficient mice, and Joel Thompson for recruitment of transwomen patients.

Go to:

Authors' contributions

RS contributed to animal care, sample collection, and data and statistical analysis. RS, CME, and SET contributed to sample analysis. WS and MG contributed to telemetry surgery and interpretation of blood pressure data, respectively. FY and SBG facilitated the development of mouse model. LT contributed to clinical data collection. RS, LT, and LC provided interpretation of findings. RS and LC wrote the manuscript. All authors read and approved the final manuscript.

Go to:

Funding

This research was supported by the National Institutes of Health Heart Lung and Blood Institute (HL073085, LC), from a postdoctoral fellowship from the American Heart Association (17POST33410015, RS), through cores supported by the National Institutes of Health General Medical Sciences (P30GM127211, LC), and the Alaska Kidney Foundation – ASN Research Grant (SBG).

Go to:

Availability of data and materials

The datasets used and/or analyzed during the current study are available from the corresponding author on reasonable request.

Go to:

Ethics approval and consent to participate

These studies were approved by the Institutional Review Board of the University of Kentucky.

Go to:

Consent for publication

We have obtained consent from all authors of this publication.

Go to:

Competing interests

The authors decalare that they have no competing interests.

Go to:

Footnotes

Publisher's Note

Go to:

References

1. Wilson PW, D'Agostino RB, Sullivan L, Parise H, Kannel WB. Overweight and obesity as determinants of cardiovascular risk: the Framingham experience. Arch Intern Med. 2002;162(16):1867–1872. doi: 10.1001/archinte.162.16.1867. [PubMed] [CrossRef] [Google Scholar]

2. Benjamin EJ, Blaha MJ, Chiuve SE, Cushman M, Das SR, Deo R, et al. Heart disease and stroke statistics-2017 update: a report from the American Heart Association. Circulation. 2017;135(10):e146–e603. doi: 10.1161/CIR.0000000000000485. [PMC free article] [PubMed] [CrossRef] [Google Scholar]

3. Jackson AS, Stanforth PR, Gagnon J, Rankinen T, Leon AS, Rao DC, et al. The effect of sex, age and race on estimating percentage body fat from body mass index: the heritage family study. Int J Obes Relat Metab Disord. 2002;26(6):789–796. doi: 10.1038/sj.ijo.0802006. [PubMed] [CrossRef] [Google Scholar]

4. Hales CM, Carroll MD, Fryar CD, Ogden CL. Prevalence of obesity among adults and youth: United States, 2015-2016. NCHS Data Brief. 2017;288:1–8. [PubMed] [Google Scholar]

5. Fryar CD, Ostchega Y, Hales CM, Zhang G, Kruszon-Moran D. Hypertension prevalence and control among adults: United States, 2015-2016. NCHS Data Brief. 2017;289:1–8. [PubMed] [Google Scholar]

6. Boustany CM, Bharadwaj K, Daugherty A, Brown DR, Randall DC, Cassis LA. Activation of the systemic and adipose renin-angiotensin system in rats with diet-induced obesity and hypertension. Am J Physiol Regul Integr Comp Physiol. 2004;287(4):R943–R949. doi: 10.1152/ajpregu.00265.2004. [PubMed] [CrossRef] [Google Scholar]

7. Yiannikouris F, Gupte M, Putnam K, Thatcher S, Charnigo R, Rateri DL, et al. Adipocyte deficiency of angiotensinogen prevents obesity-induced hypertension in male mice. Hypertension. 2012;60(6):1524–1530. doi: 10.1161/HYPERTENSIONAHA.112.192690. [PMC free article] [PubMed] [CrossRef] [Google Scholar]

8. Engeli S, Bohnke J, Gorzelniak K, Janke J, Schling P, Bader M, et al. Weight loss and the renin-angiotensin-aldosterone system. Hypertension. 2005;45(3):356–362. doi: 10.1161/01.HYP.0000154361.47683.d3. [PubMed] [CrossRef] [Google Scholar]

9. Landsberg L, Aronne LJ, Beilin LJ, Burke V, Igel LI, Lloyd-Jones D, et al. Obesity-related hypertension: pathogenesis, cardiovascular risk, and treatment—a position paper of the The Obesity Society and The American Society of Hypertension. Obesity (Silver Spring). 2013;21(1):8–24. doi: 10.1002/oby.20181. [PubMed] [CrossRef] [Google Scholar]

10. Cassis LA, Saye J, Peach MJ. Location and regulation of rat angiotensinogen messenger RNA. Hypertension. 1988;11(6):591–6. doi: 10.1161/01.HYP.11.6.591. [PubMed] [CrossRef] [Google Scholar]

11. Gupte M, Thatcher SE, Boustany-Kari CM, Shoemaker R, Yiannikouris F, Zhang X, et al. Angiotensin converting enzyme 2 contributes to sex differences in the development of obesity hypertension in C57bl/6 Mice. Arterioscler Thromb Vasc Biol. 2012;32(6):1392–1399. doi: 10.1161/ATVBAHA.112.248559. [PMC free article] [PubMed] [CrossRef] [Google Scholar]

12. Wang Y, Shoemaker R, Thatcher SE, Batifoulier-Yiannikouris F, English VL, Cassis LA. Administration of 17beta-estradiol to ovariectomized obese female mice reverses obesity-hypertension through an ACE2-dependent mechanism. Am J Physiol Endocrinol Metab. 2015;308(12):E1066–E1075. doi: 10.1152/ajpendo.00030.2015. [PMC free article] [PubMed] [CrossRef] [Google Scholar]

13. Yiannikouris F, Karounos M, Charnigo R, English VL, Rateri DL, Daugherty A, et al. Adipocyte-specific deficiency of angiotensinogen decreases plasma angiotensinogen concentration and systolic blood pressure in mice. Am J Physiol Regul Integr Comp Physiol. 2012;302(2):R244–R251. doi: 10.1152/ajpregu.00323.2011. [PMC free article] [PubMed] [CrossRef] [Google Scholar]

14. Gupte M, Boustany-Kari CM, Bharadwaj K, Police S, Thatcher S, Gong MC, et al. ACE2 is expressed in mouse adipocytes and regulated by a high-fat diet. Am J Physiol Regul Integr Comp Physiol. 2008;295(3):R781–R788. doi: 10.1152/ajpregu.00183.2008. [PMC free article] [PubMed] [CrossRef] [Google Scholar]

15. Lu N, Yang Y, Wang Y, Liu Y, Fu G, Chen D, et al. ACE2 gene polymorphism and essential hypertension: an updated meta-analysis involving 11,051 subjects. Mol Biol Rep. 2012;39(6):6581–6589. doi: 10.1007/s11033-012-1487-1. [PubMed] [CrossRef] [Google Scholar]

16. Zhang Q, Cong M, Wang N, Li X, Zhang H, Zhang K, et al. Association of angiotensin-converting enzyme 2 gene polymorphism and enzymatic activity with essential hypertension in different gender: a case-control study. Medicine (Baltimore). 2018;97(42):e12917. doi: 10.1097/MD.0000000000012917. [PMC free article] [PubMed] [CrossRef] [Google Scholar]

17. Brosnihan KB, Li P, Ganten D, Ferrario CM. Estrogen protects transgenic hypertensive rats by shifting the vasoconstrictor-vasodilator balance of RAS. Am J Physiol. 1997;273(6):R1908–R1915. doi: 10.1152/ajpcell.1997.273.6.C1908. [PubMed] [CrossRef] [Google Scholar]

18. Ji H, Menini S, Zheng W, Pesce C, Wu X, Sandberg K. Role of angiotensin-converting enzyme 2 and angiotensin(1-7) in 17beta-oestradiol regulation of renal pathology in renal wrap hypertension in rats. Exp Physiol. 2008;93(5):648–657. doi: 10.1113/expphysiol.2007.041392. [PubMed] [CrossRef] [Google Scholar]

19. Liu J, Ji H, Zheng W, Wu X, Zhu JJ, Arnold AP, et al. Sex differences in renal angiotensin converting enzyme 2 (ACE2) activity are 17beta-oestradiol-dependent and sex chromosome-independent. Biol Sex Differ. 2010;1(1):6. doi: 10.1186/2042-6410-1-6. [PMC free article] [PubMed] [CrossRef] [Google Scholar]

20. Matsusaka T, Niimura F, Shimizu A, Pastan I, Saito A, Kobori H, et al. Liver angiotensinogen is the primary source of renal angiotensin II. J Am Soc Nephrol. 2012;23(7):1181–1189. doi: 10.1681/ASN.2011121159. [PMC free article] [PubMed] [CrossRef] [Google Scholar]

21. Wiinberg N, Hoegholm A, Christensen HR, Bang LE, Mikkelsen KL, Nielsen PE, et al. 24-h ambulatory blood pressure in 352 normal Danish subjects, related to age and gender. Am J Hypertens. 1995;8(10 Pt 1):978–986. doi: 10.1016/0895-7061(95)00216-2. [PubMed] [CrossRef] [Google Scholar]

22. Sartori-Valinotti JC, Iliescu R, Yanes LL, Dorsett-Martin W, Reckelhoff JF. Sex differences in the pressor response to angiotensin II when the endogenous renin-angiotensin system is blocked. Hypertension. 2008;51(4):1170–1176. doi: 10.1161/HYPERTENSIONAHA.107.106922. [PubMed] [CrossRef] [Google Scholar]

23. Florian M, Lu Y, Angle M, Magder S. Estrogen induced changes in Akt-dependent activation of endothelial nitric oxide synthase and vasodilation. Steroids. 2004;69(10):637–645. doi: 10.1016/j.steroids.2004.05.016. [PubMed] [CrossRef] [Google Scholar]

24. Hart EC, Charkoudian N, Miller VM. Sex, hormones and neuroeffector mechanisms. Acta Physiol (Oxf). 2011;203(1):155–165. doi: 10.1111/j.1748-1716.2010.02192.x. [PMC free article] [PubMed] [CrossRef] [Google Scholar]

25. Mauvais-Jarvis F, Clegg DJ, Hevener AL. The role of estrogens in control of energy balance and glucose homeostasis. Endocr Rev. 2013;34(3):309–338. doi: 10.1210/er.2012-1055. [PMC free article] [PubMed] [CrossRef] [Google Scholar]

26. Reisner SL, Deutsch MB, Bhasin S, Bockting W, Brown GR, Feldman J, et al. Advancing methods for US transgender health research. Curr Opin Endocrinol Diabetes Obes. 2016;23(2):198–

207. doi: 10.1097/MED.0000000000000229. [PMC free article] [PubMed] [CrossRef] [Google Scholar]

27. Flores AR, Herman J, Gates GJ, Brown TNT. How many adults identify as transgender in the United States? Los Angeles: The Williams Institute, UCLA School of Law; 2016. Williams Institute (University of California Los Angeles. School of Law) [Google Scholar]

28. Vita R, Settineri S, Liotta M, Benvenga S, Trimarchi F. Changes in hormonal and metabolic parameters in transgender subjects on cross-sex hormone therapy: a cohort study. Maturitas. 2018;107:92–96. doi: 10.1016/j.maturitas.2017.10.012. [PubMed] [CrossRef] [Google Scholar]

29. Fernandez JD, Kendjorsky K, Narla A, Villasante-Tezanos AG, Tannock LR. Assessment of gender-affirming hormone therapy requirements. LGBT Health. 2019;6(3):101–106. doi: 10.1089/lgbt.2018.0116. [PMC free article] [PubMed] [CrossRef] [Google Scholar]

30. Davidson LM, Millar K, Jones C, Fatum M, Coward K. Deleterious effects of obesity upon the hormonal and molecular mechanisms controlling spermatogenesis and male fertility. Hum Fertil (Camb). 2015;18(3):184–193. doi: 10.3109/14647273.2015.1070438. [PubMed] [CrossRef] [Google Scholar]

31. Escobar-Morreale HF, Santacruz E, Luque-Ramirez M, Botella Carretero JI. Prevalence of 'obesity-associated gonadal dysfunction' in severely obese men and women and its resolution after bariatric surgery: a systematic review and meta-analysis. Hum Reprod Update. 2017;23(4):390–408. doi: 10.1093/humupd/dmx012. [PubMed] [CrossRef] [Google Scholar]

32. Xu X, Sun M, Ye J, Luo D, Su X, Zheng D, et al. The effect of aromatase on the reproductive function of obese males. Horm Metab Res. 2017;49(8):572–579. doi: 10.1055/s-0043-107835. [PubMed] [CrossRef] [Google Scholar]

33. Fischer M, Baessler A, Schunkert H. Renin angiotensin system and gender differences in the cardiovascular system. Cardiovasc Res. 2002;53(3):672–677. doi: 10.1016/S0008-6363(01)00479-5. [PubMed] [CrossRef] [Google Scholar]

34. Skinner SL, Lumbers ER, Symonds EM. Alteration by oral contraceptives of normal menstrual changes in plasma renin activity, concentration and substrate. Clin Sci. 1969;36(1):67–76. [PubMed] [Google Scholar]

35. Weinberger MH, Kramer NJ, Grim CE, Petersen LP. The effect of posture and saline loading on plasma renin activity and aldosterone concentration in pregnant, non-pregnant and estrogen-treated women. J Clin Endocrinol Metab. 1977;44(1):69–77. doi: 10.1210/jcem-44-1-69. [PubMed] [CrossRef] [Google Scholar]

36. Schunkert H, Danser AH, Hense HW, Derkx FH, Kurzinger S, Riegger GA. Effects of estrogen replacement therapy on the renin-angiotensin system in postmenopausal women. Circulation. 1997;95(1):39–45. doi: 10.1161/01.CIR.95.1.39. [PubMed] [CrossRef] [Google Scholar]

37. Leinung MC, Feustel PJ, Joseph J. Hormonal treatment of transgender women with oral estradiol. Transgend Health. 2018;3(1):74–81. doi: 10.1089/trgh.2017.0035. [PMC free article] [PubMed] [CrossRef] [Google Scholar]

38. Liang JJ, Jolly D, Chan KJ, Safer JD. Testosterone levels achieved by medically treated transgender women in a United States endocrinology clinic cohort. Endocr Pract. 2018;24(2):135–142. doi: 10.4158/EP-2017-0116. [PubMed] [CrossRef] [Google Scholar]

Acute and subchronic exposure to air particulate matter induces expression of angiotensin and bradykinin-related genes in the lungs and heart: Angiotensin-II type-I receptor as a molecular target of particulate matter exposure

Octavio Gamaliel Aztatzi-Aguilar, Marisela Uribe-Ramírez, José Antonio Arias-Montaño, Olivier Barbier, and Andrea De Vizcaya-Ruiz
Author information Article notes Copyright and License information Disclaimer

Go to:

Abstract

Background

Particulate matter (PM) adverse effects on health include lung and heart damage. The renin-angiotensin-aldosterone (RAAS) and kallikrein-kinin (KKS) endocrine systems are involved in the pathophysiology of cardiovascular diseases and have been found to impact lung diseases. The aim of the present study was to evaluate whether PM exposure regulates elements of RAAS and KKS.

Methods

Sprague–Dawley rats were acutely (3 days) and subchronically (8 weeks) exposed to coarse (CP), fine (FP) or ultrafine (UFP) particulates using a particulate concentrator, and a control group exposed to filtered air (FA). We evaluated the mRNA of the RAAS components At1, At2r and Ace, and of the KKS components B1r, B2r and Klk-1 by RT-PCR in the lungs and heart. The ACE and AT1R protein were evaluated by Western blot, as were HO-1 and γGCSc as indicators of the antioxidant response and IL-6 levels as an inflammation marker.

We performed a binding assay to determinate AT1R density in the lung, also the subcellular AT1R distribution in the lungs was evaluated. Finally, we performed a histological analysis of

intramyocardial coronary arteries and the expression of markers of heart gene reprogramming (Acta1 and Col3a1).

Results

The PM fractions induced the expression of RAAS and KKS elements in the lungs and heart in a time-dependent manner. CP exposure induced Ace mRNA expression and regulated its protein in the lungs. Acute and subchronic exposure to FP and UFP induced the expression of At1r in the lungs and heart. All PM fractions increased the AT1R protein in a size-dependent manner in the lungs and heart after subchronic exposure. The AT1R lung protein showed a time-dependent change in subcellular distribution. In addition, the presence of AT1R in the heart was accompanied by a decrease in HO-1, which was concomitant with the induction of Acta1 and Col3a1 and the increment of IL-6. Moreover, exposure to all PM fractions increased coronary artery wall thickness.

Conclusion

We demonstrate that exposure to PM induces the expression of RAAS and KKS elements, including AT1R, which was the main target in the lungs and the heart.

Keywords: Renin-angiotensin-aldosterone system, Kallikrein-kinin system, Particulate matter

Go to:

Background

Air quality has been associated with increases in the morbidity and mortality due not only to pulmonary diseases but also to cardiovascular diseases. While the first group of diseases can be explained by the fact that the respiratory system is the major route of exposure to air pollutants, the second group could be a consequence of intermediate steps that connect lung damage to cardiovascular alterations . Epidemiological studies indicate that particulate matter (PM) is involved in these diseases and that exposure to particulate less than 2.5 μm is a major risk factor for the promotion and exacerbation of pulmonary and heart diseases [1–4].

The main mechanisms proposed to explain PM-induced toxic effects on human health are inflammation and oxidative stress. Recently, it has been demonstrated that the inflammatory response to PM promotes accelerated clotting with the participation of IL-6 cytokine [5]. Furthermore, oxidative stress can decrease heart rate variability after acute PM exposure [6]. Both mechanisms are involved in the pathophysiology of lung and heart diseases, i.e., COPD, asthma, fibrosis, hypertension, atherosclerosis, thrombosis, heart failure, etc., and are able to regulate or promote physiological responses including the activation of macrophages and neutrophils, regulation of the vascular tone, and production of mediators of signaling pathways, amongst others.

Important endocrine systems that regulate cardiovascular physiology are the Renin-Angiotensin-Aldosterone system (RAAS) and the Kallikrein-Kinin system (KKS).

Both systems are composed of peptidase enzymes [angiotensin-I converting enzyme type-1 and -2 (ACE and ACE2, respectively) and tissue kallikrein (KLK-1)]; and receptors [angiotensin receptors type-1 and type-2 (AT1R and AT2R, respectively); and bradykinin receptors type-1 and type-2 (B1R and B2R)]; and peptide precursors [angiotensinogen and kininogen (ANG and KNG, respectively)] [7–10]. Both systems control cardiac muscle

contraction through vasoactive peptides, RAAS induces vasoconstriction through the ACE/Ang-II/AT1R axis, but by itself, RAAS can induce vasodilatation by the stimulation of NO-bradykinin dependent release through ACE2/Ang-(1-7)/Mas receptor axis [11], which also, in cooperation with B2R, AT2R induces a vasodilatation effect. This effect orchestrated by B2R, increases the release of NO through the activation of endothelial oxide nitric synthase (eNOS) [8, 12]. Vascular dilatation has been reported to be dependent of KLK-1, B2R and AT2R [13], where KLK-1 has an important role in the generation of the vasodilator peptides (bradykinin and kallidin) [14, 15].

Moreover, angiotensin-II through the AT1R promotes the activation of NADH/NADPH oxidase and the production of superoxide anion radicals as second messengers [16, 17] as well as B1R receptor does when it recognizes the des-Arg-bradykinin [18, 19]. In this sense, AT1R activation induces the expression of B1R [20, 21] and both induce a vasoconstriction effect with an increment in blood pressure [19, 22].

Furthermore, during the inflammation process RAAS and KKS are active participants of this process, AT1R is up-regulated by TNFα [23], IL-6 [24] and IL-1α, but is down-regulated by TNFα and INFγ combined [25]. Ang-II, through AT1R, induces IL-6 release and is inhibited by pyrrolidine dithiocarbamate radical scavenger [26]. On the other hand there is not enough information about cytokines regulating AT2R expression. KKS induces allodynia through B1R as part of the role in hyperalgesia [18]; macrophages release TNFα and IL-1 through the B1R pathway [27]. In lung fibroblasts B2R activation induces the release of IL-6 and IL-8 [28], and also IL-1β through a NF-κB-dependent pathway [28]. In summary, both systems control cardiac muscle contraction, levels of nitric oxide [8, 29], and are involved in the inflammatory response [30, 31] and in the blood coagulation state [32, 33].

There is a sustained cross-talk and a counterbalance between RAAS and KKS through the activation and degradation of vasoactive peptides through angiotensin-converting enzyme-I (ACE), which activates angiotensin-I to angiotensin-II and degrades bradykinin to bradykinin (1-5) [34–36]. It is important to note that one of the main metabolic functions of the lungs is the activation and degradation of these peptides [36, 37].

During pathological cardiovascular states, the RAAS is overexpressed, as demonstrated in diseases such as hypertension, atherosclerosis, heart infarction and heart failure. However, recent evidence also indicates its participation in the pulmonary fibrosis induced by bleomycin [38] and bronchial hyperresponsiveness in asthmatic patients [39].

PM exposure has been established as a risk factor for lung and cardiovascular diseases, and RAAS and KKS are involved in the pathophysiology of these afflictions. However, there is not currently enough evidence to confirm whether RAAS and KKS are involved in the response to PM exposure. Ulrich et al. demonstrated that the activity of angiotensin-converting enzyme (ACE) in plasma and its mRNA in the lung decreased after 4 or 7 days of exposure to ECH-93 PM and ozone [40]. Gunisson and Chen reported a 1.5-fold increase in the differential expression of At1r in a lung microarray of double-knockout mice (apoE -/- and LDLr-/-) exposed subchronically to ultrafine particulates (6 h/day; 5 days/week for 4 months) [41]. Li et al. observed ex-vivo vasoconstriction of pulmonary artery rings exposed to PM (1-100 μg/ml), the soluble fraction of the PM, and metals including copper and vanadium. This observation was associated with an activation of MAPK signaling. These effects were completely inhibited

by losartan and partially with captopril, a blocker of AT1R and an inhibitor of ACE, respectively [42]. Other studies using a mouse model of long-term exposure to PM2.5 reported cardiac remodeling observed to be associated with a switch to fetal reprogramming, the induction of fibrosis and hypertrophic markers and the impairment of the myocardial contraction [43, 44]. These processes have been reported to be mediated by RAAS.

There is not currently sufficient evidence to establish whether PM exposure could affect expression of RAAS and KKS elements. We therefore hypothesized that PM regulates expression of RAAS and KKS elements in the lungs, and concurrently in the heart, and these changes are accompanied by antioxidant/inflammation and myocardial gene responses.

The aim of this work was to screen for changes in some RAAS- and KKS-related elements during in vivo acute and subchronic exposures to three main airborne particle fractions (coarse, fine and ultrafine particulates) and to examine: 1) whether the effect of PM on RAAS and KKS elements expression is present in the lungs and concomitantly in the heart, 2) if there is a relationship between the exposures and antioxidant responses (heme oxygenase-1 and gamma-glutamyl-cysteine ligase), and 3) tissue damage by histological evaluation and changes in fetal gene reprogramming.

Go to:

Results and discussions

mRNA levels of angiotensin and bradykinin system related-genes in the lungs

To evaluate whether PM exposure affects the angiotensin and bradykinin systems as an initial response to the toxic effect of the three PM fractions, we evaluated the mRNA levels of three genes of each endocrine system.

We observed an increase in the Klk-1 mRNA in the lungs of the groups acutely exposed to FP and UFP, which was the only response of the bradykinin system observed after either exposure. However, the B1r and B2r mRNA levels showed a tendency to increase after the acute exposure; in the subchronic exposure, we did not observe any response of the bradykinin system genes (Table 1).

Table 1

Particulate matter effects on gene expression of angiotensin and bradykinin systems in the lungs. Semi-quantitative expression results of angiotensin-receptor type-2 (At2r), bradykinin receptor type-1 (B1r) and type-2 (B2r), and kallikrein (Klk-1) enzyme after acute and subchronic exposures

	Acute exposure			
Group Gene	FA	CP	FP	UFP
At2r	1 (0.6-1.4)	1.3 (0.61-2.17)	1.85 (1.1-2.5)	1.32 (0.5-1.9)
B1r	1 (0.9-1.1)	1.05 (0.8-1.2)	1.3 (1.01-2)	1.08 (0.9-1.1)
B2r	1.1 (0.6-1.2)	1.1 (0.9-1.77)	2 (0.9-3.1)	1.4 (1.4-1.7)
Klk-1	1 (0.94-1.1)	1.12 (0.76-1.3)	1.88 * (1.4-2)	1.43 * (1.1-2.35)

	Acute exposure			
Subchronic exposure				
Group Gene	FA	CP	FP	UFP
At2r	1 (0.8-1.15)	0.73 (0.7-1.1)	0.85 (0.5-1.1)	0.82 (0.6-1.1)
B1r	1 (0.9-1.2)	0.95 (0.9- 1.03)	1. (0.94-1.5)	1 (0.93-1.1)
B2r	1 (0.9-1.2)	1.03 (1-1.2)	1.6 (1.15-4.2)	1 (0.93-1.1)
Klk-1	1 (0.8-1.2)	0.84 (0.8-1.1)	1.78 (0.7-2.7)	0.92 (0.9-1.4)

Open in a separate window

Acute exposure was defined as 5 h per day for 3 days

Subchronic exposure was defined as 5 h per day, 4 days per week, for 8 weeks

All results were corrected using glyceraldehyde 3-phosphate dehydrogenase as a housekeeping gene

AF: Air filtered

CP: Coarse particulate

FP: Fine particulate

UFP: Ultrafine particulate

Data are showed as median and range

* Indicates significantly different from FA

Our results demonstrate that, in the lungs, the KKS system responds only after an acute exposure, and the main gene that responded to airborne particulate was Klk-1. This is a serine protease enzyme that is necessary to produce kinin peptides. On this basis, particulate less than 2.5 µm could interfere with the activation of kinin peptides, which are necessary to activate bradykinin receptors. Bradykinin receptors are involved in the regulation of nitric oxide, the main vasodilator molecule, and are implicated in inflammation and vascular tone regulation. The expression of the bradykinin receptors in the lungs was not significantly altered for any of the exposures (regardless of particle type or duration of exposure). This could have been because both receptors are constitutively expressed in the lung tissue, although they can be induced by some cytokines including IL-1 and TNFα. PM exposure is characterized by the induction of cytokine release [8], but we did not observe changes in the expression of these receptors.

On the other hand, major and significant mRNA changes were observed for the At1r and Ace angiotensin system genes in the lungs. These are two of the most important genes in this system and are therapeutic targets in conditions such as hypertension (Fig. (Fig.1).1). For both periods of exposure, we found an increase in the levels of At1r mRNA in the groups exposed to FP and UFP compared with those exposed to FA (Fig. 1a and andb).b). In contrast to the effects observed with FP and UFP fractions, we observed a decrease in At1r mRNA levels in the group subchronically exposed to CP (Fig. 1b). The At2r mRNA levels were not significantly different among any of the types of particle and exposure time conditions as

shown in Table 1. Our results for the Ace mRNA levels showed a significant increment following the acute exposures to FP and UFP, but not for the subchronic exposures (Fig. 1c and andd).d). On the other hand, the group exposed subchronically to CP responded with a large increase in the Ace mRNA relative to all other groups (Fig. 1d). It has been reported that RAAS elements can be expressed constitutively within the cells of various tissues and can have intracrine, paracrine and endocrine effects in the organism [10]. Angiotensin-II is the product of the enzymatic activity of ACE and is the ligand for AT1R and AT2R. Lung tissue expresses these three genes, which are important in the regulation of the pulmonary circulation. As a result of the exposures, At1r and Ace responded to PM, but At2r did not. This suggests that PM exposure modulates the activation of angiotensin-I and the deactivation of bradykinin by up-regulating Ace and promoting At1r up-regulation However, the regulation of At2r, which has been considered to have an antagonistic effect on the At1r signaling pathway, was not affected.

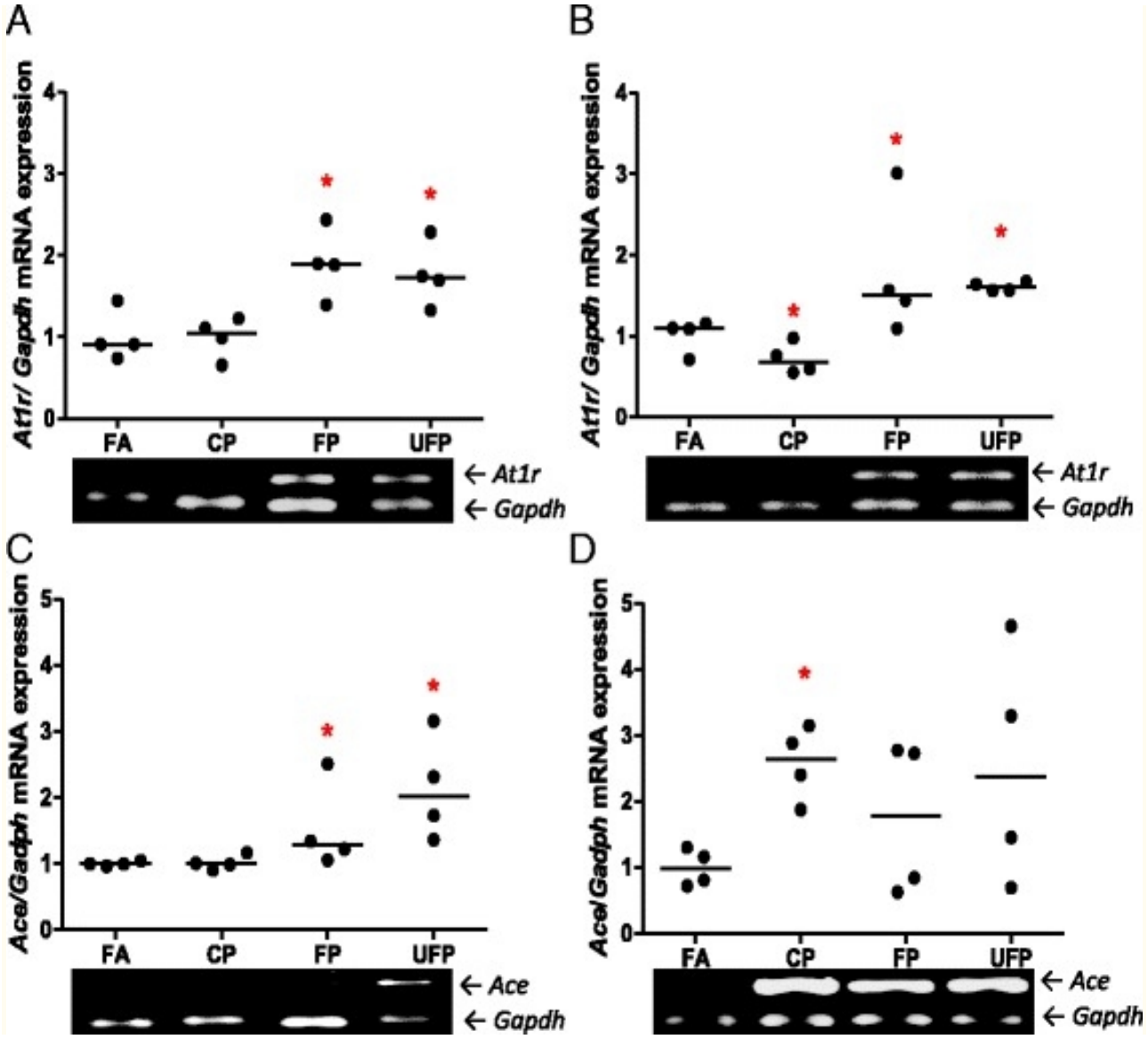

Fig. 1

Particulate matter induces lung AT1R and ACE mRNA in a size- and time-dependent manner. The animals were exposed to coarse (CP), fine (CP) and ultrafine particulate (UFP).

A control group was exposed to filtered air (FA). The semi-quantitative levels of Angiotensin Receptor Type-1 (At1r) and Angiotensin-I Converting Enzyme (Ace) mRNA after acute (3 days, 5 h/d) and subchronic (8 weeks, 5 h/d, 4 d/week) exposure are shown. Scatter dot plot shows the value of the median. Below each graph representatives gels illustrating the expression levels of mRNA are shown. * indicates significant differences among groups (n = 4 per group, $p < 0.05$)

All of these results indicate that PM can regulate two of the principal endocrine systems involved in the regulation of the cardiovascular system at mRNA level. Our data also showed that KKS responds acutely, and not subchronically. On the other hand, the expression of the RAAS genes increased at the end of both exposures, but the responses differed according to the type of particle and the specific genes affected. The mRNA levels of both endocrine systems suggest that KKS and RAAS genes are implicated in the physiological response induced by PM, and these gene expression changes may result in changes in the protein levels.

Protein levels of AT1R and ACE in the lungs

Following the screening of the expression of RAAS- and KKS-associated genes, we investigated whether the protein levels of AT1R and ACE, which demonstrated the most significant changes in the mRNA, were also altered.

In the lung total protein extracts, we observed a statistically significant reduction in the levels of the AT1R protein after acute exposures to FP or UFP (Fig. 2a). However, after the subchronic exposure, our results showed an increase in the AT1R protein levels for all three particle fractions (Fig. 2b). Moreover, we observed a decrease in the ACE protein levels after acute exposure to CP, while in the subchronic exposures, an increase in ACE levels was observed. However, for both acute and subchronic exposures to FP and UFP the ACE protein levels were variable. Therefore, although we observed a decrease in the protein levels, the differences were not statistically significant (Fig. 2c and anddd).

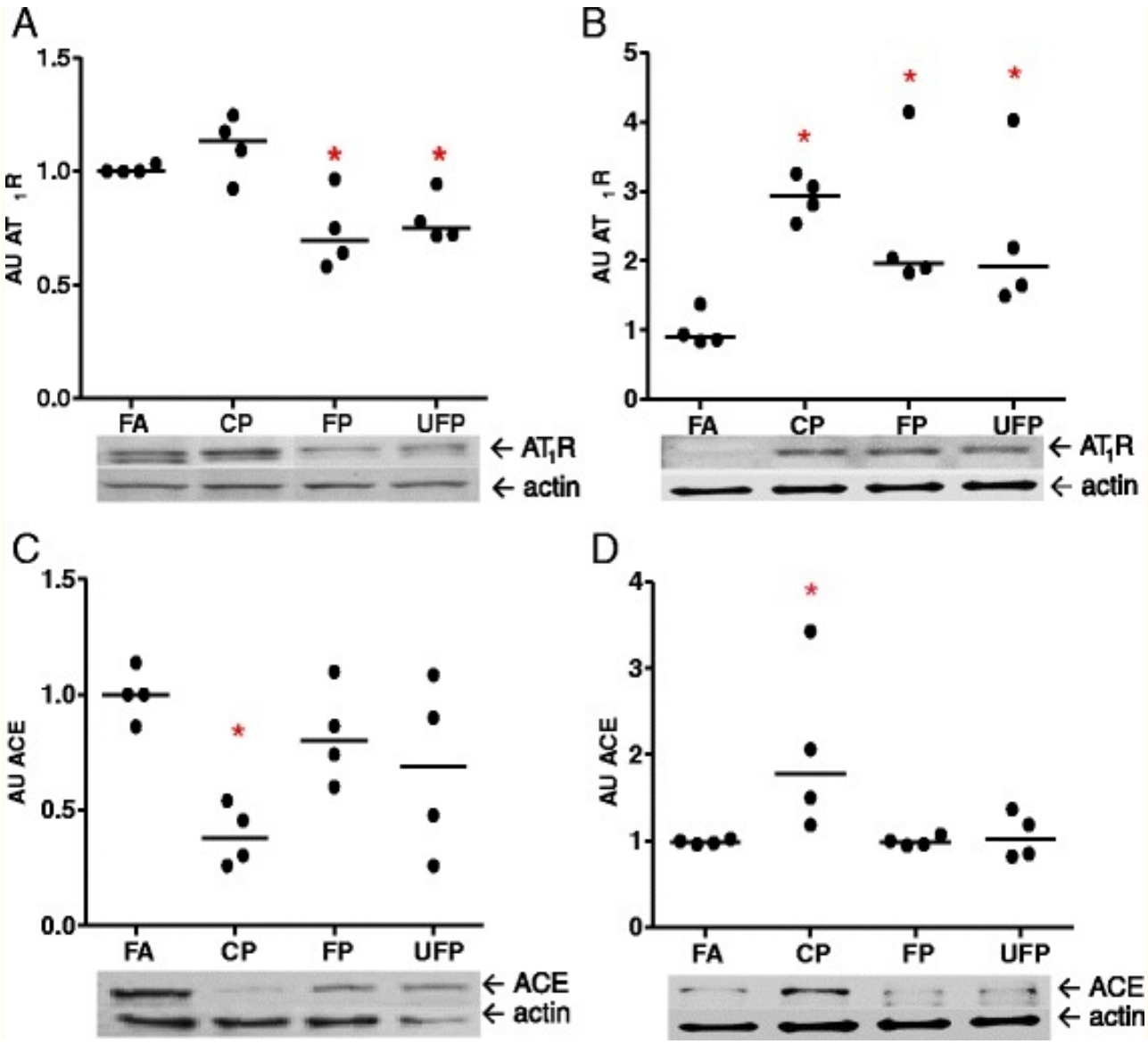

Fig. 2

Particle matter exposure regulates AT1R and ACE protein in a particle size-dependent manner. Animals were exposed to coarse (CP), fine (FP) and ultrafine particulate (UFP), or filtered air (FA). a) and b) The protein levels of Angiotensin Receptor Type-1 (AT1R) and c) and d) Angiotensin-I Converting Enzyme (ACE), after acute (3 days, 5 h/day) and subchronic (8 weeks, 5 h/day, 4 days/week) exposure, respectively, are shown as arbitrary units (AU). Scatter dot plot shows the value of the median. * indicates significant differences among groups (n = 4 per group, $p < 0.05$)

Our results show that exposure to PM was able to induce the ACE and AT1R proteins as well as mRNA. Differences were observed with respect to the particle fractions and the target proteins. Acute exposure to CP caused a down-regulation of the ACE protein, without a change of the AT1R protein levels. In contrast, the subchronic exposure to CP induced an increase in ACE protein, which was accompanied by the up-regulation of AT1R. However, FP

and UFP did not affect the ACE protein levels. Instead, AT1R was the main molecular target of the FP and UFP fractions. No differences between the FP- and UFP-induced effects on the AT1R protein levels were observed. This could be explained either by the fact that UFP are contained within the FP fraction, which precludes separation of their effects, or because they can reach the same region in the lungs, they induce similar responses.

Our data suggest that PM can regulate AT1R and ACE protein levels in the lungs in a time- and possibly a PM size-dependent manner. It is important to highlight that the CP, for which we did not expect a response, was able to modulate both genes, while the FP and UFP fractions only modulated AT1R. This evidence confirms that CP can promote pulmonary events as well as the PM smaller than 2.5 μm, and suggests a possible contribution to cardiovascular impairment as a consequence of exposure to PM.

[3H]-Angiotensin-II binding to lung membranes

Similar to other G protein-coupled receptors, upon activation AT1Rs can be internalized from the cell membrane to the cytoplasm and then can be either recycled or degraded. Because the reduction in AT1R protein after the acute exposure to FP and UFP did not match the mRNA levels, we performed a binding assay with labeled Ang-II as an alternative method to confirm the protein levels. First, we obtained a saturation curve to determine the receptor density and the affinity for [3H]-Angiotensin-II in lung membranes obtained from rats that were not used in the PM experiments. These determinations (Fig. 3a) yielded a maximum specific binding (Bmax) of 90 ± 10 fmol/mg protein (3 experiments) and an equilibrium dissociation constant (Kd) of 2.8 nM (pKd 17.2 ± 7.7).

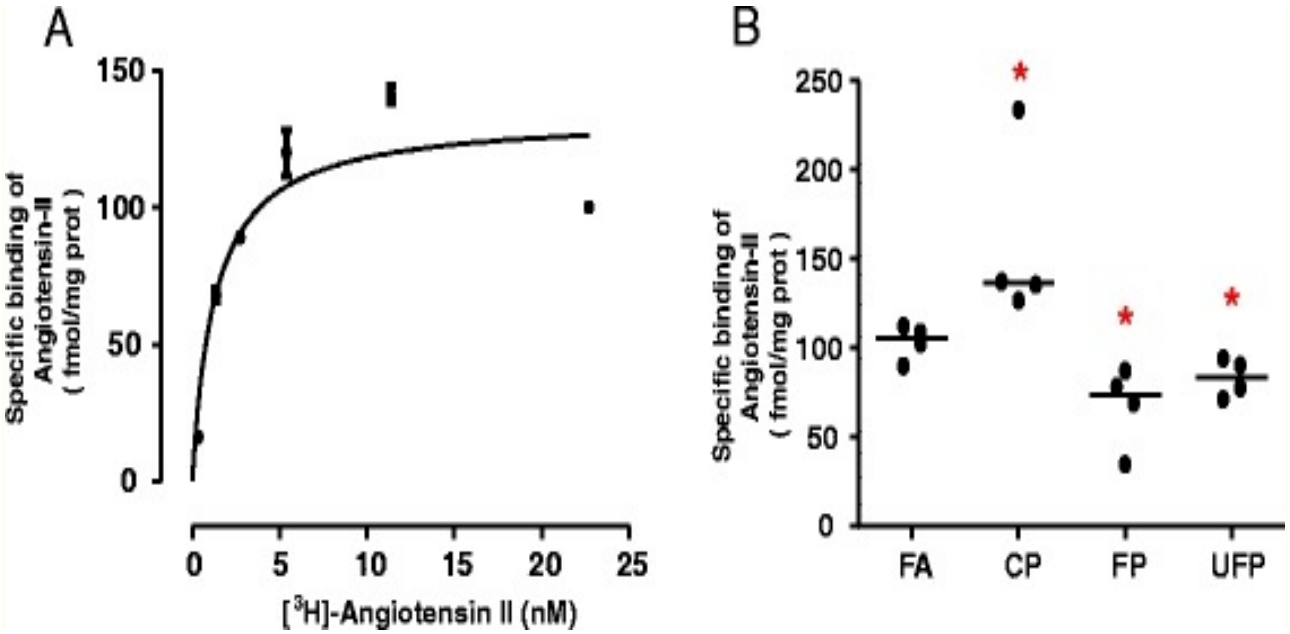

Fig. 3

Acute exposure to PM modifies [3H]-Angiotensin-II binding to the lung tissue membranes.

a) Saturation binding. Membranes, obtained from naïve animals as described in Methods, were incubated with the indicated concentrations of [3H]-Angiotensin-II. Specific receptor binding was determined by subtracting the binding in the presence of 100 μM telmisartan

from the total binding. The points show the means from quadruplicate determinations from a single experiment, which was repeated twice more with membranes obtained from different naïve animals. The line drawn is the best fit to a hyperbola. Best-fit values for the equilibrium dissociation constant (K d) and maximum binding (Bmax) are given in the text. b) Single-point determinations. Membranes were obtained from animals exposed to coarse (CP), fine (FP) and ultrafine particulate (UFP) or from the filtered air control group (FA), and then incubated with 10 nM [3H]-Angiotensin-II. Specific receptor binding was determined by subtracting the binding in the presence of 10 μM telmisartan. Scatter dot plot shows the value of the median. * Indicates significant differences among groups (n = 4 per group, $p < 0.05$)

In single-point determinations with a near saturating concentration (10 nM) of [3H]-Angiotensin-II, a reduction in the specific binding was observed in lung membranes from the animals exposed to FP and UFP. In contrast, exposure to CP increased the specific [3H]-Angiotensin-II binding (Fig. 3b).

The binding data thus showed the same pattern as the total protein detected immunologically. On this basis, we infer that the internalization and degradation of AT1R in the acute exposure could be induced by different mechanisms such as an over-activation, a target of oxidative stress and/or allosteric regulation by divalent cations, similar to observations of other GPCRs [45, 46].

AT1R levels in subcellular fractions of lung tissue

The conventional paradigm for GPCRs indicates that the activated receptors are internalized from the plasma membrane to the cytoplasm where they may be degraded or recycled [47]. However, new evidence indicates that some GPCRs can be localized in the nuclear envelope [48]. In the case of AT1R, Lu et al. reported that after 15 min of stimulation of neuronal cell cultures with Ang-II, AT1R was sequestered to the nuclear membrane [49]. However, Tadevosyan et al. [50] demonstrated that the presence of angiotensin receptors (AT1R and AT2R) in the nuclear membrane is most likely a result of intracellular synthesis and trafficking, and not the result of post-endocytotic trafficking in cardiomyocyte cultures. For these reasons, we evaluated the distribution of AT1R protein between the nuclei and the rest of the cell in the lung tissue following exposure to airborne PM in both exposure schemes (Fig. 4). For the acute exposures, we observed an increase in AT1R in the non-nuclear fraction in all exposed groups, while in the nuclear fraction we observed a reduction in protein levels (Fig. 4, upper panel). On the other hand, following the subchronic exposures, we observed the opposite response: under these conditions, we observed a decrease in AT1R levels in the non-nuclear fraction and an increase in this protein in the nuclear fraction (Fig. 4, lower panel).

Fig. 4

Particle matter modifies the AT1R subcellular distribution in lung tissue in a time-dependent manner. Representative gels of Angiotensin-II type-I receptor (AT1R) detection in lung nuclear and non-nuclear fractions after acute (upper panel) and subchronic (lower panel) exposure to coarse particulate (CP), fine particulate (FP), ultrafine particulate (UFP) or filtered air (AF). We used GAPDH and acetylated Histone-4 (H4ac) as cytosolic and nuclear quality control targets, respectively, and actin was used as a general protein loading control. Representative blot of n = 4

On the basis of our findings with respect to the subcellular distribution of AT1R in the lung tissue, we suggest that this receptor may mediate processes that include cell proliferation, survival, inflammatory responses, DNA synthesis and transcription as has been demonstrated for other GPCRs found in the nuclear envelope [48]. For example, nuclear AT1R activation has been demonstrated using isolated nuclei from fetal rat myocytes. Stimulation of these nuclei with angiotensin-II induced transcription as indicated by [α-32P] UTP incorporation, and this effect was inhibited by pertussis toxin [50].

IL-6 cytokine protein levels in lung

Pleiotropic cytokine IL-6 is involved in the acute phase of inflammation and accelerates coagulation induced by PM exposure in vivo [5]. In addition, in endothelium cells, IL-6 induced the expression of AT1R [24]. We observed a statistically significant increase in lung IL-6 protein from the acute exposure to the three PM fractions (Fig. 5a); on the other hand, in the subchronic exposure a down regulation in the three PM groups below the levels observed in the FA group was observed (Fig. 5b). Our results indicate the induction of lung IL-6 as a marker of the acute phase of the inflammation process. IL-6 could be involved in the up-regulation of AT1R in lung acute PM exposure. In contrast, in the subchronic exposure a lack of induction of lung IL-6 protein was observed and AT1R expression was increased. If a molecular communication process takes place between IL-6 and AT1R it only happens acutely, but not subchronically, yet this hypothesis needs to be confirmed.

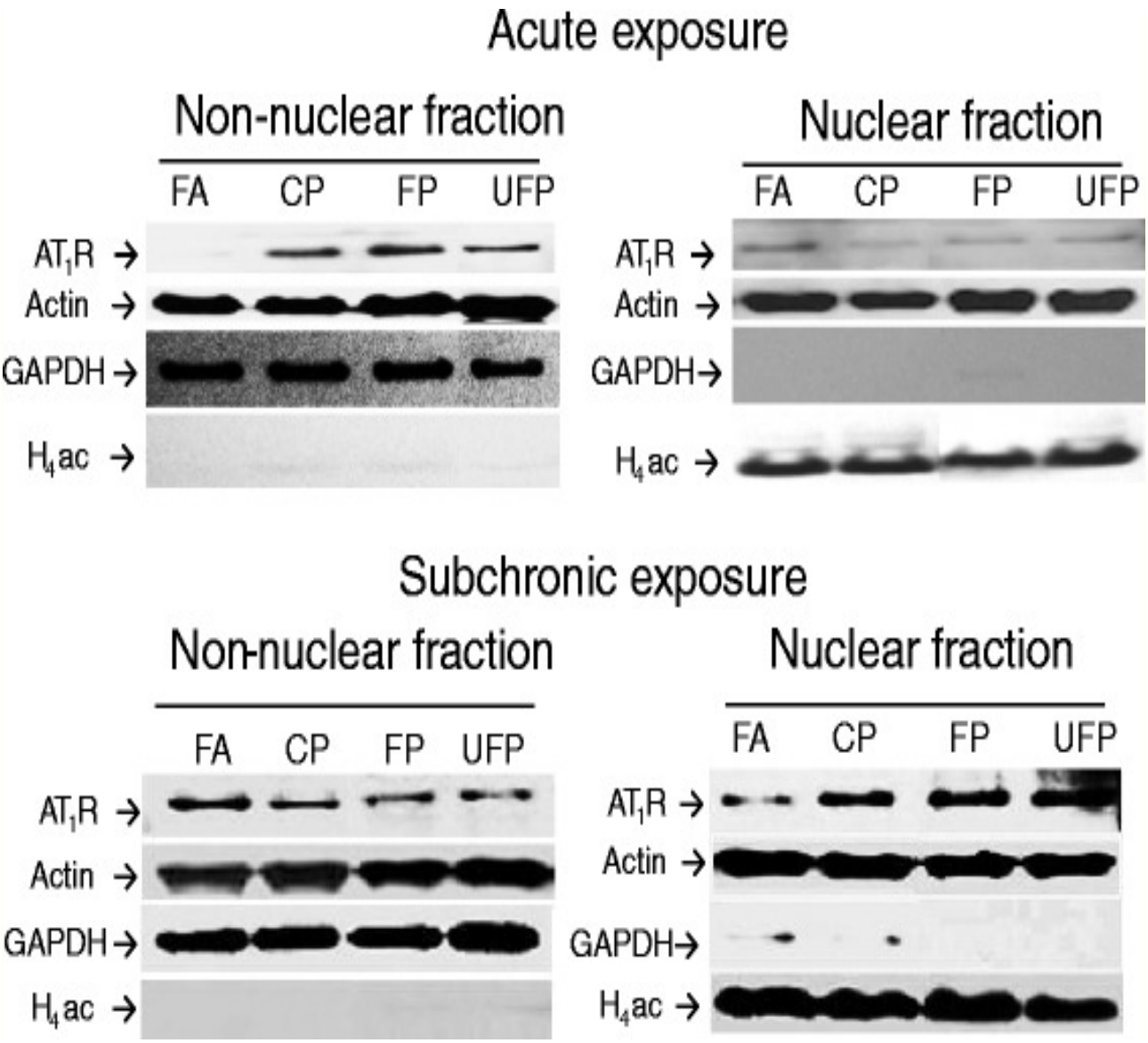

Fig. 5

Acute, but not subchronic, exposure to particle matter increases IL-6 in lungs. Animals were exposed to coarse (CP), fine (FP) and ultrafine particulate (UFP), or filtered air (FA). The protein interleukine-6 (IL-6) levels after **a**) acute (3 days, 5 h/day) and **b**) subchronic exposure (8 weeks, 5 h/day, 4 days/week), are shown as arbitrary units (AU). Scatter dot plot shows the value of the median. * indicates significant differences among groups ($n = 4$ per group, $p < 0.05$)

Expression of angiotensin and bradykinin system genes in the heart

The results obtained in the lungs suggest a contribution of the RAAS and to a lower degree, but not less important, of the KKS in the endocrine pulmonary response to PM damage. These heterogeneous responses of gene expression observed in the lungs following the acute and subchronic exposures to airborne particulate fractions could be conveyed from the lungs to the heart.

As expected, we observed a response in the mRNA levels of bradykinin-related genes in the heart following the exposure to PM. Similar to the observations in the lungs, in the heart there was an increase in Klk-1 after the acute exposure to FP that was sustained in the subchronic exposure. Additionally, we observed an increase in B1r in all groups acutely exposed to particulate (Table 2). We were not able to detect B2r in the heart samples; no positive amplification was observed in the heart samples from any of the exposure schemes. This observation confirms that, as previously reported, B2r is a receptor which has a null or low expression in the heart ventricles of the adult male rat [51–53].

Table 2

Particulate matter effects on gene expression of angiotensin and bradykinin systems in the heart. Semi-quantitative expression results for angiotensin-receptor type-2 (At2r), Bradykinin receptor type-1 (B1r) and kallikrein (Klk-1) enzyme after acute and subchronic exposures

	Acute exposure			
Group Gene	FA	CP	FP	UFP
At2r	1 (0.8-1.2)	1 (1-1.1)	1 (0.9-1.1)	1 (0.5-1)
Ace	1 (0.9-1.1)	1.6 * (1.4-1.8)	1.1 (0.9-1.3)	1.7 * (1.1-2.1)
B1r	1 (0.8-1.3)	1.7 * (1.4-2.2)	2.2 * (2.1-2.6)	1.9 * (1.3-2.4)
Klk-1	1 (0.8-1.2)	1.2 (1-1.5)	1.6 * (1.4-1.9)	1.4 * (1.2-1.5)
Subchronic exposure				
Group Gene	FA	CP	FP	UFP
At2r	1 (0.96-1.03)	0.97 (0.97-1.05)	0.92 (0.72-0.9)	0.71 * (0.7-0.8)
Ace	1 (0.9-1.1)	1 (0.9-1.1)	1 (0.9-1.3)	0.9 (0.8-1)
B1r	Not determined			
Klk-1	1 (0.9-1.1)	1.1 (0.9-1.2)	1.2 * (1.19-1.22)	1.1 (1-1.3)

Acute exposure was defined as 5 h per day for 3 days

Subchronic exposure was defined as 5 h per day, 4 days per week, during 8 weeks

All results were corrected with glyceraldehyde 3-phosphate dehydrogenase as a housekeeping gene

AF: Air filtered

CP: Coarse particulate

FP: Fine particulate

UFP: Ultrafine particulate

Data are showed as median and range

* Indicates significantly different from FA

Our results for the expression of KKS genes show that there is a differential response between the lungs and the heart: the heart responded to the exposures to the three particulate with the induction of B1r mRNA. These results suggest that the inflammatory factors or chemical components are released from the lungs and enter in the blood stream of the pulmonary circulation before being translocate to the heart. Although we observed this response to all three particulate, FP, but not UFP, was able to induce Klk-1, which indicates that there are differences between these two particle fractions and suggests that FP could affect the metabolism of kinin peptides.

With respect to the angiotensin system, the heart At2r mRNA levels were not significantly different among the acute exposure groups. In contrast, subchronic exposure to UFP caused a significant decrease in the heart At2r levels (Table 2). The Ace mRNA increased after acute exposure to either CP or UFP, but these changes did not persist in the subchronic exposure (Table 2). We observed an increase in the At1r mRNA levels after acute and subchronic exposure to FP, as well as in the group after the subchronic exposure to UFP (Fig. 6).

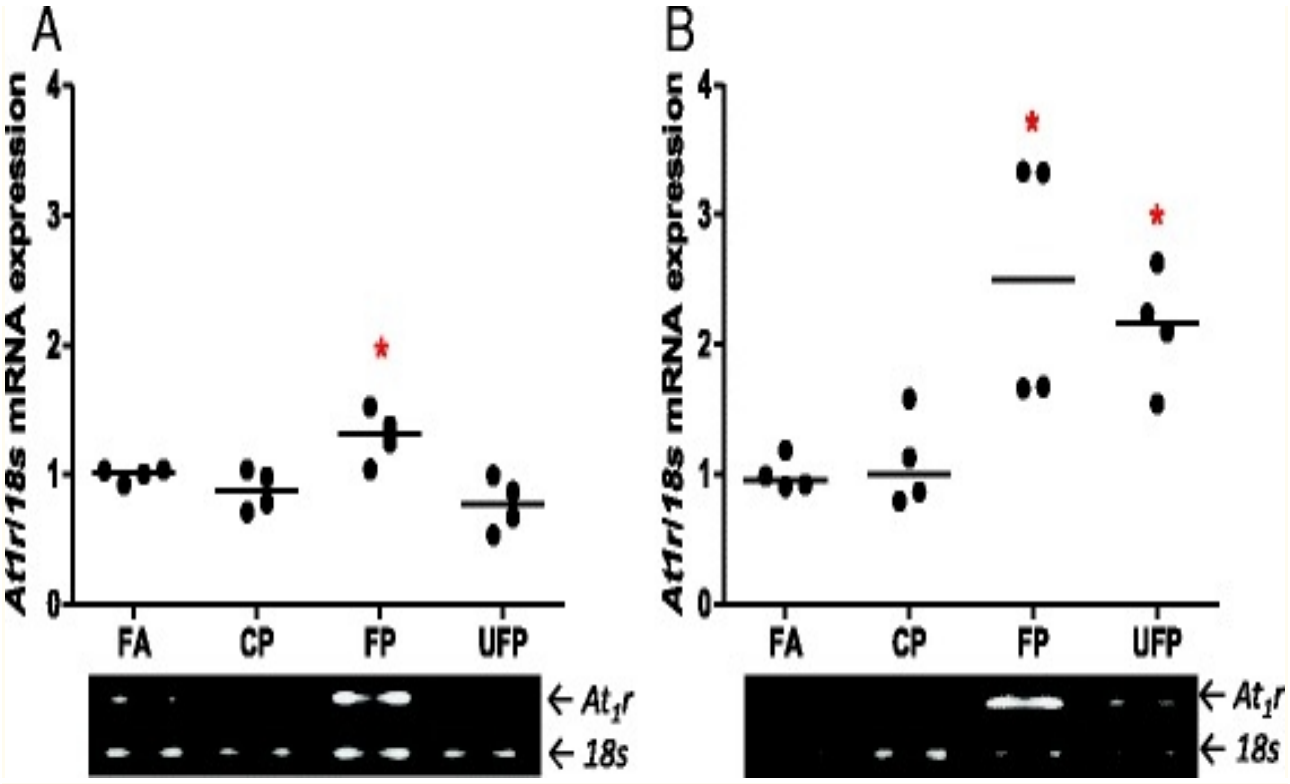

Fig. 6

Acute and subchronic exposures to fine and ultrafine PM up-regulate heart AT1R mRNA. The animals were acutely (5 h/day, 3 days) or subchronically (5 h/day, 4 days/week, 8 weeks) exposed to coarse (CP), fine (FP) and ultrafine particulate (UFP) or to filtered air (FA). Semi-quantitative levels of Angiotensin Receptor type-1 (At1r) mRNA after **a**) acute and **b**) subchronic exposures in the heart. Scatter dot plot shows the value of the median. * indicates significant differences among groups ($n = 4$ per group, $p < 0.05$)

The cardiac over-expression of AT1R has been demonstrated to be involved with the promotion and exacerbation of myocardial impairment. It is relevant to note that short PM exposure was able to

induce At1r, which was maintained in the subchronic exposure. This observation was accompanied with a down-regulation of At2r only after the subchronic exposure, indicating that exposure to PM, an environmental air pollutant, can increment the expression of At1r in the absence of counterbalancing changes in the expression of At2r.

Up-regulation of Col3a1 and Acta1 in presence of AT1R and IL-6 in the heart

Two of the main classes of response genes in the heart during pathological states of cardiac damage are the heart fetal reprogramming genes and the expression of genes involved in the deposition of the extracellular matrix. We chose alpha skeletal actin (Acta1) and collagen-III (Col3a1) as two representative markers of myocardial adaptive response to damage. We analyzed these genes in heart ventricular samples after the acute exposures, and did not observe any response in either gene (data not show). In contrast, the subchronic exposures to FP and UFP induced the up-regulation of Acta1 and Col3a1 (Fig. 7a and andbb).

Our results indicate that PM is not able to acutely up-regulate these genes, but they are increased by subchronic exposure. The presence of these two markers in various rat cardiac disease models has been described, i.e., hypertension or induced cardiac infarction [54]. FP and UFP have been associated predominantly with the enhancement of the development of cardiovascular diseases. Our results confirm that particulate less than 2.5 μm are able to up-regulate gene reprogramming in the heart, possibly by through an increase in blood pressure.

There is substantial evidence to support the concept that RAAS induces heart gene reprogramming [54–57]. For this reason, we evaluated AT1R total protein levels in samples from the subchronic exposure where we observed heart gene reprogramming. We also observed an increase in the levels of AT1R in the total protein that seems PM size-dependent, where the highest increase was observed for UFP followed by FP and to a lower degree for CP (Fig. 7c).

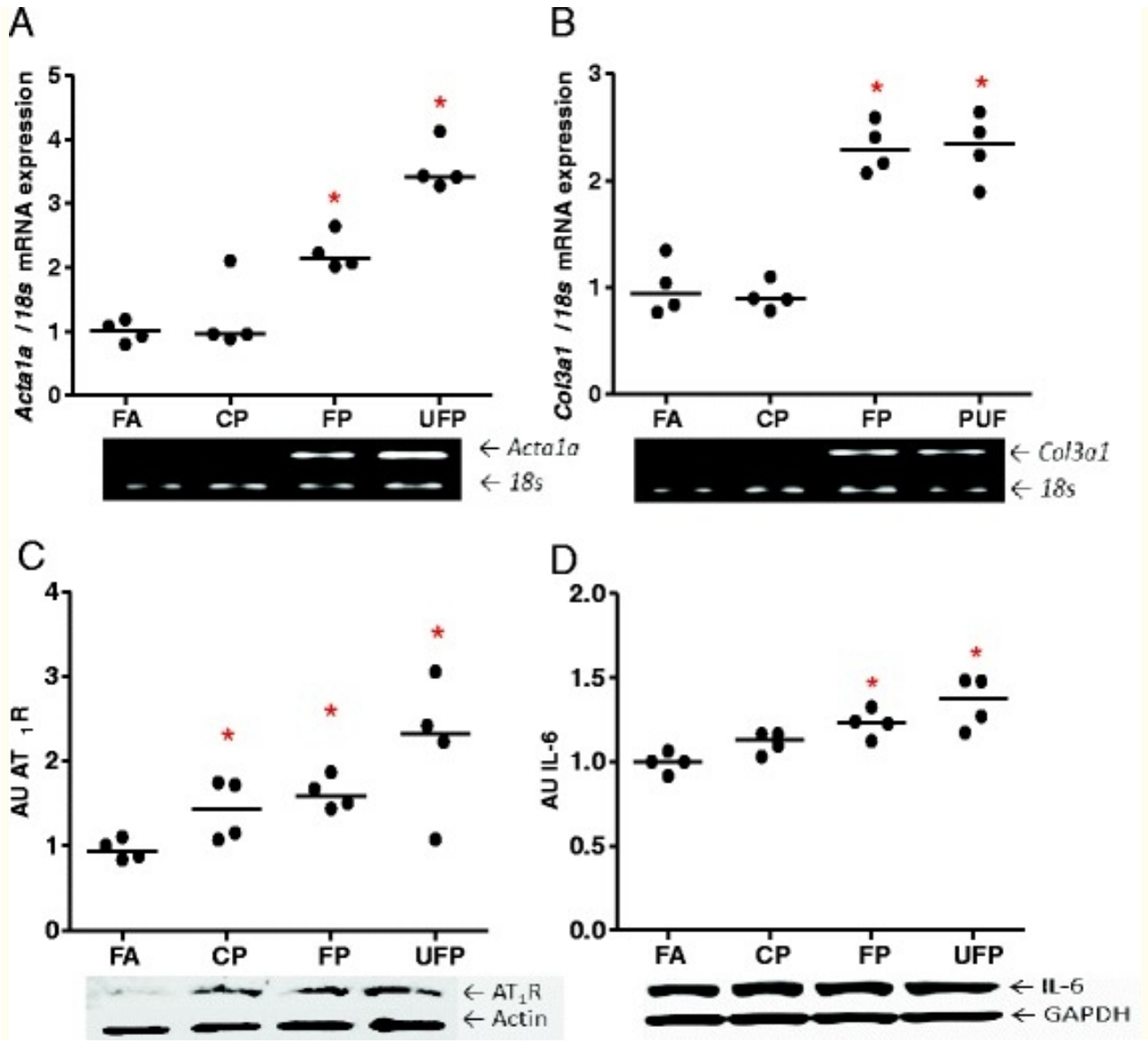

Fig. 7

Subchronic exposure to fine and ultrafine PM induces heart reprogramming and up-regulates AT1R and IL-6. The animals were subchronically exposed (5 h/day, 4 days/week for 8 weeks) to coarse (CP), fine (FP) and ultrafine particulate (UFP) or to filtered air (FA). a) Semi-quantitative levels of alpha-skeletal actin (Acta1a) mRNA and b) Semi-quantitative levels of collagen-III (Col3a1) mRNA in the heart. Protein levels of AT1R and interleukin-6 (IL-6) are expressed in arbitrary units (AU), c) and d), respectively. Scatter dot plot shows the value of the median. * indicates significant differences among groups (n = 4 per group, $p < 0.05$)

IL-6 cytokine is involved in the induction of AT1R in the endothelium; also Ang-II through AT1R induces the expression of cardiotrophin-1, leukemia inhibitory factor and IL-6, all which are members of IL-6 family. In rodent cardiac fibroblast these cytokines induce cardiomyocyte hypertrophy through the activation of gp130, which is a IL-6 receptor [58]. In

this sense, we evaluated IL-6 protein levels, as a marker of inflammation response, in the heart and observed an increment in IL-6 that could be size-dependent where FP and UFP showed statistical significant differences (Fig. 7d) and they have the same tendency as the AT1R in the heart. Our findings suggest that IL-6 and AT1R are induced in heart by PM exposure and is possibly size particulate-dependent; also, IL-6 and AT1R show the same behavior as cardiac reprogramming genes induced by FP and UFP.

Histology of intramyocardial coronary arteries

One effect of RAAS in the heart tissue is hypertrophy and proliferation of the smooth muscle cells of the blood vessels. We evaluated the thickness of the intramyocardial coronary arteries (we considered only arteries found within the myocardium wall, but not in the epicardium or endocardium) as a morphological effect in myocardial tissue induced from the particle exposure and found that the exposure to the three particle fractions increased the intramyocardial coronary artery wall thickness (Fig. 8a and andc).c). This result is consistent with the induction of AT1R with the three fractions and suggests the activation of RAAS.

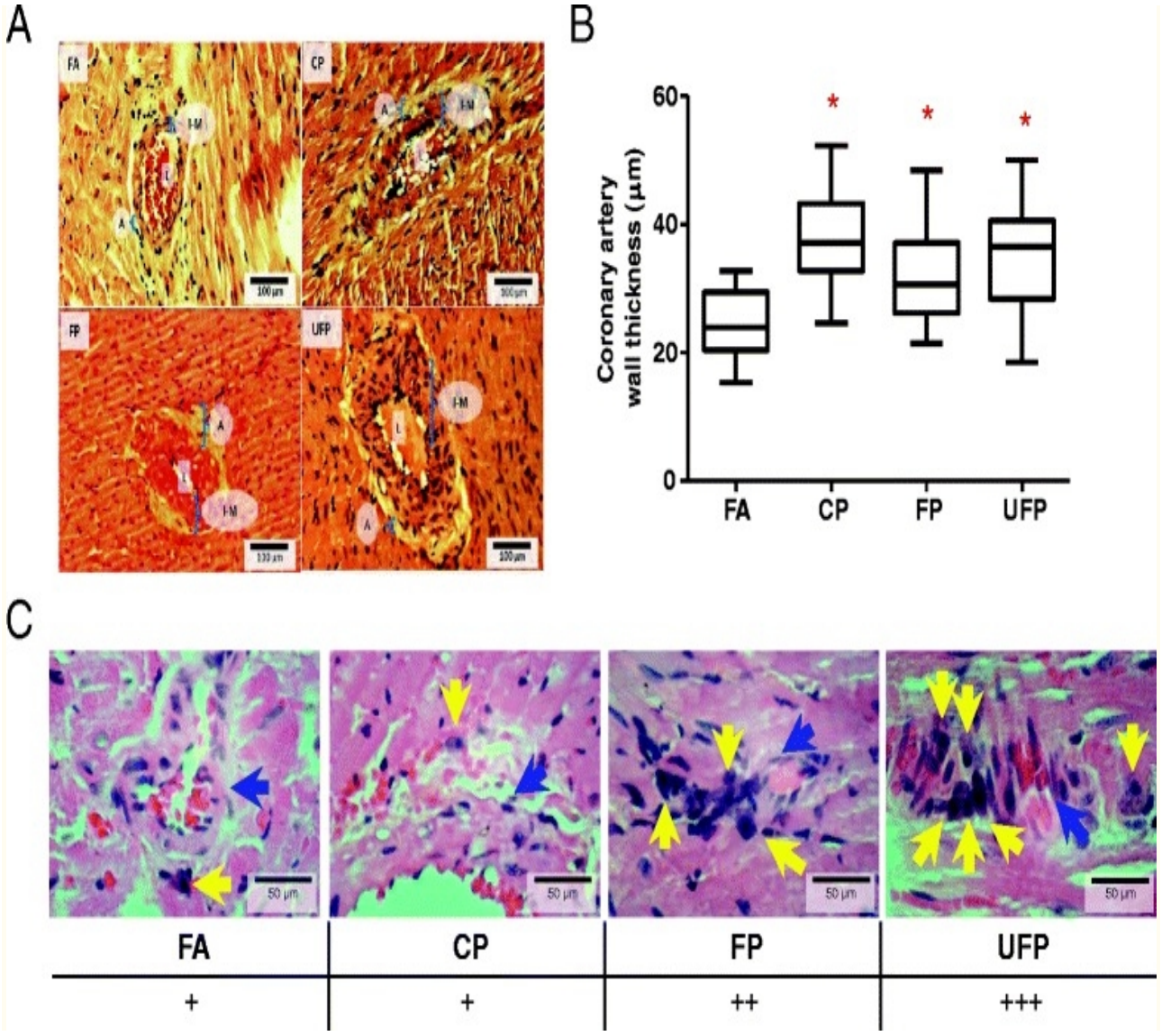

Fig. 8

Subchronic PM exposure increases intramyocardial coronary artery wall thickness independently of PM size. Hematoxylin & Eosin staining of 5 μm myocardial slices. **a**) Representative slides of the hearts from rats exposed to Filtered Air (FA), coarse (CP), fine (FP) and ultrafine (UFP) particulates for 5 h/day, 4 days/week for 8 weeks. **b**) Box plot of ten random measurements of each coronary artery wall measured in the tissues. **c**) Semi-quantitative analysis of the presence of mononuclear cells in heart coronary arteries in the groups exposed to FP and UFP. L: Artery lumen; A: Tunica adventitia; I-M: Tunica intima-media. Yellow arrows indicate mononuclear cells and blue arrows indicate a blood vessel. Scatter dot plot shows the value of the median. * indicates significant differences among groups ($n = 4$ per group, $p < 0.05$)

It has been proposed that particulate less than 2.5 μm can pass through the lung respiratory and vascular walls and reach the heart through the pulmonary circulation [48, 59]. A particular observation in this study was the presence of mononuclear cells, which seem to be macrophages as they display fried egg-like morphology, next to the arteries in the heart from the UFP group and to a minor degree from the FP group (Fig. 8c). This observation suggests an immune cellular response at the end of the subchronic exposure to FP and UFP.

Lungs and heart subchronic antioxidant response

Finally, one of the most important responses to particulate exposure is the antioxidant defense. We evaluated the protein levels of γ-glutamyl-cysteine-synthetase catalytic subunit (γGCSc), and heme oxygenase type-1 (HO-1) in the lungs and heart after subchronic exposure to airborne PM. We did not observe significant changes in γGCSc protein levels in either tissue (data not shown). However, the lung levels of HO-1 seem to decrease in a particulate size-dependent manner, where the greatest down-regulation was observed in the UFP group (Fig. 9a). The same tendency was observed for the heart levels of HO-1, but only the effects of UFP were statistically significant (Fig. 9b).

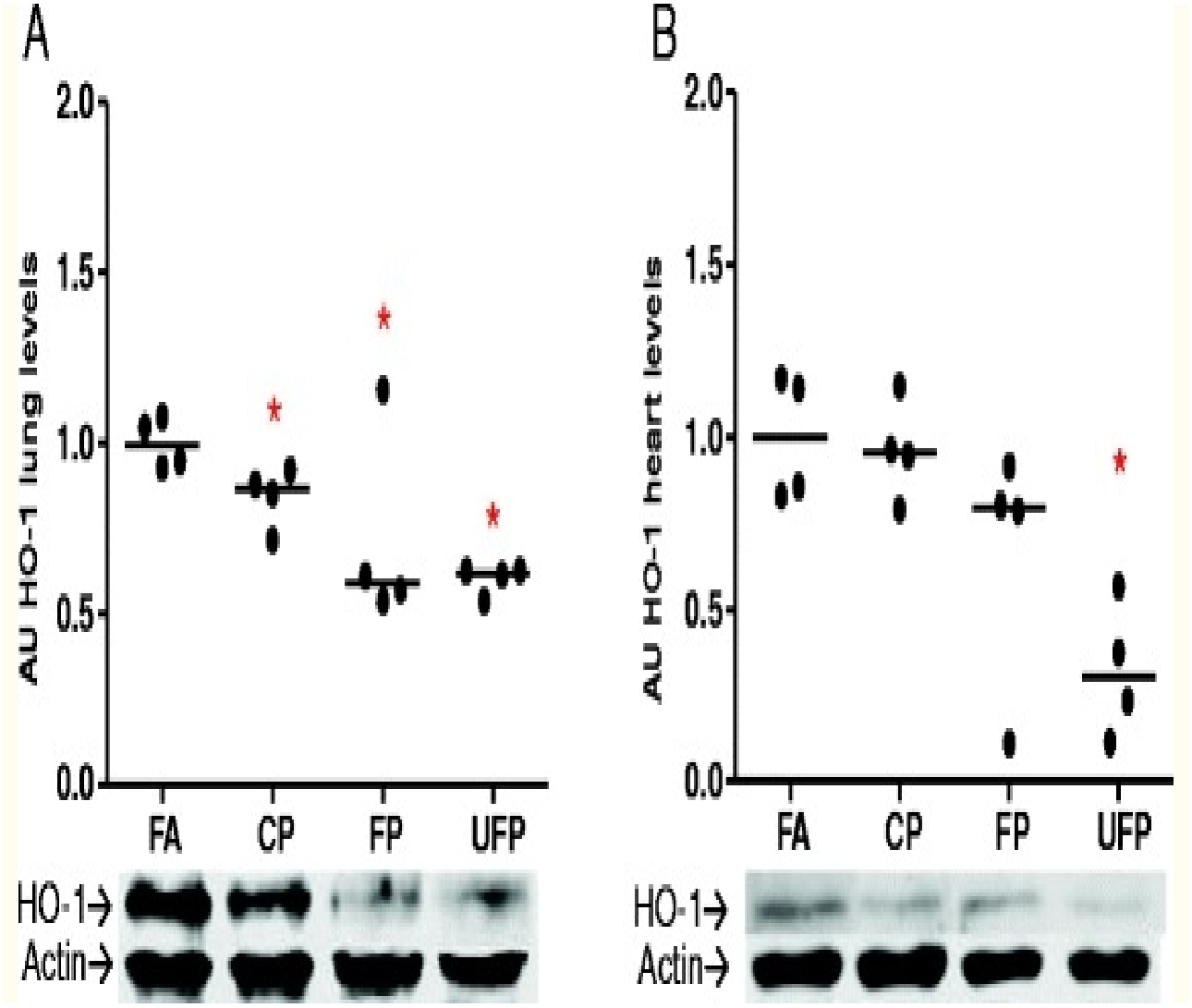

Fig. 9

Particle size-dependent decreases in heme oxygenase-1 after subchronic exposure in the lungs and heart. Animals were exposed subchronic to coarse (CP), fine (FP) and ultrafine particulate (UFP) or to filtered air as a control (FA) for 8 weeks (5 h/day, 4 days/week). Protein levels of heme oxygenase-1 (HO-1) in arbitrary units (AU) in lungs **a**) and heart **b**). Scatter dot plot shows the value of the median. * indicates significant differences among groups ($n = 4$ per group, $p < 0.05$)

We did not observe differences in γGCSc protein levels in lungs and heart even though glutathione is one of the first antioxidant defenses against oxidative stress. Also, although γGCSc is involved in the de novo synthesis of glutathione the toxic effect of PM may be directly modifying the reduced and oxidized glutathione ratio and diminish total glutathione levels, as it has been reported for different progressive lung diseases [60]. Also, other antioxidant response elements such as ascorbic acid, which is abundant in the rat lung, or HO-1 and bilirubin in the cardiovascular system, could be involved in the response against PM-induced oxidative toxicity [61].

HO-1 is an inducible stress protein enzyme that has major role in cytoprotective defense against apoptosis, inflammation and oxidative stress through the catabolism of the heme moiety and the release of Fe2+, biliverdin and CO. The latter two metabolites are implicated in the antioxidant

response and vascular tone, respectively [62–64]. Low HO-1 levels have also been shown to be associated with an impairment of the cardiovascular system [65] and the development of lung diseases [66]. In addition, HO-1 levels can be down-regulated at the mRNA and protein levels by angiotensin-II through AT1R in rat vascular smooth muscle cells [67]. Evidence from in vitro models (RAW 264.7, THP-1, BEAS-2B and A549 cells) exposed to PM indicated that the induction of HO-1 depended on the PAH content of the PM [68–70]. However, exposure of A549 cells to 9,10-phenanthraquinone down-regulated the expression of HO-1 [71]. Acute in vivo studies demonstrate increases in HO-1 protein and mRNA. Nevertheless, in older current smokers, HO-1 mRNA is down-regulated [72]. Furthermore, it has been observed in human populations that a larger size of the dinucleotide repeat polymorphism (GT) n in the HO-1 gene confers a low induction of mRNA by tobacco smoke and is related to the development of emphysema [73]. The same polymorphism has been associated with a low induction and the development of coronary artery disease [74]. Moreover, oxidative stress during the subchronic exposure to PM is likely to be neutralized by non-enzymatic antioxidants derived from enzymatic antioxidant elements, such as heme-metabolism/HO-1/bilirubin-biliverdin biochemical route, these products, bilirubin and biliverdin, play the main antioxidant role, thus the induction of HO-1 is probably not the primarily antioxidant biomarker in response to the subchronic exposure.

General overview

PM pollution contributes to the development of cardiovascular diseases. Our results indicate that in addition to inflammation and oxidative stress, exposure to PM induces an endocrine response through the expression of some RAAS and KKS elements. This effect could be dependent on the particle size, the tissue type and the time of exposure, and could participate in cardiovascular events.

The KKS acute exposure response was characterized by the induction of the Klk-1 in the lungs and heart of the groups exposed to FP and UFP. Expression of Klk-1 leads to the generation of kinin peptides through the breakdown of KNG in tissues. However, this enzyme also can have other substrates such as pro-renin, pro-insulin, LDL, the precursor of atrial natriuretic factor, pro-collagenase, vasoactive intestinal peptide and ANG. Despite the many substrates of KLK-1, it has been reported that KLK-1 improves cardiac physiology reducing blood pressure, prevents the increment in heart mass, reduces the septal thickness and cardiomyocyte size in hypertrophic animal models after aortic constriction. Also, in these animals KLK-1 contributes to decrease the NADPH oxidase activity and increases NO production through B2R [75]. Moreover, klk-1 null mice do not show alteration in blood pressure but exhibited abnormal structures (thin wall and diminished mass of the left ventricle) and functions (reduced cardiac output, stroke volume and left ventricular fractional shortening) of the heart [76].

The above evidence indicates the importance of KLK-1 in the physiology of the cardiovascular system, in addition, kallikrein family genes have been proposed as emerging new markers for the development of cancer [77], and have been weakly associated with the development of lung diseases. It has been demonstrated that KLK-1 is abundant in the lung lavage from asthmatic patients challenged with allergen [78], as well as in an allergic sheep model. Furthermore, a monoclonal antibody to KLK1 inhibited allergen-induced late-phase bronchoconstriction and airway hyper-responsiveness to carbachol. Additionally, in human

tracheobronchial epithelial cells, this antibody blocked oxidative stress-induced epidermal growth factor receptor activation and mucus hypersecretion [79].

This evidence suggests that in the lung KLK-1 seems to be involved in the triggering of local inflammatory response, through breakage of KNG zymogen to bradykinin and kallidin by KLK-1. Bradykinin and kallidin are further broken by the membrane-bound carboxypeptidase-M into des-Arg-bradykinin and des-Arg-kallidin peptides, which activates B1R that is an important inflammatory mediator [8].

For these reasons, the induction of Klk1 by FP and UFP suggests that the generation of kinin peptides or other substrates of KLK1 could be modified by the PM-induced activation.

The bradykinin receptors did not show a response in the lungs at any time of exposure. However, in the heart, the expression of B1r increased after the acute exposure in the three PM-exposed groups. B1r can be induced by inflammatory cytokines, and it can regulate the induction of iNOS enzyme. Thus, our results indicate that the three fractions of particulate could induce the release of secondary mediators from the lungs to the heart, where they were able to induce B1r.

With respect to RAAS, we observed that At2r did not change significantly at any exposure times in the lungs. In the heart, we only observed a decrease in the mRNA for this receptor after the subchronic exposure to UFP. The lack of response of At2r indicates that PM mainly promotes At1r expression more than the other mRNAs.

Ace is of particular interest because it can be a target of PM toxicity due to having a zinc prosthetic group that could be replaced by other divalent cations. Furthermore, this enzyme can activate angiotensin and degrade bradykinin. We observed that the ACE mRNA and protein in the lungs were regulated mainly by CP, and not by FP and UFP, most likely because CP can only reach the bronchial branches and does not penetrate the lungs as deeply as FP and UFP. Future studies should be conducted to determine whether ACE protein is degraded or is released from the lungs to the blood stream after acute exposure to PM. This is important given that new evidence indicates a novel pathway in which activated ACE can be released from the cell membrane [80–83].

The principal finding of our work was that PM regulates AT1R after acute and subchronic exposure. Although CP did not induce the mRNA for AT1R, it was able to increase the protein levels of this receptor as observed using the binding assay and Western blotting. The potential mechanism for the increase in AT1R protein without the mRNA up-regulation in the CP group, it could be explained as reported by Mori et al. [84], cis-acting sequences in the AT1R gene and the glucocorticoid-responsiveness elements control the transduction process, however, AUG codon in the 5'-leader of AT1R transcripts play a role in the translation regulation of AT1R protein, future research is necessary to confirm this hypothesis. These results confirmed that CP may contribute in the development or promotion of lung and heart diseases, through the increase of Ang-II binding and the regulation of ACE.

With respect to FP and UFP, we know that the UFP fraction is included within the FP fraction. For some parameters that we evaluated, such as mRNA and protein levels, both fractions induced the same degree of response in the lungs. However, we were able to distinguish different responses between the fractions in the heart expression of Acta1, HO-1 and AT1R proteins. Thus, differences between FP and UFP can be attributed to the different

composition and the deposition sites in the respiratory tract reached by these two different particulate types.

Particle chemical composition has an important role in particle-induced toxicity because it can promote oxidative stress through chemical catalysis or metabolism and can enhance inflammatory responses. Previously, the chemical composition of PM10 and PM2.5, including the metal and organic partial composition was reported by Guerra et al. [85]. The total metal mass concentrations of the CP and FP were 5488.89 and 2992.11 ng/m3, respectively. We estimated the percent of each metal mass contribution from the total metal mass of CP and FP based on the results from Guerra et al. [85] (Table 3). For ten metals (Fe, Zn, Pb, Mn, Cr, Cu, Ni, V, Co and Cd), we found that the element with greatest mass contribution to CP and FP was Fe, at 38.5 and 48.4 %, respectively. The second most abundant element contributing to the CP and FP masses was Zn, at 37.9 and 12.1 %, respectively. The rest of the metals had a minor contributions to particle mass (less than 12 %), but some elements are more abundant in FP than CP. For example we found more Cd in FP than CP (44.6 times), followed by Co (6.7 times); V (5.1 times); Cu (2.6 times); Mn (2.2 times) and Pb (1.2 times). Biologically relevant effects of the particle composition on RAAS were reported by Li et al. [42], who demonstrated that particle constituents such as V and Cu induce pulmonary artery vasoconstriction through AT1R and ACE. According to the authors, other metals including Ni, Fe, Mn, Zn and Al produced a weak or no effect on vasoconstriction. Based on the percent contribution to the mass, Zn was one of the most abundant. It was shown that Zn contained in PM inhibits total cardiac aconitase activity, induces mitochondrial DNA damage, and causes modest changes in the cardiac expression of mRNAs involved in signaling, ion channel function, oxidative stress, mitochondrial fatty acid metabolism and cell cycle regulation [86].

Table 3

Metal mass contribution in coarse (CP) and fine PM (FP) from subchronic exposure

Metal	CP %	FP %
Fe	38.5	48.4
Zn	37.9	12.1
Mn	5.0	11.1
Pb	6.9	8.3
Cu	4.0	10.3
Cr	4.8	1.7
V	1.0	5.0
Co	0.2	1.2
Cd	0.03	1.2
Ni	1.7	0.7

On the basis of the information presented above and considering the metal composition of the PM in our study, we suggest that the biological effects observed could be related to the presence of divalent metals that are able to mimic prosthetic groups, such as Zn in the ACE enzyme, or mediate oxidative stress and promote inflammation and thus up-regulate AT1R. Although CP and FP share some components, we suggest that the biological effect attributed to PM-associated metal content is related to the sites in the lungs reached by the particulate and their potential to translocate beyond the lungs.

In this study it was not possible to assess UFP mass and collect it for chemical determination. However, evidence in the literature [87–89] allows to propose the participation of divalent metals (i.e., Zn, Cu, Cd, etc.) as the UFP-chemical components mostly involved in the induction of the effect on RAAS and KKS. Moreover, we do not discard that some other components (i.e., endotoxin and possibly other metals) may also contribute to induce this effect as a secondary response of the release of inflammatory mediators.

While particle composition and possibly oxidative stress could explain the expression of AT1R, the second most important mechanism of toxicity from the exposure to PM is the inflammatory process. Two cytokines associated with AT1R expression are the pleiotropic cytokine IL-6 [24, 90] and growth factor TGF-β [91, 92], both of which are also involved in the pathological states of lung and heart disease. We evaluated IL-6 levels as an inflammation marker as well as an AT1R inductor. We observed that an inflammation response was present in our experimental model in the lungs and heart. These data suggest that IL-6 may participate in the regulation of AT1R in the acute phase of the PM exposure but not in the subchronic exposure in the lung. We suggest that in the subchronic exposure the RAAS by itself maintains the induction of AT1R, or inflammatory and/or oxidative stress responses in the lungs may also be involved. On the other hand, heart IL-6 levels in the subchronic exposure seem to increment in a size-dependent manner as well as we observed in the heart AT1R protein. However, future studies should focus to establish whether IL-6 is determinant in the induction of AT1R in the heart since it has been reported that cytokines such as TNFα [23] and IL-1α [25] are involved in the induction of AT1R in rat cardiac fibroblast and smooth muscle cells, respectively.

It is important to highlight that the differences in the PM concentration achieved in the chambers could directly influence the biological responses observed in the present study. The chamber PM concentrations were ~32 μg/m3 for CP, ~178 μg/m3 for FP, and ~107 μg/m3 for UFP. These concentrations suggest the possibility that the highest biological responses should be observed in PM concentration-response relationship, nevertheless, our data seems to indicate that the molecular targets (e.g., AT1R, HO-1 etc.) respond in a particulate size-dependent manner. However, some biological responses were independent of the concentration or the particle size such as the B1r expression in heart in the acute exposure, lung IL-6 levels or the intramyocardial thickness, and could be influenced by PM composition, yet this hypothesis needs to be confirmed. Moreover, we have to consider that our results, based in our experimental design, have uncertainty from other factors that include the detailed PM chemical content, the retained dose and the intrinsic biological background.

Future directions of our study should focus in AT1R independent ligand-activation since it has been reported that AT1R can function as a mechanoreceptor that under mechanical stretch in vitro may induce RAAS elements [93, 94], and probably the physical interaction of PM with AT1R in the cellular membrane may influence the activation of AT1R pathway.

Finally, our results demonstrate that the three fractions of PM were able to modulate their effects through the deregulation of two endocrine systems involved in pulmonary and cardiovascular pathology. These effects could result from the development of the inflammation and oxidative stress processes feeding back on the response of the RAAS.

In this sense our results suggest that the cardiac effect of PM is consequent to a neuro-endocrine stimulation, which includes RAAS and KKS response, probably by mediating vascular tone dysfunction (i.e., hypertension) in the lung as well as in the heart. The augmented AT1R expression observed in this study in the lungs and heart may be related with both processes.

Go to:

Conclusion

Exposure to PM is detrimental to human health. Oxidative stress and inflammation are the major mechanisms that contribute to the impairment of the lung and cardiovascular systems. Furthermore, in the present study we observed that PM induces the expression of the endocrine system RAAS and KKS elements in a time- and probably in a particulate size-dependent manner. PM primarily promotes the expression of AT1R in the lungs and heart, which appears to be involved in the depletion of the antioxidant HO-1, as well as the tissue remodeling and heart gene reprogramming resulting from a subchronic exposure to FP and UFP, concomitantly, PM induces acute IL-6 response in the lung and subchronic response in the heart. Thus, these findings contribute to the understanding of the underlying mechanisms involved in the development of cardiac disease associated with PM exposure.

Go to:

Methods

Inhalation exposure

The present study was carried out in the north of Mexico City, an area with high traffic affluence and industrial activity [95], during the months of May to July, 2009. The particulate concentrator was localized within the Animal Care Unit at CINVESTAV-IPN.

Male Sprague Dawley rats (purchased from Harlan, Mexico; 4 rats/group) were exposed acutely (3 days, 5 h per day) and subchronically (8 weeks, 4 days/week, 5 h per day) to coarse (CP), fine (FP), or ultrafine (UFP) particulate using an aerosol enrichment concentrator system. A control group was exposed to filtered air (FA). The FP fraction was defined as particulate less than or equal to 2.5 μm, which includes the UFP fraction. The particulate concentration in the exposure chambers was 32, 178 and 107 μg/m3 for CP, FP, and UFP, respectively. Simultaneous air ambient concentration of PM10 and PM2.5 were monitored and those results were accompanied with the partial chemical composition of PM10 and PM2.5 in the study developed and reported by Guerra-García et al. [85].

At the end of the each exposure (24 h after the last exposure), the animals were anesthetized (i.p. 10-20 mg/kg of sodium pentobarbital) and euthanized by exsanguination. The lung and heart tissues were dissected and frozen in liquid nitrogen and stored at -70 °C until analysis. A ventricular slice of the heart was fixed in 10 % buffered formaldehyde and embedded in paraffin for histological analysis.

Semi-quantitative reverse transcription-polymerase chain reaction

Total RNA was isolated from the lungs and heart using TRIzol reagent (Invitrogen™, Life Technologies, Thermo Fisher Scientific, Carlsbad, CA, USA). cDNA synthesis was performed with 3 μg of total RNA according to the manufacturer's instructions (SuperScript II, Invitrogen™, Life Technologies, Thermo Fisher Scientific, Carlsbad, CA, USA). Specific oligonucleotides were designed for each gene (Table 4) using GeneRunner software, and we confirmed their amplification using Primer-BLAST [http://www.ncbi.nlm.nih.gov/tools/primer-blast/]. **We chose three RAAS genes (At1r, At2r and Ace) and three KKS genes (B1r, B2r and Klk-1) on the basis of their roles as the effectors and mediators of the metabolism of the active peptides. To evaluate heart gene reprogramming, we evaluated the mRNA levels of Acta1 and Col3a1.** We used 18S and Gapdh as housekeeping genes. After PCR amplification, the PCR products were loaded and subjected to electrophoresis in 1.5 % agarose gels, stained with ethidium bromide and photodocumented in a transilluminator (UVP EC3 imaging system, UVP Inc., Upland, CA, USA). Densitometry was performed with the software Image J (National Institutes of Health, USA).

Table 4

Oligonucleotides used for PCR amplification. The gene name, the sequence of forward (Fw) and reverse (Rv) oligonucleotide, the PCR product and the Genbank ID are shown

Gen	Olinucleotides	PCR product (pb)	Genbank ID
At1r	Fw 5'-AATATTTGGAAACAGCTTGGT-3' Rv 5'-ATGATGATGCAGGTGACTTTG-3'	331	[GenBank: NM_030985]
At2r	Fw 5'-TAGTTCCCCTTGTTTGGTG-3' Rv 5'-GAGGATGGCAAAAGGAAGT-3'	428	[GenBank: NM_012494]
Ace	Fw 5'-CCAACAAGACTGCCACCTG-3' Rv 5'-GTACTGGTGACATCGAGGTTG-3'	457	[GenBank: NM_012544]
B1r	Fw 5'-AGCATCTTCCTGGTGGTGG-3' Rv 5'-CCAGCAGACCAGGAAGGAG-3'	420	[GenBank: NM_030851]
B2r	Fw 5'-GAGATCTACCTGGGCAACCT-3' Rv 5'-AGGAAGGTGCTGATCTGGAA-3'	599	[GenBank: NM_173100]
Klk-1	Fw 5'-CCCTCACCCTGACTTCAAC-3' Rv 5'-TCACACACTGGAGCTCATC-3'	236	[GenBank: 001005382]
Acta1	Fw 5'-ACATCGACATCAGGAAGGAC-3' Rv 5'-CGTCGTACTCCTGCTTGGT-3'	234	[GenBank: NM_019212]
Col3a1	Fw 5'-AGGGTGATCGTGGTGAAAA-3' Rv 5'-TCCTCGATGTCCTTTGATG-3'	239	[GenBank: NM_032085]
18S	Fw 5'-GCAGCTAGGAATAATGGAATA-3' Rv 5'-GACTTTCGTTCTTGATTAATGA-3'	188	[GenBank: NR_046237]
Gapdh	Fw 5'-ACCACAGTCCATGCCATCAC-3' Rv 5'-TGCCAGTGAGCTTCCCGTT-3'	166	[GenBank: NM_017008]

Western blot

To obtain the total protein, the lung samples were homogenized with Nonidet-P40 buffer (150 mM NaCl, 1 % NP40, 50 mM Tris–HCl, pH 8.0, and protease inhibitors) and centrifuged at 10,000 rpm 4 °C. The supernatant was collected and stored at -70 °C until use.

Nuclear and non-nuclear cell fractions were obtained following the Abcam protocol. Briefly, the tissue was homogenized with cytoplasmic buffer (250 mM sucrose, 20 mM HEPES pH 7.4, 10 mM KCl, 1.5 mM MgCl2, 1 mM EDTA, 1 mM EGTA, 1 mM DTT). The homogenate was centrifuged at 3000 rpm for 5 min, and the supernatant (non-nuclear fraction) was removed. The nuclear pellet was dispersed with a pipette, and then the first step was repeated to remove cytosolic contaminants from the pellet. The nuclear pellet was resuspended in the nuclear buffer (cytoplasmic buffer with 10 % glycerol and 0.1 % SDS). Finally, the nuclear pellet was sonicated on ice and centrifuged at 10,000 rpm, and the supernatant was removed and stored at -70 °C. The protein concentrations were determined using Bradford protein assay. A 6× Laemmli buffer was added to 30 µg of protein, and the sample was loaded in 12 % SDS-polyacrylamide gel and transferred to a PVDF membrane.

The membranes were blocked for 1 h with 5 % of not-fat milk. The membranes were then incubated overnight with primary antibodies to AT1R (1:600, rabbit polyclonal AT1 306 antibody, Sc-579), ACE (1:1000; goat polyclonal ACE N-20 antibody, Sc-12184), HO-1 (1:500, rabbit polyclonal HO-1 H-105 antibody, Sc-10789) and γ-GCSc (1:600, rabbit polyclonal γ-GCSc H-338 antibody, Sc-22755) all from Santa Cruz Biotechnology (Delaware Ave, Santa Cruz, CA, USA). HRP-conjugated secondary antibodies (Bio-Rad laboratories, Hercules, CA, USA) were incubated 1 h at a dilution of 1:10,000. Immunoreactivity was detected using ECL western blotting detection reagents (GE health care, Buckinghamshire HP7 9NA, UK). The bands were visualized by exposure to x-ray film. The x-ray film was photodocumented with a UVP (UVP EC3 imaging system, UVP Inc., USA). We used α-actin (donated by Dr. Hernández- Hernández, CINVESTAV-IPN) as an internal control to correct for protein loading. For the subcellular fractions, we used GAPDH (1:1000, mouse monoclonal GAPDH 6C5 antibody, Sc-32,233) and acetyl-Histone-4 (1:1000, mouse monoclonal Ac-Histone H4 Ser 1/Lys 5/Lys 8/Lys 12 antibody, Sc-34,263) to confirm the purity of the fractions.

[3H]-Angiotensin-II binding to lung cell membranes

The lung tissue samples were placed in 10 ml of lysis buffer (10 mM Tris–HCl, 1 mM EGTA, pH 7.4 at 4 °C) and homogenized with a Polytron (3 cycles, 5 s each). The homogenate was centrifuged (1,000×g, 10 min, 4 °C), the pellet was discarded and the supernatant was centrifuged at 42,000×g (20 min, 4 °C). The resulting pellet was resuspended in lysis buffer and centrifuged again (42,000 × g, 20 min, 4 °C). The pellet (membranes) was resuspended in incubation buffer (20 mM Tris–HCl, 5 mM MgCl2, 100 mM NaCl, 2 mg/ml bovine serum albumin (BSA); pH 7.4 at 4 °C), and the suspension was immediately used in binding assays. The protein contents were determined by the Bradford assay, using BSA as standard.

Saturation analysis was carried out in 100 µl of incubation buffer containing [Tyrosil-3,5-3H (N)]-Angiotensin-II (ARC inc., Saint Louis, MO, USA) (0.5-40 nM) and ~40 µg protein. For single-point experiments, the incubations contained 10 nM [3H]-Angiotensin-II. The samples were equilibrated for 60 min at 25 °C in a water bath with continuous gentle rocking, and the incubations were terminated by filtration through Whatman GF/B glass fiber paper, pre-soaked in 0.3 % polyethylenimine. Non-specific binding was determined as the binding insensitive to 100 µM of the antagonist

telmisartan (Sigma Aldrich, USA). The filters were washed 3 times with 1 ml ice-cold Tris–HCl buffer (20 mM, pH 7.4), soaked in 3 ml scintillator, and the tritium content was determined by liquid scintillation spectroscopy (Multi-purpose Scintillation Counter, Beckman LS-6500). The saturation binding data were fit with a hyperbolic function using non-linear regression with GraphPad Prism 5 (Graph Pad Software, San Diego, CA, USA).

Histology

Slides of 5 μm sections of the heart tissues were stained with Hematoxylin/Eosin stain. We photographed all of the intramyocardial coronary arteries observed in the slides (two slides from each tissue sample). We performed a blinded analysis of the measure of the thickness using Image J. Twenty radial measurements for each artery from the intima to the adventitia wall were registered. For the statistical analysis we used the median of each artery; we included in the analysis between 15 to 25 arteries per group. Semi-quantitative analysis of mononuclear cells in heart tissue was performed counting the number of fields with mononuclear cells per slide.

Statistical analysis

All statistical analyses were performed using SigmaPlot version 11.0. We performed descriptive statistical analyses. To compare the four groups, we performed Kruskal-Wallis test, considering non-normal data distribution. Student Newman-Keul's post-hoc test was used for all pair-wise comparisons. We considered the differences to be statistically significant when $P \leq 0.05$. All comparisons were performed with respect to filtered air as the control group.

Go to:

Acknowledgement

This work was funded by Conacyt [Consejo Nacional de Ciencia y Tecnología] Grant No. 57752 and 167778.

Go to:

Footnotes

Competing interest

The authors declare that they have no competing interests.

Authors' contributions

OGAA proposed the molecular targets, carried out the molecular biology, the binding assay, analyzed the data and wrote the manuscript. TMUR participated in the animal exposure and Western blot analyses. JAAM supervised the binding assay and data analysis. OB participated in the data analysis and study supervision. ADVR devised and developed the animal exposure, carried out its design and coordination, and supervised the draft of the manuscript. All authors read and approved the final manuscript.

Go to:

Contributor Information

Octavio Gamaliel Aztatzi-Aguilar, Email: moc.liamg@iztatzammag.

Marisela Uribe-Ramírez, Email: moc.oohay@ebirumt.

José Antonio Arias-Montaño, Email: xm.vatsevnic.oisif@sairaaj.

Olivier Barbier, Email: xm.vatsevnic@reibrabo.

Andrea De Vizcaya-Ruiz, Phone: ++ 52 (55) 5747 3800, Email: xm.vatsevnic@ayacziva.

Go to:

References

1. Pope CA, III, Dockery DW. Health effects of fine particulate air pollution: lines that connect. J Air Waste Manage Assoc. 2006;56:709–742. doi: 10.1080/10473289.2006.10464485. [PubMed] [CrossRef] [Google Scholar]

2. Simkhovich BZ, Kleinman MT, Kloner RA. Air pollution and cardiovascular injury: epidemiology, toxicology, and mechanisms. J Am Coll Cardiol. 2008;52:719–726. doi: 10.1016/j.jacc.2008.05.029. [PubMed] [CrossRef] [Google Scholar]

3. Pope CA, Burnett RT, Thurston GD, Thun MJ, Calle EE, Krewski D, et al. Cardiovascular mortality and long-term exposure to particulate air pollution epidemiological evidence of general pathophysiological pathways of disease. Circulation. 2004;109:71–77. doi: 10.1161/01.CIR.0000108927.80044.7F. [PubMed] [CrossRef] [Google Scholar]

4. Donaldson K, Stone V, Seaton A, MacNee W. Ambient particle inhalation and the cardiovascular system: potential mechanisms. Environ Health Perspect. 2001;109:523. doi: 10.1289/ehp.01109s4523. [PMC free article] [PubMed] [CrossRef] [Google Scholar]

5. Mutlu GM, Green D, Bellmeyer A, Baker CM, Burgess Z, Rajamannan N, et al. Ambient particulate matter accelerates coagulation via an IL-6–dependent pathway. J Clin Invest. 2007;117:2952–2961. doi: 10.1172/JCI30639. [PMC free article] [PubMed] [CrossRef] [Google Scholar]

6. Rhoden CR, Wellenius GA, Ghelfi E, Lawrence J, González-Flecha B. PM-induced cardiac oxidative stress and dysfunction are mediated by autonomic stimulation. Biochim Biophys Acta Gen Subj. 2005;1725:305–313. doi: 10.1016/j.bbagen.2005.05.025. [PubMed] [CrossRef] [Google Scholar]

7. Sharma JN. Role of tissue kallikrein–kininogen–kinin pathways in the cardiovascular system. Arch Med Res. 2006;37:299–306. doi: 10.1016/j.arcmed.2005.08.001. [PubMed] [CrossRef] [Google Scholar]

8. Kuhr F, Lowry J, Zhang Y, Brovkovych V, Skidgel R. Differential regulation of inducible and endothelial nitric oxide synthase by kinin B1 and B2 receptors. Neuropeptides. 2010;44:145–154. doi: 10.1016/j.npep.2009.12.004. [PMC free article] [PubMed] [CrossRef] [Google Scholar]

9. Thomas WG, Mendelsohn FA. Angiotensin receptors: form and function and distribution. Int J Biochem Cell Biol. 2003;35:774–779. doi: 10.1016/S1357-2725(02)00263-7. [PubMed] [CrossRef] [Google Scholar]

10. Lavoie JL, Sigmund CD. Minireview: overview of the renin-angiotensin system—an endocrine and paracrine system. Endocrinology. 2003;144:2179–2183. doi: 10.1210/en.2003-0150. [PubMed] [CrossRef] [Google Scholar]

11. Iwai M, Horiuchi M. Devil and angel in the renin–angiotensin system: ACE–angiotensin II–AT1 receptor axis vs. ACE2–angiotensin-(1–7)–Mas receptor axis. Hypertens Res. 2009;32:533–536. doi: 10.1038/hr.2009.74. [PubMed] [CrossRef] [Google Scholar]

12. Tsutsumi Y, Matsubara H, Masaki H, Kurihara H, Murasawa S, Takai S, et al. Angiotensin II type 2 receptor overexpression activates the vascular kinin system and causes vasodilation. J Clin Invest. 1999;104:925. doi: 10.1172/JCI7886. [PMC free article] [PubMed] [CrossRef] [Google Scholar]

13. Bergaya S, Hilgers RH, Meneton P, Dong Y, Bloch-Faure M, Inagami T, et al. Flow-dependent dilation mediated by endogenous kinins requires angiotensin AT2 receptors. Circ Res. 2004;94:1623–1629. doi: 10.1161/01.RES.0000131497.73744.1a. [PubMed] [CrossRef] [Google Scholar]

14. Bhoola K, Figueroa C, Worthy K. Bioregulation of kinins: kallikreins, kininogens, and kininases. Pharmacol Rev. 1992;44:1–80. [PubMed] [Google Scholar]

15. Yousef GM, Diamandis EP. The New Human Tissue Kallikrein Gene Family: Structure, Function, and Association to Disease 1. Endocr Rev. 2001;22:184–204. [PubMed] [Google Scholar]

16. Rueckschloss U, Quinn MT, Holtz J, Morawietz H. Dose-dependent regulation of NAD (P) H oxidase expression by angiotensin II in human endothelial cells protective effect of angiotensin II type 1 receptor blockade in patients with coronary artery disease. Arterioscler Thromb Vasc Biol. 2002;22:1845–1851. doi: 10.1161/01.ATV.0000035392.38687.65. [PubMed] [CrossRef] [Google Scholar]

17. Rajagopalan S, Kurz S, Münzel T, Tarpey M, Freeman BA, Griendling KK, et al. Angiotensin II-mediated hypertension in the rat increases vascular superoxide production via membrane NADH/NADPH oxidase activation. Contribution to alterations of vasomotor tone. J Clin Invest. 1996;97:1916. doi: 10.1172/JCI118623. [PMC free article] [PubMed] [CrossRef] [Google Scholar]

18. Dias JP, Talbot S, Sénécal J, Carayon P, Couture R. Kinin B1 receptor enhances the oxidative stress in a rat model of insulin resistance: outcome in hypertension, allodynia and metabolic complications. PLoS One. 2010;5 doi: 10.1371/journal.pone.0012622. [PMC free article] [PubMed] [CrossRef] [Google Scholar]

19. Ni A, Yin H, Agata J, Yang Z, Chao L, Chao J. Overexpression of kinin B1 receptors induces hypertensive response to des-Arg9-bradykinin and susceptibility to inflammation. J Biol Chem. 2003;278:219–225. doi: 10.1074/jbc.M209490200. [PubMed] [CrossRef] [Google Scholar]

20. Morand-Contant M, Anand-Srivastava MB, Couture R. Kinin B1 receptor upregulation by angiotensin II and endothelin-1 in rat vascular smooth muscle cells: receptors and mechanisms. Am J Physiol Heart Circ Physiol. 2010;299:H1625–H1632. doi: 10.1152/ajpheart.00735.2009. [PubMed] [CrossRef] [Google Scholar]

21. Kintsurashvili E, Duka I, Gavras I, Johns C, Farmakiotis D, Gavras H. Effects of ANG II on bradykinin receptor gene expression in cardiomyocytes and vascular smooth muscle cells. Am J Physiol Heart Circ Physiol. 2001;281:H1778–H1783. [PubMed] [Google Scholar]

22. Harrison-Bernard LM, El-Dahr SS, O'Leary DF, Navar LG. Regulation of angiotensin II type 1 receptor mRNA and protein in angiotensin II–induced hypertension. Hypertension. 1999;33:340–346. doi: 10.1161/01.HYP.33.1.340. [PubMed] [CrossRef] [Google Scholar]

23. Gurantz D, Cowling RT, Villarreal FJ, Greenberg BH. Tumor necrosis factor-α upregulates angiotensin II type 1 receptors on cardiac fibroblasts. Circ Res. 1999;85:272–279. doi: 10.1161/01.RES.85.3.272. [PubMed] [CrossRef] [Google Scholar]

24. Wassmann S, Stumpf M, Strehlow K, Schmid A, Schieffer B, Böhm M, et al. Interleukin-6 induces oxidative stress and endothelial dysfunction by overexpression of the angiotensin II type 1 receptor. Circ Res. 2004;94:534–541. doi: 10.1161/01.RES.0000115557.25127.8D. [PubMed] [CrossRef] [Google Scholar]

25. Sasamura H, Nakazato Y, Hayashida T, Kitamura Y, Hayashi M, Saruta T. Regulation of vascular type 1 angiotensin receptors by cytokines. Hypertension. 1997;30:35–41. doi: 10.1161/01.HYP.30.1.35. [PubMed] [CrossRef] [Google Scholar]

26. Kranzhöfer R, Schmidt J, Pfeiffer CA, Hagl S, Libby P, Kübler W. Angiotensin induces inflammatory activation of human vascular smooth muscle cells. Arterioscler Thromb Vasc Biol. 1999;19:1623–1629. doi: 10.1161/01.ATV.19.7.1623. [PubMed] [CrossRef] [Google Scholar]

27. Tiffany CW, Burch RM. Bradykinin stimulates tumor necrosis factor and interleukin-1 release from macrophages. FEBS Lett. 1989;247:189–192. doi: 10.1016/0014-5793(89)81331-6. [PubMed] [CrossRef] [Google Scholar]

28. Hayashi R, Yamashita N, Matsui S, Fujita T, Araya J, Sassa K, et al. Bradykinin stimulates IL-6 and IL-8 production by human lung fibroblasts through ERK-and p38 MAPK-dependent mechanisms. Eur Respir J. 2000;16:452–458. doi: 10.1034/j.1399-3003.2000.016003452.x. [PubMed] [CrossRef] [Google Scholar]

29. Yayama K, Okamoto H. Angiotensin II-induced vasodilation via type 2 receptor: Role of bradykinin and nitric oxide. Int Immunopharmacol. 2008;8:312–318. doi: 10.1016/j.intimp.2007.06.012. [PubMed] [CrossRef] [Google Scholar]

30. Brasier AR, Recinos A, Eledrisi MS. Vascular inflammation and the renin-angiotensin system. Arterioscler Thromb Vasc Biol. 2002;22:1257–1266. doi: 10.1161/01.ATV.0000021412.56621.A2. [PubMed] [CrossRef] [Google Scholar]

31. Kaplan AP, Joseph K, Silverberg M. Pathways for bradykinin formation and inflammatory disease. J allergy clin immunol. 2002;109:195–209. doi: 10.1067/mai.2002.121316. [PubMed] [CrossRef] [Google Scholar]

32. Dielis AW, Smid M, Spronk HM, Hamulyak K, Kroon AA, ten Cate H, et al. The Prothrombotic Paradox of Hypertension Role of the Renin-Angiotensin and Kallikrein-Kinin Systems. Hypertension. 2005;46:1236–1242. doi: 10.1161/01.HYP.0000193538.20705.23. [PubMed] [CrossRef] [Google Scholar]

33. Remková A, Remko M. The role of renin-angiotensin system in prothrombotic state in essential hypertension. Physiol Res. 2010;59. [PubMed]

34. Campbell D. Towards understanding the kallikrein-kinin system: insights from measurement of kinin peptides. Braz J Med Biol Res. 2000;33:665–677. doi: 10.1590/S0100-879X2000000600008. [PubMed] [CrossRef] [Google Scholar]

35. Su JB. Different cross-talk sites between the renin–angiotensin and the kallikrein–kinin systems. J Renin-Angiotensin-Aldosterone Syst. 2013;1470320312474854. [PubMed]

36. Schmaier AH. The kallikrein-kinin and the renin-angiotensin systems have a multilayered interaction. Am J Physiol Regul, Integr Comp Physiol. 2003;285:R1–R13. doi: 10.1152/ajpregu.00535.2002. [PubMed] [CrossRef] [Google Scholar]

37. Gillis C. Metabolism of vasoactive hormones by lung. Anesthesiology. 1973;39:626–632. doi: 10.1097/00000542-197312000-00015. [PubMed] [CrossRef] [Google Scholar]

38. Zhang L, Wang H, Xiao Y, Cai Y, Ren J. Early lung injury contributes to lung fibrosis via AT1 receptor in rats. Acta Pharmacol Sin. 2007;28:227–237. doi: 10.1111/j.1745-7254.2007.00493.x. [PubMed] [CrossRef] [Google Scholar]

39. Myou S, Fujimura M, Kamio Y, Ishiura Y, Kurashima K, Tachibana H, et al. Effect of losartan, a type 1 angiotensin II receptor antagonist, on bronchial hyperresponsiveness to methacholine in patients with bronchial asthma. Am J Respir Crit Care Med. 2000;162:40–44. doi: 10.1164/ajrccm.162.1.9907127. [PubMed] [CrossRef] [Google Scholar]

40. Ulrich MM, Alink GM, Kumarathasan P, Vincent R, Boere AJF, Cassee FR. Health effects and time course of particulate matter on the cardiopulmonary system in rats with lung inflammation. J Toxicol Environ Health A. 2002;65:1571–1595. doi: 10.1080/00984100290071676. [PubMed] [CrossRef] [Google Scholar]

41. Gunnison A, Chen LC. Effects of subchronic exposures to concentrated ambient particles in mice: VI. gene expression in heart and lung tissue. Inhal toxicol. 2005;17:225–233. doi: 10.1080/08958370590912851. [PubMed] [CrossRef] [Google Scholar]

42. Li Z, Carter JD, Dailey LA, Huang Y-CT. Pollutant particles produce vasoconstriction and enhance MAPK signaling via angiotensin type I receptor. Environ Health Perspect. 2005;113:1009. doi: 10.1289/ehp.7736. [PMC free article] [PubMed] [CrossRef] [Google Scholar]

43. Wold LE, Ying Z, Hutchinson KR, Velten M, Gorr MW, Velten C, et al. Cardiovascular remodeling in response to long-term exposure to fine particulate matter air pollution. Circ Heart Fail. 2012;5:452–461. doi: 10.1161/CIRCHEARTFAILURE.112.966580. [PMC free article] [PubMed] [CrossRef] [Google Scholar]

44. Ying Z, Yue P, Xu X, Zhong M, Sun Q, Mikolaj M, et al. Air pollution and cardiac remodeling: a role for RhoA/Rho-kinase. Am JPhysiol Heart Circ Physiol. 2009;296:H1540. doi: 10.1152/ajpheart.01270.2008. [PMC free article] [PubMed] [CrossRef] [Google Scholar]

45. Rosati AM, Traversa U. Mechanisms of inhibitory effects of zinc and cadmium ions on agonist binding to adenosine A1 receptors in rat brain. Biochem Pharmacol. 1999;58:623–632. doi: 10.1016/S0006-2952(99)00135-5. [PubMed] [CrossRef] [Google Scholar]

46. Hubbard PC, Lummis SC. Zn < sup > 2 + </sup > enhancement of the recombinant 5-HT < sub > 3</sub > receptor is modulated by divalent cations. Eur J Pharmacol. 2000;394:189–197. doi: 10.1016/S0014-2999(00)00143-6. [PubMed] [CrossRef] [Google Scholar]

47. Marinissen MJ, Gutkind JS. G-protein-coupled receptors and signaling networks: emerging paradigms. Trends Pharmacol Sci. 2001;22:368–376. doi: 10.1016/S0165-6147(00)01678-3. [PubMed] [CrossRef] [Google Scholar]

48. Boivin B, Vaniotis G, Allen BG, Hebert TE. G protein-coupled receptors in and on the cell nucleus: a new signaling paradigm? J Recep Signal Transduction. 2008;28:15–28. doi: 10.1080/10799890801941889. [PubMed] [CrossRef] [Google Scholar]

49. Lu D, Yang H, Shaw G, Raizada MK. Angiotensin II-Induced Nuclear Targeting of the Angiotensin Type 1 (AT1) Receptor in Brain Neurons 1. Endocrinology. 1998;139:365–375. [PubMed] [Google Scholar]

50. Tadevosyan A, Maguy A, Villeneuve LR, Babin J, Bonnefoy A, Allen BG, et al. Nuclear-delimited angiotensin receptor-mediated signaling regulates cardiomyocyte gene expression. J Biol Chem. 2010;285:22338–22349. doi: 10.1074/jbc.M110.121749. [PMC free article] [PubMed] [CrossRef] [Google Scholar]

51. Figueroa CD, Marchant A, Novoa U, Förstermann U, Jarnagin K, Schölkens B, et al. Differential distribution of bradykinin B2 receptors in the rat and human cardiovascular system. Hypertension. 2001;37:110–120. doi: 10.1161/01.HYP.37.1.110. [PubMed] [CrossRef] [Google Scholar]

52. McEachern AE, Shelton ER, Bhakta S, Obernolte R, Bach C, Zuppan P, et al. Expression cloning of a rat B2 bradykinin receptor. Proc Natl Acad Sci. 1991;88:7724–7728. doi: 10.1073/pnas.88.17.7724. [PMC free article] [PubMed] [CrossRef] [Google Scholar]

53. Madeddu P, Emanueli C, Varoni MV, Demontis MP, Anania V, Gorioso N, et al. Regulation of bradykinin B2-receptor expression by oestrogen. Br J Pharmacol. 1997;121:1763–1769. doi: 10.1038/sj.bjp.0701255. [PMC free article] [PubMed] [CrossRef] [Google Scholar]

54. Kim S, Iwao H. Molecular and cellular mechanisms of angiotensin II-mediated cardiovascular and renal diseases. Pharmacol Rev. 2000;52:11–34. [PubMed] [Google Scholar]

55. Paradis P, Dali-Youcef N, Paradis FW, Thibault G, Nemer M. Overexpression of angiotensin II type I receptor in cardiomyocytes induces cardiac hypertrophy and remodeling. Proc Natl Acad Sci. 2000;97:931–936. doi: 10.1073/pnas.97.2.931. [PMC free article] [PubMed] [CrossRef] [Google Scholar]

56. Kim S, Ohta K, Hamaguchi A, Yukimura T, Miura K, Iwao H. Angiotensin II induces cardiac phenotypic modulation and remodeling in vivo in rats. Hypertension. 1995;25:1252–1259. doi: 10.1161/01.HYP.25.6.1252. [PubMed] [CrossRef] [Google Scholar]

57. Tsybouleva N, Zhang L, Chen S, Patel R, Lutucuta S, Nemoto S, et al. Aldosterone, through novel signaling proteins, is a fundamental molecular bridge between the genetic defect and the cardiac phenotype of hypertrophic cardiomyopathy. Circulation. 2004;109:1284–1291. doi: 10.1161/01.CIR.0000121426.43044.2B. [PMC free article] [PubMed] [CrossRef] [Google Scholar]

58. Sano M, Fukuda K, Kodama H, Pan J, Saito M, Matsuzaki J, et al. Interleukin-6 family of cytokines mediate angiotensin II-induced cardiac hypertrophy in rodent cardiomyocytes. J Biol Chem. 2000;275:29717–29723. doi: 10.1074/jbc.M003128200. [PubMed] [CrossRef] [Google Scholar]

59. Schmid O, Möller W, Semmler-Behnke MA, Ferron G, Karg E, Lipka J, et al. Dosimetry and toxicology of inhaled ultrafine particles. Biomarkers. 2009;14:67–73. doi: 10.1080/13547500902965617. [PubMed] [CrossRef] [Google Scholar]

60. Gould NS, Day BJ. Targeting maladaptive glutathione responses in lung disease. Biochem Pharmacol. 2011;81:187–193. doi: 10.1016/j.bcp.2010.10.001. [PMC free article] [PubMed] [CrossRef] [Google Scholar]

61. Cross CE, van der Vliet A, O'Neill CA, Louie S, Halliwell B. Oxidants, antioxidants, and respiratory tract lining fluids. Environ Health Perspect. 1994;102:185. doi: 10.1289/ehp.94102s10185. [PMC free article] [PubMed] [CrossRef] [Google Scholar]

62. Otterbein LE, Choi AM. Heme oxygenase: colors of defense against cellular stress. Am J PhysioLung Cell Mol Physiol. 2000;279:L1029–L1037. [PubMed] [Google Scholar]

63. Abraham NG, Kappas A. Heme oxygenase and the cardiovascular–renal system. Free Radic Biolo Med. 2005;39:1–25. doi: 10.1016/j.freeradbiomed.2005.03.010. [PubMed] [CrossRef] [Google Scholar]

64. Ryter SW, Otterbein LE, Morse D, Choi AM. Heme oxygenase/carbon monoxide signaling path-ways: Regulation and functional significance. In Oxygen/Nitrogen Radicals: Cell Injury and Disease. Springer; 2002. pp. 249–263. [PubMed] [Google Scholar]

65. Idriss NK, Blann AD, Lip GY. Hemoxygenase-1 in cardiovascular disease. J Am Coll Cardiol. 2008;52:971–978. doi: 10.1016/j.jacc.2008.06.019. [PubMed] [CrossRef] [Google Scholar]

66. Fredenburgh LE, Perrella MA, Mitsialis SA. The role of heme oxygenase-1 in pulmonary disease. Am J Respir Cell Mol Biol. 2007;36:158–165. doi: 10.1165/rcmb.2006-0331TR. [PMC free article] [PubMed] [CrossRef] [Google Scholar]

67. Ishizaka N, Griendling KK. Heme oxygenase-1 is regulated by angiotensin II in rat vascular smooth muscle cells. Hypertension. 1997;29:790–795. doi: 10.1161/01.HYP.29.3.790. [PubMed] [CrossRef] [Google Scholar]

68. Li N, Wang M, Oberley TD, Sempf JM, Nel AE. Comparison of the pro-oxidative and proinflammatory effects of organic diesel exhaust particle chemicals in bronchial epithelial cells and macrophages. JImmunol. 2002;169:4531–4541. doi: 10.4049/jimmunol.169.8.4531. [PubMed] [CrossRef] [Google Scholar]

69. Danielsen PH, Møller P, Jensen KA, Sharma AK, Wallin H, Bossi R, et al. Oxidative stress, DNA damage, and inflammation induced by ambient air and wood smoke particulate matter in human A549 and THP-1 cell lines. Chem Res Toxicol. 2011;24:168–184. doi: 10.1021/tx100407m. [PubMed] [CrossRef] [Google Scholar]

70. Li N, Sioutas C, Cho A, Schmitz D, Misra C, Sempf J, et al. Ultrafine particulate pollutants induce oxidative stress and mitochondrial damage. Environ Health Perspect. 2003;111:455. doi: 10.1289/ehp.6000. [PMC free article] [PubMed] [CrossRef] [Google Scholar]

71. Sugimoto R, Kumagai Y, Nakai Y, Ishii T. 9, 10-Phenanthraquinone in diesel exhaust particles downregulates Cu, Zn–SOD and HO-1 in human pulmonary epithelial cells: Intracellular iron scavenger 1, 10-phenanthroline affords protection against apoptosis. Free Radic Biol Med. 2005;38:388–395. doi: 10.1016/j.freeradbiomed.2004.11.003. [PubMed] [CrossRef] [Google Scholar]

72. Suzuki M, Betsuyaku T, Ito Y, Nagai K, Nasuhara Y, Kaga K, et al. Down-regulated NF-E2–related factor 2 in pulmonary macrophages of aged smokers and patients with chronic obstructive pulmonary disease. Am J Respir Cell Mol Biol. 2008;39:673–682. doi: 10.1165/rcmb.2007-0424OC. [PubMed] [CrossRef] [Google Scholar]

73. Yamada N, Yamaya M, Okinaga S, Nakayama K, Sekizawa K, Shibahara S, et al. Microsatellite polymorphism in the heme oxygenase-1 gene promoter is associated with susceptibility to emphysema. Am J Hum Genet. 2000;66:187–195. doi: 10.1086/302729. [PMC free article] [PubMed] [CrossRef] [Google Scholar]

74. Kaneda H, Ohno M, Taguchi J, Togo M, Hashimoto H, Ogasawara K, et al. Heme oxygenase-1 gene promoter polymorphism is associated with coronary artery disease in Japanese patients with coronary risk factors. Arterioscler Thromb Vasc Biol. 2002;22:1680–1685. doi: 10.1161/01.ATV.0000033515.96747.6F. [PubMed] [CrossRef] [Google Scholar]

75. Li H-J, Yin H, Yao Y-Y, Shen B, Bader M, Chao L, et al. Tissue kallikrein protects against pressure overload-induced cardiac hypertrophy through kinin B2 receptor and glycogen synthase kinase-3β activation. Cardiovasc Res. 2007;73:130–142. doi: 10.1016/j.cardiores.2006.10.014. [PMC free article] [PubMed] [CrossRef] [Google Scholar]

76. Meneton P, Bloch-Faure M, Hagege AA, Ruetten H, Huang W, Bergaya S, et al. Cardiovascular abnormalities with normal blood pressure in tissue kallikrein-deficient mice. Proc Natl Acad Sci. 2001;98:2634–2639. doi: 10.1073/pnas.051619598. [PMC free article] [PubMed] [CrossRef] [Google Scholar]

77. Borgoño CA, Diamandis EP. The emerging roles of human tissue kallikreins in cancer. Nat Rev Cancer. 2004;4:876–890. doi: 10.1038/nrc1474. [PubMed] [CrossRef] [Google Scholar]

78. Christiansen SC, Proud D, Sarnoff RB, Juergens U, Cochrane CG, Zuraw BL. Elevation of tissue kallikrein and kinin in the airways of asthmatic subjects after endobronchial allergen challenge. Am Rev Respir Dis. 1992;145:900–905. doi: 10.1164/ajrccm/145.4_Pt_1.900. [PubMed] [CrossRef] [Google Scholar]

79. Sexton D, Chen T, Martik D, Kuzmic P, Kuang G, Chen J, et al. Specific inhibition of tissue kallikrein 1 with a human monoclonal antibody reveals a potential role in airway diseases. Biochem J. 2009;422:383–392. doi: 10.1042/BJ20090010. [PubMed] [CrossRef] [Google Scholar]

80. Takimoto M, Mitani H, Hori S, Kimura M, Bandoh T, Okada T. Expression, secretion, and inhibition of angiotensin-converting enzyme in cultured human bronchial epithelial cells. Eur J Pharmacol. 1999;370:169–177. doi: 10.1016/S0014-2999(99)00116-8. [PubMed] [CrossRef] [Google Scholar]

81. Kohlstedt K, Gershome C, Friedrich M, Muller-Esterl W, Alhenc-Gelas F, Busse R, et al. Angiotensin-converting enzyme (ACE) dimerization is the initial step in the ACE inhibitor-induced ACE signaling cascade in endothelial cells. Mol Pharmacol. 2006;69:1725–1732. doi: 10.1124/mol.105.020636. [PubMed] [CrossRef] [Google Scholar]

82. Kohlstedt K, Shoghi F, Müller-Esterl W, Busse R, Fleming I. CK2 phosphorylates the angiotensin-converting enzyme and regulates its retention in the endothelial cell plasma membrane. Circ Res. 2002;91:749–756. doi: 10.1161/01.RES.0000038114.17939.C8. [PubMed] [CrossRef] [Google Scholar]

83. Kohlstedt K, Busse R, Fleming I. Signaling via the angiotensin-converting enzyme enhances the expression of cyclooxygenase-2 in endothelial cells. Hypertension. 2005;45:126–132. doi: 10.1161/01.HYP.0000150159.48992.11. [PubMed] [CrossRef] [Google Scholar]

84. Mori Y, Matsubara H, Murasawa S, Kijima K, Maruyama K, Tsukaguchi H, et al. Translational regulation of angiotensin II type 1A receptor role of upstream AUG triplets. Hypertension. 1996;28:810–817. doi: 10.1161/01.HYP.28.5.810. [PubMed] [CrossRef] [Google Scholar]

85. Guerra R, Vera-Aguilar E, Uribe-Ramirez M, Gookin G, Camacho J, Osornio-Vargas A, et al. Exposure to inhaled particulate matter activates early markers of oxidative stress, inflammation and unfolded protein response in rat striatum. Toxicol Lett. 2013;222:146–154. doi: 10.1016/j.toxlet.2013.07.012. [PMC free article] [PubMed] [CrossRef] [Google Scholar]

86. Kodavanti UP, Schladweiler MC, Gilmour PS, Wallenborn JG, Mandavilli BS, Ledbetter AD, et al. The role of particulate matter-associated zinc in cardiac injury in rats. Environ Health Perspect. 2008;13–20. [PMC free article] [PubMed]

87. Hughes LS, Cass GR, Gone J, Ames M, Olmez I. Physical and chemical characterization of atmospheric ultrafine particles in the Los Angeles area. Environ Sci Technol. 1998;32:1153–1161. doi: 10.1021/es970280r. [CrossRef] [Google Scholar]

88. Utsunomiya S, Jensen KA, Keeler GJ, Ewing RC. Direct identification of trace metals in fine and ultrafine particles in the Detroit urban atmosphere. Environ Sci Technol. 2004;38:2289–2297. doi: 10.1021/es035010p. [PubMed] [CrossRef] [Google Scholar]

89. Lin C-C, Chen S-J, Huang K-L, Hwang W-I, Chang-Chien G-P, Lin W-Y. Characteristics of metals in nano/ultrafine/fine/coarse particles collected beside a heavily trafficked road. Environ Sci Technol. 2005;39:8113–8122. doi: 10.1021/es048182a. [PubMed] [CrossRef] [Google Scholar]

90. Barnes PJ. The cytokine network in asthma and chronic obstructive pulmonary disease. J Clin Invest. 2008;118:3546–3556. doi: 10.1172/JCI36130. [PMC free article] [PubMed] [CrossRef] [Google Scholar]

91. Camoretti-Mercado B, Solway J. Transforming growth factor-β1 and disorders of the lung. Cell Biochem Biophys. 2005;43:131–148. doi: 10.1385/CBB:43:1:131. [PubMed] [CrossRef] [Google Scholar]

92. Rosenkranz S. TGF-β1 and angiotensin networking in cardiac remodeling. Cardiovasc Res. 2004;63:423–432. doi: 10.1016/j.cardiores.2004.04.030. [PubMed] [CrossRef] [Google Scholar]

93. Zou Y, Akazawa H, Qin Y, Sano M, Takano H, Minamino T, et al. Mechanical stress activates angiotensin II type 1 receptor without the involvement of angiotensin II. Nat Cell Biol. 2004;6:499–506. doi: 10.1038/ncb1137. [PubMed] [CrossRef] [Google Scholar]

94. Malhotra R, Sadoshima J, Brosius FC, Izumo S. Mechanical stretch and angiotensin II differentially upregulate the renin-angiotensin system in cardiac myocytes in vitro. Circ Res. 1999;85:137–146. doi: 10.1161/01.RES.85.2.137. [PubMed] [CrossRef] [Google Scholar]

95. De Vizcaya-Ruiz A, Gutiérrez-Castillo M, Uribe-Ramirez M, Cebrián M, Mugica-Alvarez V, Sepúlveda J, et al. Characterization and in vitro biological effects of concentrated particulate matter from Mexico City. Atmos Environ. 2006;40:583–592. doi: 10.1016/j.atmosenv.2005.12.073. [CrossRef] [Google Scholar]

Spike Protein

The researchers, led by Jason McLellan of the University of Texas at Austin, defined the structure of 2019-nCoV's spike protein using a technique called cryogenic electron microscopy, or "Cryo-EM". This involves cooling the protein to below -150℃, so that it crystallises and then its structure can be determined with near-atomic resolution.

The newly discovered molecular structure of the 2019-nCoV spike protein, which the virus uses as a 'key' to gain access to human cells. Wrapp et al. 2019/Science

They also identified the "keyhole", the host cell receptor: it is a human protein called angiotensin converting enzyme 2 (ACE2). This is the same human receptor protein targeted by the earlier SARS coronavirus.

But, disturbingly, the researchers found that 2019-nCoV binds to ACE2 with much higher affinity (10-20 times higher!) than SARS. In other words, 2019-nCoV's "key" is a lot "stickier" than the SARS one. It's like a SARS "key" covered in superglue. This means that once it's in the lock, it's far less likely to be shaken loose and is therefore presumably more effective at invading our cells.

https://science.sciencemag.org/content/sci/early/2020/02/19/science.abb2507.full.pdf

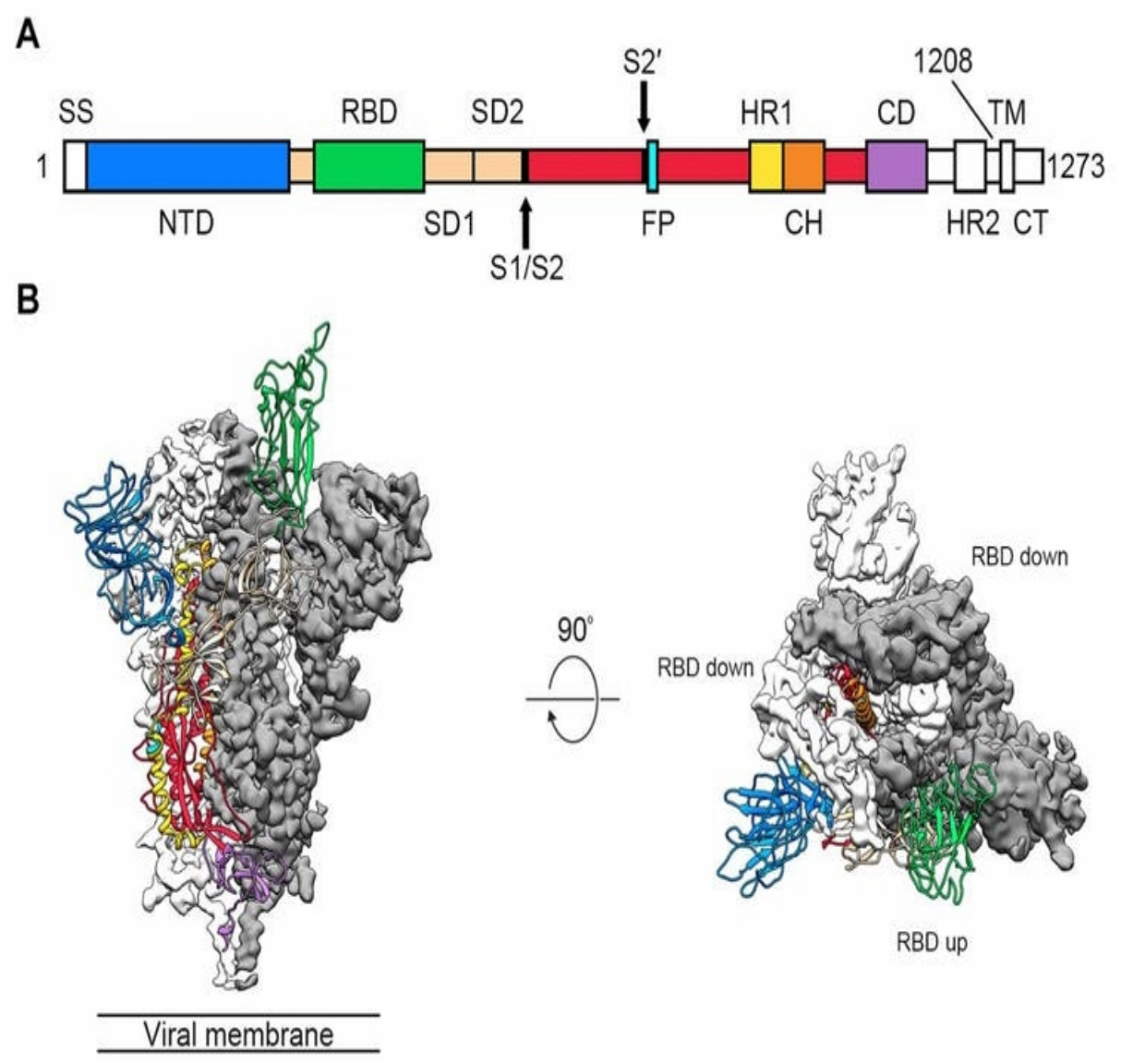

Antibodies against trimeric S glycoprotein protect hamsters against SARS-CoV challenge despite their capacity to mediate Fc RII-dependent entry into B cells *in vitro*

Yiu Wing Kam [a,*,1], Francois Kien [a,1], Anjeanette Roberts [c,1], Yan Chung Cheung [b], Elaine W. Lamirande [c], Leatrice Vogel [c], Shui Ling Chu [a], Jane Tse [a], Jeannette Guarner [d], Sherif R. Zaki [d], Kanta Subbarao [c], Malik Peiris [b], B´eatrice Nal [a], Ralf Altmeyer [e]

[a] *HKU-Pasteur Research Centre, 8 Sassoon Road, Hong Kong SAR, China*

Department of Microbiology, The University of Hong Kong, Hong Kong SAR, China Laboratory of Infectious Diseases, NIAID, National Institutes of Health, MSC-8007, 50 South Drive, Bethesda, MD 20892-8007, USA [d] *Centers for Disease Control and Prevention, Atlanta, GA 30333, USA* [e] *CombinatorX, 11 Biopolis Way, Helios #08-05/06, Singapore 128667*

Received 12 March 2006; received in revised form 30 July 2006; accepted 10 August 2006 Available online 22 August 2006

Abstract

Vaccine-induced antibodies can prevent or, in the case of feline infectious peritonitis virus, aggravate infections by coronaviruses. We investigated whether a recombinant native full-length S-protein trimer (triSpike) of severe acute respiratory syndrome coronavirus (SARS- CoV) was able to elicit a neutralizing and protective immune response in animals and analyzed the capacity of anti-S antibodies to mediate antibody-dependent enhancement (ADE) of virus entry *in vitro* and enhancement of replication *in vivo*. SARS-CoV-specific serum and mucosal immunoglobulins were readily detected in immunized animals. Serum IgG blocked binding of the S-protein to the ACE2 receptor and neutralized SARS-CoV infection *in vitro*. Entry into human B cell lines occurred in a Fc RII-dependent and ACE2-independent fashion indicating that ADE of virus entry is a novel cell entry mechanism of SARS-CoV. Vaccinated animals showed no signs of enhanced lung pathology or hepatitis and viral load was undetectable or greatly reduced in lungs following challenge with SARS-CoV. Altogether our results indicate that a recombinant trimeric S protein was able to elicit an efficacious protective immune response *in vivo* and warrant concern in the safety evaluation of a human vaccine against SARS-CoV.

Keywords: **SARS-CoV; Protection; ADE**

1. Introduction

Coronavirus infections of the human respiratory tract occur frequently. Infections by HCoV-229E and HCoV-OC43 account for 15% of all common colds in humans and recently identified human coronavirus NL63 and HKU1 are associ- ated with acute respiratory distress syndrome and pneumonia [1,2]. While most coronavirus infections are mild and self- limiting, infections by severe acute respiratory syndrome coronavirus (SARS-CoV) result in high mortality and mor- bidity [3]. There is currently no vaccine available against any human coronavirus infection.

The S-protein is a 150-180 kDa highly glycosylated trimeric class-I fusion protein [4,5] responsible for receptor binding, virus-membrane fusion and tissue tropism. Angiotensin con- verting enzyme 2 (ACE2) has been identified as the functional receptor for virus entry into susceptible target cells [6,7], but C-type lectin L-SIGN (CD209L) has also been shown to mediate virus

The viral surface Spike glycoprotein (S) is the key target for protective neutralizing antibodies against coronaviruses.

* Corresponding author at: HKU-Pasteur Research Centre, Dexter HC Man Building, 8, Sassoon Road, Pokfulam, Hong Kong, China. Tel.: +852 2816 8402; fax: +852 2872 5782.
E-mail address: Jasonkamyiuwing@yahoo.com.hk (Y.W. Kam).
[1] Contributed equally to this work.

uptake [8]. S-mediated viral entry occurs in a pH-dependent manner [9,10] and can be inhibited by S-specific sera [11]. Neutralizing antibodies are broadly elicited in patients with SARS [12] and passive transfer of S-specific antibodies, including monoclonal antibodies directed against the receptor-binding domain (RBD) of S [13], to na¨ıve ani- mals confer protection to SARS-CoV

challenge indicating that the humoral immune response alone can protect against SARS-CoV [14-18].

SARS vaccine candidates should induce strong protective immunity against infection and person-to-person transmission which requires a humoral immune response at both systemic and mucosal levels and absence of immunopathol- ogy. Different vaccine candidates have been explored for SARS including DNA [19], Modified Vaccinia virus Ankara (MVA) [16] subunit vaccine [20] or inactivated virus vaccine [21-23] and they all have been shown to induce neutraliz- ing and protective responses. While protection was achieved in the mouse with a recombinant MVA virus expressing S protein [16], vaccination with a different MVA-S construct failed to elicit a sustained serum neutralizing anti- body titer to SARS-CoV in ferrets and subsequent challenge with SARS-CoV was associated with hepatitis [24]. *In vitro* data also demonstrate that anti-S immune responses can enhance SARS-CoV entry into target cells. Yang and col- leagues showed that entry of SARS-CoV pseudotype viruses, expressing the palm civet S-protein, into a human renal epithelial cell-line was enhanced by human S-specific neu- tralizing antibodies [25]. Such *in vitro* detectable facilitating antibodies can be correlated with disease enhancement in feline infectious peritonitis virus-infected cats (FIPV) and it has been shown that vaccine-induced anti-S antibodies and macrophage-expressed Fc receptors (FcR) are key factors of antibody-dependent enhancement (ADE) [26,27] in cats.

Animal models for SARS are useful to evaluate the neu- tralizing or enhancing capacity of antibodies *in vivo*. Several animal models have been proposed for SARS including mice, ferrets, hamsters, rhesus and cynomologus macaques [15,28-30]. The hamster is an interesting small animal model as it reproduces several pathological features of human SARS including high titer replication of SARS-CoV in lungs and nasal turbinates and marked lung pathology including cellular necrosis and inflammatory cell infiltrates [30]. In the present study, we analyzed the immune response to a recombinant native full-length S protein trimer of SARS-CoV. Neutralizing and enhancing activity could be detected in sera of immunized animals and human convalescent SARS patient sera *in vitro* while challenge experiments in hamsters indicate complete protection and absence of disease enhancement *in vivo*.

2. Materials and methods

2.1. Cell lines and expression vectors

Human Raji B and BHK-21 cells were cultured as described previously [31,32]. HEK293T, VeroE6, FRhK-4 and murine macrophagic J774A1 cell lines were cultured at 37 °C, 5% CO_2, in Dulbecco's modified Eagle medium supplemented with 10% FBS, 100 U penicillin/ml, 100 g streptomycin/ml. Optimized DNA and Semliki Forest Virus expression vectors encoding SARS-CoV S-protein fused to a C-terminal FLAG-sequence were described previously [33].

2.2. Immunoaffinity purification and biochemical analysis of S-protein

For protein production BHK cells were cultured in the presence or absence of cycloheximide (100 g/ml), added at 7 h pre-harvest. Fourteen hours post-infection/transfection BHK-21 cells were lysed (20 mM Tris-HCl pH 7.5, 150 mM NaCl, 2 mM EDTA, 1% Triton X-100) and incubated for 5 min on ice. The collected lysate was vortexed, incubated for another 15 min on ice prior to centrifugation at 13,000 rpm for 15 min. Recombinant S-protein was immunopurified using anti-FLAG M2 mAb-coated agarose beads (Sigma) as described previously [31]. The quantity and quality of recombinant S-protein was assessed by SDS-PAGE and Western Blot using BAP-FLAG protein and microBSA methods as standards for protein quantification [31,32]. Mouse sera were diluted (1/500) prior to Western Blot analysis and immune complexes detected with HRP-conjugated anti-mouse IgG (H + L) (1/1000) (Zymed), followed by visualization of the bands on X-ray film (Kodak) using chemiluminescence (Amersham Biosciences).

2.3. Immunization with triSpike

Balb/c mice 6-8 weeks old (n = 3 per group) were immunized intraperitoneally (i.p.) with 20 g of purified triSpike or triSpike in 1 mg of aluminium hydroxide gel (alum) on days 0, 16 and 32. Animals in the control group received PBS with 1 mg of alum on the same days. Blood samples were col- lected by saphenous vein bleeding at indicated time points in accordance with local guidelines and sera were prepared and heat-inactivated. Fecal samples [34] and nasal lavages [35] were prepared as described previously. HRP-conjugated anti-mouse IgG (H + L) or IgA (1/1000) (Zymed) were used to detect the existence of IgG or IgA antibody against triSpike in immunized mice fecal and nasal lavage sample. Absence of blood contamination was confirmed using the Hema-Screen occult blood detection kit (Stanbio Laboratory). Antibodies from fecal samples were used at a final dilution of 1/500 and nasal lavage sample at 1/25 dilution for Western Blot analy- sis.

Six to eight week old female golden Syrian hamsters (n = 4 per group) were immunized subcutaneously (s.c.) with 2, 10 or 20 g of purified triSpike in 2 mg of alum on d0, d21 and d42 at HKU-Pasteur Research Centre, Hong Kong, China. A parallel experiment in 5-week-old hamsters was performed

at the NIAID, NIH, Bethesda, Maryland with immunization of 2, 10 or 50 g of purified triSpike in 1 mg of alum on d0, d21 and d42.

2.4. Flow cytometry and ACE2 binding assay

Recombinant S-protein expressing BHK-21 cells were detached with 5 mM EDTA and incubated for 45 min at 4 ˚C with the diluted hamster sera (1/100), washed, fixed with 3.2% of PFA for 5 min at 4 ˚C and labeled with the FITC-conjugated goat anti-Syrian hamster IgG (Santa Cruz Biotechnology) for 30 min at 4 ˚C. Cells were ana- lyzed by flow cytometer (FACSCalibur, BD). All steps were blocked with 3% normal goat serum (Zymed). Fluo- rescence values are expressed as mean fluorescence inten- sity (MFI). ACE2 binding assays were performed by incu- bating soluble ACE2 receptor with S-protein coated on agarose beads as described previously [33]. For inhibition of binding analysis, protein-coated beads were pre-incubated with sera for 1 h at 4 ˚C before incubation with soluble ACE2. The beads were washed four times with lysis buffer (20 mM Tris-HCl 7.5, 150 mM NaCl, 2 mM EDTA, 1% Triton X-100) prior to SDS-PAGE and Western Blot anal- ysis. *2.5. Serum-neutralization assay* Neutralization assays were carried on FRhK-4 cells using SARS-CoV strain HKU-39849 (Department of Microbiol- ogy, HKU) as follows. One hundred $TCID_{50}$ of SARS-CoV were incubated for 2 h at 37 ˚C with serial 2-fold dilutions of heat-inactivated mouse sera in quadruplicate. Virus antibody mix was then added to cells in 96-well plates and plates were incubated at 37 ˚C with microscopic examination for cyto- pathic effect (cpe) after a 4-day incubation. Neutralization titers were calculated by the Reed & Muench formula and are expressed as the reciprocal of the serum dilution which neutralized cpe in 50% of the wells [36]. Table 1

2.6. SARS-CoV pseudotype particles

Recombinant SARS-CoVpp lentiviral vectors expressing a luciferase reporter gene were produced from HEK293T cells as described previously [37] using 10 g of plasmid pNL4.3.Luc R−E−pro− [11] and 10 g of plasmid pCDNA- S-FLAG encoding codon-optimized SARS-CoV S protein [33]. For ADE assays, 25 L of serial 2-fold dilutions of heat-inactivated murine or hamster sera were incubated for 1 h at 37 ˚C with 25 L of pseudovirus (50 ng p24). Fifty micro- liters of Raji cells, at 2 × 10^6 cell/mL previously washed three times with serum-free RPMI, were added to the antibody-SARS-CoVpp mixture in a 96-well plate. After adsorption for 1 h at 37 ˚C, 100 L of RPMI 1640 containing 5% FCS were added. Medium was renewed 16 h later and incubated for an additional 48 h, washed in PBS, lysed and luciferase activ- ity measured for 10 sec in a MicroBeta Jet Counter (Perkin Elmer) according to the instructions provided by the sup- plier (Promega). For ADE blocking assays, Raji cells were pre-incubated for 15 min at 4 ˚C with 10 g/mL of murine monoclonal antibody directed against human CD32 (Fc RII, BD Pharmingen) or goat polyclonal antibody directed against human ACE2 (R&D Systems) prior to infection with SARS-CoVpp.

2.7. SARS-CoV challenge and viral load titration in hamsters, histopathology and blood chemistry

On day 56 (14 days following the last immunization), 48 anesthetized hamsters received 100 l (10^3 $TCID_{50}$) of SARS-CoV (strain Urbani) intranasally (Table 1). Hamsters were euthanatized by lethal intraperitoneal injection with sodium pentobarbital (200 l/hamster) on days 2 and 5 fol- lowing challenge when peak virus replication, and pneu- monitis are anticipated and on day 21 post challenge to look for possible late changes in histopathology. Sixteen of forty eight SARS-CoV-inoculated hamsters were sacri- ficed 2 days post-challenge. Lungs were harvested and pro- cessed for viral titration. Groups of 16 SARS-CoV-inoculated hamsters were sacrificed 5 and 21 days post-challenge and lungs and livers were harvested and processed for pathology studies. Tissue samples were homogenized and virus titers

Group (# Hms)	Days 0, 21, 42 Inoculum (dose)		Day 56 SARS	Day of sacrifice	Organs harvested for
1 (4)	PBS	IN	58	Viral titers	
2 (4)	ST 2	g IN	58	Viral titers 3 (4)	ST 10 g IN 58
	Viral titers 4 (4)	ST 50	g IN	58	Viral titers
5 (4)	PBS	IN	61	**Pathology** (in 10% buffered formalin)	
6 (4)	ST 2	g IN	61	**Pathology** (in 10% buffered formalin)	
7 (4)	ST 10	g IN	61	**Pathology** (in 10% buffered formalin)	
8 (4)	ST 50	g IN	61	**Pathology** (in 10% buffered formalin)	
9 (4)	PBS	IN	77	**Pathology** (in 10% buffered formalin)	
10 (4)	ST 2	g IN	77	**Pathology** (in 10% buffered formalin)	
11 (4)	ST 10	g IN	77	**Pathology** (in 10% buffered formalin)	
12 (4)	ST 50	g IN	77	**Pathology** (in 10% buffered formalin)	

were determined in VeroE6 cell monolayers as described previously [30].

Four hamsters per group, immunized and challenged as described above, were sacrificed at 5 days post-challenge and an additional four hamsters per group (with one addi- tional hamster in the 50 g/dose group) were sacrificed 21 days following challenge. Lungs were evaluated for pneu- monitis and consolidation as previously described [30]. A colorimetric immunoalkaline phosphatase IHC method was used to identify SARS-CoV antigens [30]. Hamster serum samples were analyzed for the levels of aspartate aminotrans- ferase (AST), alanine aminotransferase (ALT), alkaline phos- phatase (ALP), gamma-glutamyl transferase (GGT), blood urea nitrogen (BUN) and total bilirubin using blood chem- istry analyzer (Analytics, MedTec Lab).

3. Results

3.1. Production of immunopurified trimeric S-protein with native antigenicity

Full-length, codon-optimized SARS-CoV S-protein fused to a C-terminal FLAG was purified by a single-step immunoaffinity protocol to over 90% purity with an aver- age yield of 3 g of pure S-protein per 10^6 cells, i.e. 1.5 mg/L (Fig. 1A). Analysis of the apparent molecular weight of the protein by SDS-PAGE and Western Blot under non-reducing conditions revealed the predominant trimeric nature of the antigen (Fig. 1B, lane 1). Trimers dissoci- ate into monomers when the protein is heat-denatured in the presence of SDS indicating that monomers are asso- ciated non-covalently (Fig. 1B, lane 2). Higher molecular weight DTT-sensitive aggregates were observed when the protein was not heat denatured prior to SDS-PAGE (Fig. 1B, lane 3). As expected, trimers and aggregates dissociate completely into monomers when heat-denatured in SDS and DTT (Fig. 1B, lane 4). Monomers derived from SDS/heat-denatured trimers have a slightly greater electrophoretic mobility than monomers derived from SDS/heat/DTT denatured trimers indicating that intramolecular disulfide bonds lead to a more compact three dimensional conformation of the Spike monomer. The trimeric and monomeric S-protein frequently migrate as doublets (Fig. 1B) [33]. These represent high-mannose glycoforms from proteins that reside in the ER at the time of lysis and glycoforms from proteins that have acquired complex *N*-glycans in the median-Golgi [33]. triSpike has native antigenicity shown by reactivity with sera from 10 convalescent SARS patients by Western Blot and FACS (data not shown). **The native fold was further underscored by the specific binding of the triSpike protein with soluble ACE2 receptor (Fig. 2E, lane 2). Altogether our results strongly argue that purified triSpike molecules mimic the native trimeric S-protein on the virion surface.**

3.2. triSpike induces antibodies against SARS-CoV S-protein in mice and hamsters

Immunogenicity of triSpike was assessed by immuniza- tion with three different doses with or without adjuvant (alum) in mice or hamsters (Fig. 2). Immunization of mice with triSpike alone induced low levels of anti-S antibod- ies (Fig. 2A, dl5). However a single subsequent injection of triSpike induced detectable levels of antibodies against S-protein (Fig. 2A, d30) which could be further boosted by a third injection (Fig. 2A, d49). Sera were reactive against mono-, di- and trimers of S-proteins carrying either high- mannose or complex *N*-glycosylation. Analysis of individ-

Fig. 1. Biochemical characterization of purified trimeric SARS-CoV S-protein (triSpike). (A) Silver staining of immunopurified triSpike, lane M contains a pre-stained protein marker and lane 1 had 720 ng of purified triSpike. (B) triSpike was expressed in BHK-21 cells in the presence of cycloheximide. Recombinant triSpike purification was performed by immunoaffinity as described in Section 2. Eluted protein was treated as indicated and analyzed by 4-8% Tris-Acetate SDS-PAGE gel and Western Blot using M2 monoclonal antibody against the FLAG peptide. Sizes of molecular weight markers are indicated on the right (HiMark™ Pre-stained HMW Protein Standard, Invitrogen).

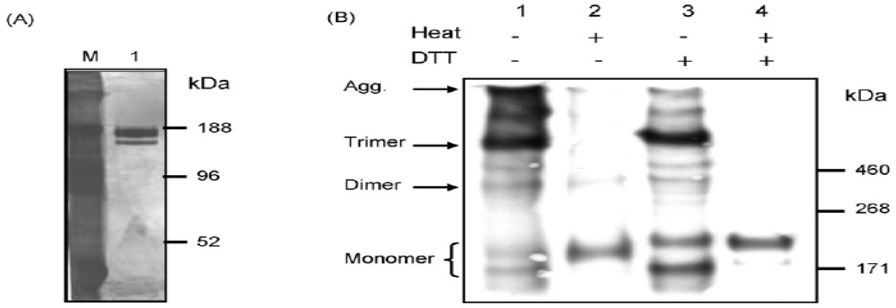

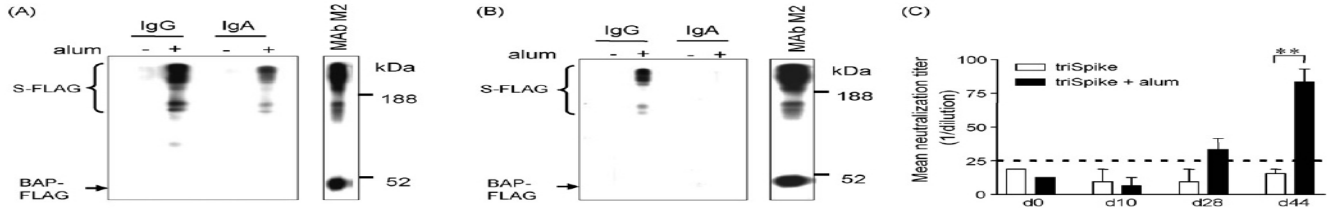

Fig. 2. Immunogenicity of triSpike. Sera collected at indicated time points from vaccinated mice or hamsters were analyzed for reactivity with triSpike. (A) Western Blot analysis of pooled sera from immunized mice with or without alum adjuvant. Sera were collected and used at 1/1000 dilution against S-FLAG that was separated under conditions that allowed simultaneous detection of mono-, di-, and trimers of S-protein. A SARS patient serum (SARS), a rabbit serum against S1 and M2 monoclonal antibody against the FLAG peptide was used as control. FLAG-tagged bacterial alkaline phosphatase (BAP-FLAG) was used to assess the presence of antibodies against the FLAG tag. Immune complexes were detected with HRP-conjugated goat anti-mouse, -human or -rabbit IgG polyclonal antibody. Sizes of molecular weight markers are indicated on the right. (B) Reactivity of immune sera from pooled immunized hamster with live BHK-21 cells expressing S-protein at the plasma membrane using FACS analysis. Values were expressed as mean ± standard deviations. (C) Effect of alum adjuvant on longevity of neutralizing response in mouse sera against SARS-CoV (determined on FRhK-4 cells). Values were expressed as mean ± standard deviations. (D) Dose effect of triSpike immunization with alum adjuvant on neutralizing response against SARS-CoV in hamsters (determined on FRhK-4 cells). Values were expressed as mean ± standard deviations. (E) Inhibition of S-protein binding to ACE2 by sera from immunized mice. S-protein coated beads were pre-incubated with sera prior to incubation with soluble ACE2 (sACE2) and detection of the receptor was performed with a polyclonal goat-anti human ACE2 antibody. BAP-FLAG coated beads were used as control.

ual serum samples from d49 confirmed the homogeneity of the antibody response in individual mice (data not shown). When triSpike was used in combination with alum adju- vant (Fig. 2A) a very similar response was observed, except that the level of anti-S IgG was slightly higher after the second injection (Fig. 2A, d30) and a third injection did not increase the anti-S serum antibody level (Fig. 2A, d49). Neither triSpike nor triSpike with alum adjuvant immuniza- tion induced antibodies directed against the FLAG peptide (Fig. 2A, lower panels).

In a next step we analyzed the dose response and booster immunization effect in hamsters, immunized with 2, 10 or 20 g triSpike plus alum, by FACScan. The first immunization with all three doses resulted in a moderate anti-S antibody response (Fig. 2B, d20). A second injection strongly increased anti-S antibody levels (Fig. 2B, d41), while no further increase in anti-S antibody level was seen after a third injection (Fig. 2B, d55). There is no significant dose-dependent antibody response as 2 g triSpike plus alum immunization seems to induce maximum antibody response in hamster model. Analysis of individual serum samples from d55 confirmed the homogeneity of the antibody response in individual hamster (data not shown). Altogether these results indicate that an optimal anti-S antibody response might require two doses of triSpike (2 g) immunization in alum adjuvant.

3.3. Neutralizing antibodies in sera from triSpike

vaccinated mice and hamsters

We next evaluated the neutralizing activity of sera from triSpike vaccinated mice. Serial dilutions of sera were tested for their neutralizing activity of cpe induced by SARS-CoV replication in FRhK-4 cells (neutralization of 100 $TCID_{50}$). Injection of triSpike with alum adjuvant induces higher neutralization titers compared to triSpike alone (Fig. 2C). Antibody titers in triSpike with alum immunized animals remained at high levels until day 87 (1/6400) while neutralizing titers dropped rapidly from day 49 to day 87 in animals injected with triSpike alone (from 1/4800 to 1/600). Subsequently, a dose-response experiment was performed in ham- sters. Sera from hamsters immunized with at least two doses as low as 2 g effectively neutralized 100 $TCID_{50}$ of SARS-CoV on FRhK-4 cells (Fig. 2D). Boosting effect with a third injection was limited with all three doses. Maximum antibody levels were obtained in animals immunized with 20 g.

3.4. Neutralizing sera block spike binding to the ACE2 receptor

We next investigated the mechanism of neutralization by analyzing the capacity of sera to block the interaction between immunopurified triSpike coated on agarose beads with puri- fied soluble human ACE2, the SARS-CoV entry receptor [6,7]. Fig. 2E shows that sera from triSpike + alum immu- nized mice (lane 3) but not from control animals (lane 4) neutralized S-protein binding to ACE2 receptor. These results suggest inhibition of receptor binding as the key mechanism of neutralization in triSpike immunized animals.

3.5. Mucosal IgG and IgA response in mice

Detection of SARS-CoV in intestinal tissue of fatal SARS cases indicated that the gastrointestinal tract is another target for SARS-CoV infection [38]. Hence, a vaccine candidate should ideally induce protective response in mucosal sites. Previous study suggested the induction of IgG response in serum (systemic response) and IgA response in stool (mucosal response) samples against *Yersinia pestis* using intraperitoneal immunization [39]. To address this question antibody were prepared from fecal samples of immunized animals. Occult blood detection showed absence of blood contamination (data not shown) indicating that the samples were not contaminated by serum antibodies. Western Blot using antibodies isolated from fecal samples revealed that mucosal IgG and IgA were induced by triSpike plus alum but not by triSpike alone (Fig. 3A). These antibodies were able to neutralize SARS-CoV infection of FRhK-4 cells (Fig. 3C). Altogether, we conclude that triSpike plus alum immunization induced antigen-specific IgG and IgA in the gastrointestinal tract.

Mice were also analyzed for the presence of anti-S antibodies in nasal lavage samples. Occult blood detection indicated the absence of blood contamination in the sample. Western Blot analysis using antibodies isolated from nasal lavage revealed the induction of a mucosal IgG response only after triSpike plus alum immunization but not after triSpike immunization alone (Fig. 3B). We were unable to detect any IgA response in either group and anti-S antibodies in nasal lavage samples did not neutralize SARS-CoV (Fig. 3B). Fur- ther studies are required to address the respective role of IgA and IgG in the neutralizing activity, epitope specificity and antibody titer in the neutralization mechanism.

3.6. Antibody-dependent enhancement (ADE) of viral entry into human B cells

We investigated whether vaccine-induced anti-S antibod- ies against triSpike could mediate ADE of SARS-CoV entry into FcR expressing cell lines. SARS pseudotype particles (SARS-CoVpp) were generated for this study. These recom-

Fig. 3. Induction of mucosal immune response in triSpike plus alum vaccinated mice. (A) Antibodies prepared from fecal samples collected at day 44 post-immunization were reacted against S-protein as described in Fig. 2A. Immune complexes were detected with HRP-conjugated goat anti-mouse IgG or IgA polyclonal antibody. (B) Similar as (A) except that Western Blot analysis was performed with pooled nasal lavage samples collected at day 65. (C). Antibodies prepared from fecal samples of vaccinated mice were analyzed for neutralizing activity against SARS-CoV infection on FRhK-4 cells. Weak neutralizing activity was detected after the third immunization only. Asterisk (**) indicates the value of $p < 0.01$ in two-tailed t tests. Values were expressed as mean ± standard deviations.

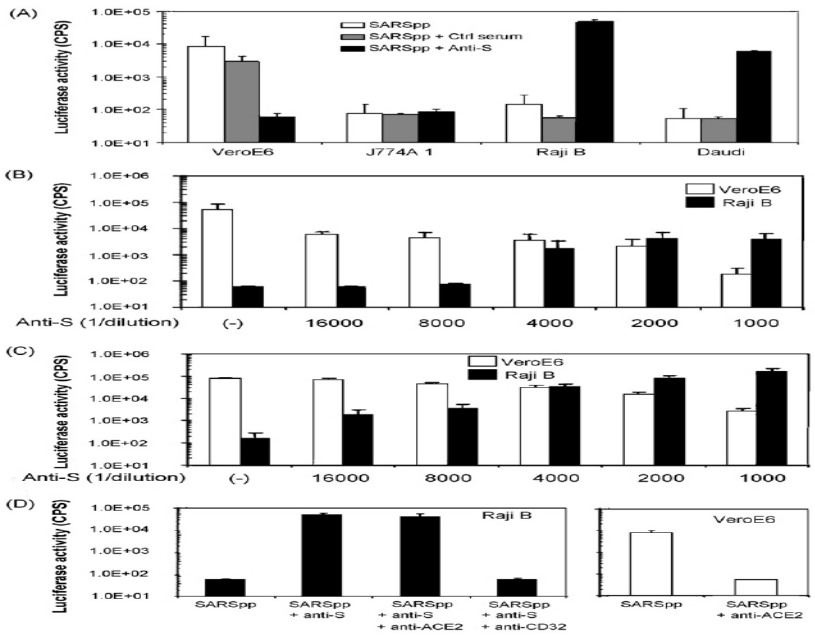

Fig. 4. Analysis of antibody-dependent enhancement of SARS-CoVpp entry. (A) Analysis of various cell lines for ADE of Spike-mediated viral entry. SARS- CoVpp were incubated with a 1/1000 dilution of sera from mice immunized with triSpike and transduction was measured as SARS-CoVpp-expressed luciferase activity. (B) Serial dilutions of sera from mice immunized with triSpike neutralize SARS-CoVpp transduction of VeroE6 cells and enhance transduction of Raji B cells. (C) Same as (B) except that sera from hamsters immunized with triSpike were used. (D) Fc RII (CD32) involvement in antibody-dependent enhancement of SARS-CoVpp entry. Same as (C), SARS-CoVpp were incubated with a 1/1000 dilution of sera and Raji cells pre-incubated with 10 mg/mL of a mAb against ACE2 or CD32 (left panel) prior to infection. Inhibition of SARS-CoVpp entry by the mAb against ACE2 was controlled on VeroE6 cells (right panel). All experiments were performed in triplicates and data are presented as mean ± standard deviations.

binant viruses encoding the luciferase reporter gene and expressing the SARS-CoV Spike protein at the virion surface have been shown to faithfully mimic the SARS-CoV entry process [9-11]. We infected cells with SARS-CoVpp in the presence or absence of heat-inactivated serum from triSpike immunized mice and hamsters as well as sera from ten convalescent SARS patients. Transduction of FcR-negative VeroE6 cells with SARS-CoVpp was reduced in a dose-dependent manner when pseudovirus was pre-incubated with S-specific antisera (Fig. 4B & C). When SARS-CoVpp were pre-incubated with heat-inactivated S-specific mouse or ham- ster sera a dose-dependent enhancement of ACE2-negative Raji B and Daudi cell transduction was observed (Fig. 4A-C). Only background level of transduction was detected in the absence of serum or in the presence of sera from the na¨ıve control group. When Raji B cells were pre-incubated with a monoclonal antibody (mAb) against human Fc RII (CD32) SARS-CoVpp transduction was reduced to background lev-

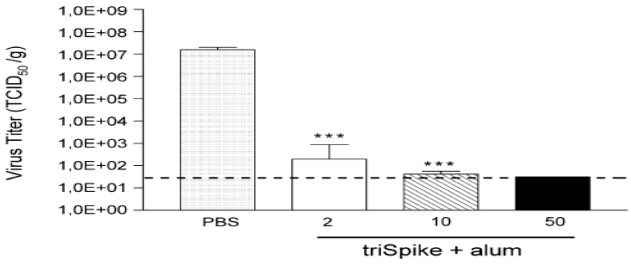

Fig. 5. Protection of triSpike-immunized hamsters from SARS-CoV challenge. Hamsters were inoculated intranasally with 10^3 $TCID_{50}$ of SARS-CoV (Urbani strain) and virus titers in lung homogenates were determined. Error bars indicated standard errors and asterisk (***) indicate the value of $p < 0.001$ in two-tailed t tests. Values were expressed as $TCID_{50}$ per g of lung tissue.

els demonstrating that pseudovirus entry was Fc RII dependent (Fig. 4D). Furthermore ADE could be abrogated by pre-incubating the pseudovirus-antibody mix with protein G, demonstrating that the process is mediated by the Fc portion of the antibody (data not shown). Interestingly, a mAb against ACE2 blocked transduction of VeroE6 cells by SARS-CoVpp but not on Raji B cells by SARS-CoVpp- antibody complexes indicating that Fc RII mediated virus entry does not require ACE2 for virus-cell membrane fusion (Fig. 4D). Only a low level of SARS-CoVpp transduction was observed with the J774A1 murine macrophage cell line despite the presence of Fc RII receptor. ADE was not lim- ited to vaccine-induced anti-S sera from mice and hamsters. Eight out of ten sera from convalescent SARS patients also showed enhancement of Raji B cell transduction despite the capacity of 10/10 sera to neutralize virus entry into VeroE6 cells (data not shown). Our results demonstrate that S-specific antibodies can induce a shift in cell tropism of SARS- CoV towards human Fc RII expressing cells. Antibody- and Fc RII-dependent but ACE2-independent virus entry and fusion is a novel mechanism by which SARS-CoV can enter into target cells.

3.7. Protection of immunized hamsters from SARS-CoV challenge

Syrian golden hamsters were immunized 3 times at bi-weekly intervals with 2 g, 10 g or 50 g of triSpike plus alum and challenged intranasally with 10^3 $TCID_{50}$/hamster of SARS-CoV. Hamsters receiving triSpike vaccine were significantly protected from SARS-CoV challenge compared to mock immunized controls (Fig. 5). Complete protection was observed following three doses of 50 g (mean viral titer below the limit of detection) and partial protection was observed in hamsters receiving the lowest dose. Half the hamsters receiving three doses of 2 g triSpike vaccine showed complete protection from challenge. Mean viral titers for the group were $10^{2.3}$ $TCID_{50}$/g tissue. Seventy-five percent of hamsters receiving three doses of 10 g triSpike vaccine showed complete protection from challenge. One hamster for this group had viral titers just above the limit of detection at 10^2 TCIDso/g tissue. In comparison of four mock immunized hamsters had similar high titers of SARS-CoV present with a mean viral titer of $10^{7.2}$ TCIDso/g tissue. Patterns or consistent elevations of liver enzymes were not observed in any group following any immunization or SARS-CoV challenge (data not shown).

3.8. Histopathology

Five days following SARS-CoV challenge mock immunized hamsters had severe pneumonitis and consolidation in comparison to triSpike immunized hamsters where 9/12 had mild, 2/12 had moderate and only 1/12 had severe pneumonitis and none had pulmonary consolidation. The data indicate that regardless of the dose administered the vaccine significantly protects from the occurrence and severity of pneumonitis following SARS-CoV challenge. In contrast to previously published data where pneumonitis and consolidation were completely cleared by day 14 post-challenge, moderate (1/4) to severe pneumonitis (3/4) was observed 21 days post-challenge in mock immunized hamsters. In triSpike immunized hamsters 21 days post-challenge, pneumonitis was completely cleared (3/13) or reduced to mild (8/12) or moderate (2/12) levels. The variation between these observations and previously reported observations in the time to resolution of pneumonitis is likely due to changes in tissue processing. Lungs were inflated with formalin in these studies and were not in the previous report [30]. Nevertheless, consistent with previously reported data, 21 days after challenge pulmonary consolidation was absent in all groups including the mock immunized controls.

Histopathological analyses of livers at both days 5 (3/16) and 21 (4/17) post-challenge revealed very rare foci of hepatic cellular necrosis. These foci were observed in both mock immunized and triSpike immunized hamsters post-challenge and did not show any correlation with either pre-challenge neutralizing antibody titers or liver enzyme levels (pre- or post-challenge). Furthermore, SARS-CoV antigen was not detected by immunohistochemical staining.

4. Discussion

There is currently no licensed vaccine against a human coronavirus. Vaccines against animal coronaviruses have been successfully generated, e.g. transmissible gastroenteritis virus (TGEV) [40]. However, the development of a vaccine against FIPV has proven difficult due to immune enhancement of disease in vaccinated cats. Receptors binding viral envelope glycoproteins are prime targets for neutralizing antibodies [41]. We hypothesized that a SARS-CoV enve-

lope with native trimeric conformation would be optimal for induction of conformation-dependent neutralizing anti- bodies targeting multiple epitopes. Full-length coronavirus Spike glycoproteins with an intact transmembrane domain were previously shown to assemble into rosettes generating highly immunogenic enveloped lipid spheres [42]. Biochem- ical characterization of the S-protein immunogen showed that purified recombinant S protein migrates in SDS-PAGE with an apparent molecular weight >500 kDa, suggesting that it is a trimer. The correctly folded S protein is a complex- glycosylated, non-covalently linked homotrimeric glycoprotein which is not cleaved by intracellular proteases during exit to the cell surface. These results are in agreement with data obtained by others for SARS [5] and other coronaviruses [4]. Immunopurified preparations of full-length S trimer (triSpike) contain correctly folded S protein but also mannosylated high molecular weight forms, which are likely ER retained proteins that are not yet correctly folded or being degraded. Indeed, high-mannose forms are purged from the ER, as evidenced by pulse-chase experiments [33] and by treatment of S expressing cells with translation inhibitor cycloheximide. Correct folding and native conformation of triSpike was confirmed by binding to soluble ACE2 recep- tor. Preliminary results obtained with two soluble forms of the S-protein ectodomain, Secd (aa1-1184) and S1 (aa1- 757), show that Secd migrates with the apparent molecular weight of a trimer (>500 kDa), consistent with the model that trimerization domains are located within the membrane proximal S2 domain, while S1 migrates with the apparent molecular weight of a monomer (data not shown). These findings are in agreement with previous reports showing that coronavirus MHV and TGEV S proteins are trimers [4,43].

Immunization studies in mice and hamsters demonstrated that triSpike is highly immunogenic and induces a long-lasting neutralizing response which remains stable for up to 6 months (neutralization titer 1/800) when the immunogen is administered with alum, an adjuvant licensed for use in humans [44]. Mucosal immunity can provide a first-line defense mechanism against viral infection in the respiratory tract or intestinal lumen where SARS-CoV replicates [45,46]. Our results show that a neutralizing IgG and IgA response can be induced through immunization with S protein adjuvanted in alum. The induction of anti-S IgA, absent from nasal lavage samples in this study, might be critical for improved neutral- ization activity [47].

Several studies have previously pointed towards the receptor binding domain (RBD) within S1 as key target for neutralizing antibodies [48,49]. A human mAb from a non-immune human antibody library was described which blocked association of S-protein with ACE2 [50]. In our experiment sera collected from Secd and S1 immunized animals also neutralized SARS-CoV (unpublished data) suggesting that the key neutralization epitopes are located in the S1 domain and that correct conformation of the monomer alone is sufficient to achieve a neutralizing response. Our data show that a purified protein vaccine can induce such blocking antibodies with high efficiency. Indeed neutralizing sera from our vaccinated mice prevented triSpike binding to soluble human ACE2 receptor indicating that the RBD is accessible to antibodies and suggesting receptor binding inhibition as key mechanism of virus neutralization in triSpike immunized animals. However, blocking of receptor binding might not be the sole mechanism of virus neutralization. Neutralization with antibodies against the putative S2 protein [51] suggest that antibodies can also block post binding steps, e.g. conformational transitions of the S2 subunit required for membrane fusion.

Antibody-dependent enhancement (ADE) of infection has been described for several viruses, e.g. Dengue virus, Human Immunodeficiency Virus, Ebola virus and FIPV [26,52-55]. ADE occurs when a virus-antibody complex interacts with FcR or complement to trigger virus uptake or alternatively when antibodies induce conformational changes in envelope glycoproteins that are required for virus-cell membrane fusion [56]. Antibody-dependent conformational changes have previously been reported for a civet cat strain of SARS-CoV which showed enhanced entry into a human renal epithelial cell-line in the presence of human monoclonal antibodies against human strain of SARS-CoV Spike [25]. We could exclude this mechanism of enhancement as sera from triSpike vaccinated mice did neutralize, rather than enhance, virus infection on VeroE6 cells. However, we observed that sera from triSpike vaccinated mice or hamsters showed a 100-1000 fold increase in virus entry into Fc RII positive, ACE2-negative human B cells. ADE was still observed when the complement was inactivated by heat treatment of sera but could be abrogated by protein G and an anti-Fc RII antibody, demonstrating that ADE is mediated by the Fc region of the antibody and the Fc RII receptor. Interestingly, the R/R131 genotype of the human Fc RIIA receptor was recently correlated with severity of disease in SARS patients [57]. Our results show that anti-ACE2 antibody did not reduce transduction by pseudovirus-antibody complexes indicating that Spike-mediated virus cell entry and membrane fusion can occur through an ACE2-independent mechanism. Together with previously described data, our results suggest that pseudovirus-antibody complexes might be endocytosed via Fc RII, followed by protease cleavage of S in the endosome [58,59] and S2-mediated membrane fusion in a low pH endosomal compartment [9,60].

ADE in the FIPV model has been linked to specific enhancing non-neutralizing epitopes and enhancing non-neutralizing IgG2a antibodies [61,62]. Analysis of monoclonal antibodies against S should provide evidence whether antibody subclass or specific epitopes are involved in the enhancement mechanism. Interestingly, we observed the enhancement phenotype only in human B cell lines but not in mouse macrophages despite the presence of Fc RII. Reasons for this are unclear, but the respective role of activating and inhibiting human Fc RII which have identical extracellular

but heterologous intracellular domains and signaling capac- ities might play a role [63]. ADE in SARS-CoV entry is not restricted to vaccine-induced anti-S antibodies but can also be observed with SARS patient sera. Eight out of ten sera capa- ble of neutralizing infection on VeroE6 cells were found to enhance transduction of B cell lines. B cells have been shown to be only occasionally infected in patients with SARS [64]. However, enhanced viral entry into B cells could have a pro- found effect on pathogenesis even if ensuing viral replication in this cell type is abortive. Vaccine-induced antibodies that enhance entry of virus could increase the frequency of B cell infection in vaccinated subjects and alter disease on subse- quent exposure to SARS-CoV.

Vaccine-mediated protection against SARS-CoV infection in mice has been demonstrated using different vac- cine approaches [19,20,65]. However, mice do not replicate SARS-CoV to high titers and do not show pronounced pathol- ogy in lungs [15]. On the contrary, ferrets [28], cynomolgus macaques [29] and hamsters [30] have been shown to support high titer replication of SARS-CoV in the respiratory tract associated with pneumonitis. In order to assess the respective role of neutralization or ADE *in vivo* we performed SARS- CoV challenge experiments in hamsters vaccinated with three doses of 2, 10 or 50 g of protein in alum adjuvant. All vac- cinated groups showed a significant decrease of viral load at 3 days post challenge by at least four orders of magnitude without signs of enhanced lung pathology. The rare foci of hepatocyte necrosis that we observed in these hamsters did not correlate with pre-challenge neutralizing antibody titers, liver enzyme levels (pre- or post-challenge), or immunohis- tochemical detection of SARS-CoV antigen suggesting that hepatic cellular necrosis is unrelated to SARS-CoV immu- nization or infection in Syrian golden hamsters. This contrasts with a report of hepatitis 28 days following challenge with SARS-CoV in ferrets vaccinated with a poorly immunogenic recombinant MVA vaccine expressing SARS-CoV spike pro- tein [24].

Altogether our results indicate that a recombinant trimeric S protein was able to elicit a protective immune response *in vivo* but if the observation of enhanced entry into B cells *in vitro* can be shown to have an *in vivo* correlate, this would warrant concern in the safety evaluation of a human vaccine against SARS-CoV.

Acknowledgements

We wish to thank Cheman Chan, Pierre Corby, Jean-Claude Manuguerra, Isabelle Staropoli and Marc Daeron for expert advice and helpful discussions. This work was supported by the European Commission (EPISARS con- tract SP22-CT-2004-511063), the "Programme de Recherche en R´ eseaux Franco-Chinois -Epid´ emie du SARS: de l'´ emergence au contrˆ and the Public Health Research ole Grant A195357 from the National Institute of Allergy and Infectious Disease, USA.

References

[1] van der Hoek L, Pyrc K, Jebbink MF, Vermeulen-Oost W, Berkhout RJ, Wolthers KC, et al. Identification of a new human coronavirus. Nat Med 2004;10(4):368-73.
[2] Woo PC, Lau SK, Chu CM, Chan KH, Tsoi HW, Huang Y, et al. Characterization and complete genome sequence of a novel coron- avirus, coronavirus HKU1, from patients with pneumonia. J Virol 2005;79(2):884-95.
[3] Peiris JS, Guan Y, Yuen KY. Severe acute respiratory syndrome. Nat Med 2004;10(12 Suppl):S88-97.
[4] Bosch BJ, van der Zee R, de Haan CA, Rottier PJ. The coronavirus spike protein is a class I virus fusion protein: structural and functional char- acterization of the fusion core complex. J Virol 2003;77(16):8801-11.
[5] Song HC, Seo MY, Stadler K, Yoo BJ, Choo QL, Coates SR, et al. Syn- thesis and characterization of a native, oligomeric form of recombinant severe acute respiratory syndrome coronavirus spike glycoprotein. J Virol 2004;78(19):10328-35.
[6] Li W, Moore MJ, Vasilieva N, Sui J, Wong SK, Berne MA, et al. Angiotensin-converting enzyme 2 is a functional receptor for the SARS coronavirus. Nature 2003;426(6965):450-4.
[7] Wang P, Chen J, Zheng A, Nie Y, Shi X, Wang W, et al. Expression cloning of functional receptor used by SARS coronavirus. Biochem Biophys Res Commun 2004;315(2):439-44.
[8] Jeffers SA, Tusell SM, Gillim-Ross L, Hemmila EM, Achenbach JE, Babcock GJ, et al. CD209L (L-SIGN) is a receptor for severe acute respiratory syndrome coronavirus. Proc Natl Acad Sci USA 2004;101(44):15748-53.
[9] Yang ZY, Huang Y, Ganesh L, Leung K, Kong WP, Schwartz O, et al. pH-dependent entry of severe acute respiratory syndrome coronavirus is mediated by the spike glycoprotein and enhanced by dendritic cell transfer through DC-SIGN. J Virol 2004;78(11):5642-50.
[10] Simmons G, Reeves JD, Rennekamp AJ, Amberg SM, Piefer AJ, Bates P. Characterization of severe acute respiratory syndrome-associated coronavirus (SARS-CoV) spike glycoprotein-mediated viral entry. Proc Natl Acad Sci USA 2004;101(12):4240-5.
[11] Hofmann H, Hattermann K, Marzi A, Gramberg T, Geier M, Krumbiegel M, et al. S protein of severe acute respiratory syndrome-associated coronavirus mediates entry into hepatoma cell lines and is targeted by neutralizing antibodies in infected patients. J Virol 2004;78(12):6134-42.
[12] Nie Y, Wang G, Shi X, Zhang H, Qiu Y, He Z, et al. Neutralizing anti- bodies in patients with severe acute respiratory syndrome-associated coronavirus infection. J Infect Dis 2004;190(6):1119-26.
[13] Greenough TC, Babcock GJ, Roberts A, Hernandez HJ, Thomas Jr WD, Coccia JA, et al. Development and characterization of a severe acute respiratory syndrome-associated coronavirus-neutralizing human mon- oclonal antibody that provides effective immunoprophylaxis in mice. J Infect Dis 2005;191(4):507-14.
[14] ter Meulen J, Bakker AB, van den Brink EN, Weverling GJ, Martina BE, Haagmans BL, et al. Human monoclonal antibody as prophylaxis for SARS coronavirus infection in ferrets. Lancet 2004;363(9427):2139-41.
[15] Subbarao K, McAuliffe J, Vogel L, Fahle G, Fischer S, Tatti K, et al. Prior infection and passive transfer of neutralizing antibody prevent replication of severe acute respiratory syndrome coronavirus in the respiratory tract of mice. J Virol 2004;78(7):3572-7.
[16] Bisht H, Roberts A, Vogel L, Bukreyev A, Collins PL, Murphy BR, et al. Severe acute respiratory syndrome coronavirus spike protein expressed by attenuated vaccinia virus protectively immunizes mice. Proc Natl Acad Sci USA 2004;101(17):6641-6.
[17] Traggiai E, Becker S, Subbarao K, Kolesnikova L, Uematsu Y, Gis- mondo MR, et al. An efficient method to make human monoclonal antibodies from memory B cells: potent neutralization of SARS coro- navirus. Nat Med 2004;10(8):871-5.
[18] Sui J, Li W, Roberts A, Matthews LJ, Murakami A, Vogel L, et al. Evaluation of human monoclonal antibody 80R for immunoprophy-

[20] laxis of severe acute respiratory syndrome by an animal study, epitope mapping, and analysis of spike variants. J Virol 2005;79(10):5900-6. Yang ZY, Kong WP, Huang Y, Roberts A, Murphy BR, Subbarao K, et al. A DNA vaccine induces SARS coronavirus neutralization and protective immunity in mice. Nature 2004;428(6982):561-4.

[21] Bisht H, Roberts A, Vogel L, Subbarao K, Moss B. Neutralizing anti- body and protective immunity to SARS coronavirus infection of mice induced by a soluble recombinant polypeptide containing an N-terminal segment of the spike glycoprotein. Virology 2005;334(2):160-5.

[22] Zhou Z, Post P, Chubet R, Holtz K, McPherson C, Petric M, et al. A recombinant baculovirus-expressed S glycoprotein vaccine elicits high titers of SARS-associated coronavirus (SARS-CoV) neutralizing antibodies in mice. Vaccine 2006;24(17):3624-31.

[23] See RH, Zakhartchouk AN, Petric M, Lawrence DJ, Mok CP, Hogan RJ, et al. Comparative evaluation of two severe acute respiratory syndrome (SARS) vaccine candidates in mice challenged with SARS coronavirus. J Gen Virol 2006;87(Pt 3):641-50.

[24] Qin E, Shi H, Tang L, Wang C, Chang G, Ding Z, et al. Immunogenicity and protective efficacy in monkeys of purified inactivated Vero-cell SARS vaccine. Vaccine 2006;24(7):1028-34.

[25] Weingartl H, Czub M, Czub S, Neufeld J, Marszal P, Gren J, et al. Immunization with modified vaccinia virus Ankara-based recombinant vaccine against severe acute respiratory syndrome is associated with enhanced hepatitis in ferrets. J Virol 2004;78(22):12672-6.

[26] Yang ZY, Werner HC, Kong WP, Leung K, Traggiai E, Lanzavec- chia A, et al. Evasion of antibody neutralization in emerging severe acute respiratory syndrome coronaviruses. Proc Natl Acad Sci USA 2005;102(3):797-801.

[27] Vennema H, de Groot RJ, Harbour DA, Dalderup M, Gruffydd-Jones T, Horzinek MC, et al. Early death after feline infectious peritonitis virus challenge due to recombinant vaccinia virus immunization. J Virol 1990;64(3):1407-9.

[28] Olsen CW, Corapi WV, Ngichabe CK, Baines JD, Scott FW. Mono- clonal antibodies to the spike protein of feline infectious peritonitis virus mediate antibody-dependent enhancement of infection of feline

[29] macrophages. J Virol 1992;66(2):956-65.

Martina BE, Haagmans BL, Kuiken T, Fouchier RA, Rimmelzwaan GF, Van Amerongen G, et al. Virology: SARS virus infection of cats and

[30] ferrets. Nature 2003;425(6961):915.

Fouchier RA, Kuiken T, Schutten M, van Amerongen G, van Doornum GJ, van den Hoogen BG, et al. Aetiology: Koch's postulates fulfilled for SARS

[31] virus. Nature 2003;423(6937):240.

Roberts A, Vogel L, Guarner J, Hayes N, Murphy B, Zaki S, et al. Severe acute respiratory syndrome coronavirus infection of golden Syr- ian hamsters. J Virol 2005;79(1):503-11.

[32] Lozach PY, Lortat-Jacob H, de Lacroix de Lavalette A, Staropoli I, Foung S, Amara A, et al. DC-SIGN and L-SIGN are high affinity binding receptors for hepatitis C virus glycoprotein E2. J Biol Chem

[33] 2003;278(22):20358-66.

Staropoli I, Chanel C, Girard M, Altmeyer R. Processing, stability, and receptor binding properties of oligomeric envelope glycoprotein from a primary HIV-1 isolate. J Biol Chem 2000;275(45):35137-45.

[34] Nal B, Chan C, Kien F, Siu L, Tse J, Chu K, et al. Differential matura- tion and subcellular localization of severe acute respiratory syndrome coronavirus surface proteins S, M and E. J Gen Virol 2005;86(Pt 5): 1423-34.

[35] Matoba N, Magerus A, Geyer BC, Zhang Y, Muralidharan M, Alf- sen A, et al. A mucosally targeted subunit vaccine candidate elic- iting HIV-1 transcytosis-blocking Abs. Proc Natl Acad Sci USA 2004;101(37):13584-9.

[36] Wu HY, Russell MW. Induction of mucosal and systemic immune responses by intranasal immunization using recombinant cholera toxin B

[37] subunit as an adjuvant. Vaccine 1998;16(2-3):286-92.

Reed LJ, Munich H. A simple method for estimating fifty percent end- points. Am J Hyg 1938;27:493-7.

Lozach PY, Amara A, Bartosch B, Virelizier JL, Arenzana-Seisdedos F, Cosset FL, et al. C-type Lectins L-SIGN and DC-SIGN capture and transmit infectious hepatitis C virus pseudotype particles. J Biol Chem 2004;279(31):32035-45.

[38] Shi X, Gong E, Gao D, Zhang B, Zheng J, Gao Z, et al. Severe acute respiratory syndrome associated coronavirus is detected in intestinal tissues of fatal cases. Am J Gastroenterol 2005;100(1):169-76.

[39] Reddin KM, Easterbrook TJ, Eley SM, Russell P, Mobsby VA, Jones DH, et al. Comparison of the immunological and protective responses elicited by microencapsulated formulations of the F1 antigen from *Yersinia pestis*. Vaccine 1998;16(8):761-7.

[40] Gomez N, Carrillo C, Salinas J, Parra F, Borca MV, Escribano JM. Expression of immunogenic glycoprotein S polypeptides from trans- missible gastroenteritis coronavirus in transgenic plants. Virology 1998;249(2):352-8.

[41] He Y, Zhou Y, Liu S, Kou Z, Li W, Farzan M, et al. Receptor-binding domain of SARS-CoV spike protein induces highly potent neutraliz- ing antibodies: implication for developing subunit vaccine. Biochem Biophys Res Commun 2004;324(2):773-81.

[42] Anton IM, Gonzalez S, Bullido MJ, Corsin M, Risco C, Langeveld JP, et al. Cooperation between transmissible gastroenteritis coronavirus (TGEV) structural proteins in the in vitro induction of virus-specific antibodies. Virus Res 1996;46(1-2):111-24.

[43] Delmas B, Laude H. Assembly of coronavirus spike protein into trimers and its role in epitope expression. J Virol 1990;64(11):5367-75.

[44] Gupta RK, Siber GR. Adjuvants for human vaccines-current status, problems and future prospects. Vaccine 1995;13(14):1263-76.

[45] van Ginkel FW, Nguyen HH, McGhee JR. Vaccines for mucosal immunity to combat emerging infectious diseases. Emerg Infect Dis 2000;6(2):123-32.

[46] Lee JS, Poo H, Han DP, Hong SP, Kim K, Cho MW, et al. Mucosal immunization with surface-displayed severe acute respiratory syn- drome coronavirus spike protein on *Lactobacillus casei* induces neu- tralizing antibodies in mice. J Virol 2006;80(8):4079-87.

[47] Renegar KB, Small Jr PA, Boykins LG, Wright PF. Role of IgA versus IgG in the control of influenza viral infection in the murine respiratory tract. J Immunol 2004;173(3):1978-86.

[48] He Y, Lu H, Siddiqui P, Zhou Y, Jiang S. Receptor-binding domain of severe acute respiratory syndrome coronavirus spike protein contains multiple conformation-dependent epitopes that induce highly potent neutralizing antibodies. J Immunol 2005;174(8):4908-15.

[49] He Y, Zhu Q, Liu S, Zhou Y, Yang B, Li J, et al. Identification of a crit- ical neutralization determinant of severe acute respiratory syndrome (SARS)-associated coronavirus: importance for designing SARS vac- cines. Virology 2005;334(1):74-82.

[50] Sui J, Li W, Murakami A, Tamin A, Matthews LJ, Wong SK, et al. Potent neutralization of severe acute respiratory syndrome (SARS) coronavirus by a human mAb to S1 protein that blocks receptor asso- ciation. Proc Natl Acad Sci USA 2004;101(8):2536-41.

[51] Zhang H, Wang G, Li J, Nie Y, Shi X, Lian G, et al. Identification of an antigenic determinant on the S2 domain of the severe acute respi- ratory syndrome coronavirus spike glycoprotein capable of inducing neutralizing antibodies. J Virol 2004;78(13):6938-45.

[52] Halstead SB. Neutralization and antibody-dependent enhancement of dengue viruses. Adv Virus Res 2003;60:421-67.

[53] Halstead SB, Shotwell H, Casals J. Studies on the pathogenesis of dengue infection in monkeys. II. Clinical laboratory responses to het- erologous infection. J Infect Dis 1973;128(1):15-22.

[54] Fust G. Enhancing antibodies in HIV infection. Parasitology 1997;115(Suppl):S127-40.

[55] Takada A, Watanabe S, Okazaki K, Kida H, Kawaoka Y. Infectivity-enhancing antibodies to Ebola virus glycoprotein. J Virol 2001;75(5):2324-30.

[56] Takada A, Kawaoka Y. Antibody-dependent enhancement of viral infection: molecular mechanisms and in vivo implications. Rev Med Virol 2003;13(6):387-98.

[57] Yuan FF, Tanner J, Chan PK, Biffin S, Dyer WB, Geczy AF, et al. Influence of FcgammaRIIA and MBL polymorphisms on severe acute respiratory syndrome. Tissue Antigens 2005;66(4):291-6.

[58] Simmons G, Gosalia DN, Rennekamp AJ, Reeves JD, Diamond SL, Bates P. Inhibitors of cathepsin L prevent severe acute res- piratory syndrome coronavirus entry. Proc Natl Acad Sci USA 2005;102(33):11876-81.

[59] Matsuyama S, Ujike M, Morikawa S, Tashiro M, Taguchi F. Protease-mediated enhancement of severe acute respiratory syn- drome coronavirus infection. Proc Natl Acad Sci USA 2005;102(35): 12543-7.

[60] Bosch BJ, Martina BE, Van Der Zee R, Lepault J, Haijema BJ, Versluis C, et al. Severe acute respiratory syndrome coronavirus (SARS-CoV) infection inhibition using spike protein heptad repeat-derived peptides. Proc Natl Acad Sci USA 2004;101(22):8455-60.

[61] Olsen CW, Corapi WV, Jacobson RH, Simkins RA, Saif LJ, Scott FW. Identification of antigenic sites mediating antibody-dependent enhancement of feline infectious peritonitis virus infectivity. J Gen Virol 1993;74(Pt 4):745-9.

[62] Corapi WV, Darteil RJ, Audonnet JC, Chappuis GE. Localization of antigenic sites of the S glycoprotein of feline infectious peritonitis virus involved in neutralization and antibody-dependent enhancement. J Virol 1995;69(5):2858-62.

[63] Daeron M. Structural bases of Fc gamma R functions. Int Rev Immunol 1997;16(1-2):1-27.

[64] Gu J, Gong E, Zhang B, Zheng J, Gao Z, Zhong Y, et al. Mul- tiple organ infection and the pathogenesis of SARS. J Exp Med 2005;202(3):415-24.

[65] Stadler K, Roberts A, Becker S, Vogel L, Eickmann M, Kolesnikova L, et al. SARS vaccine protective in mice. Emerg Infect Dis 2005;11(8):1312-4.

BMC Proc. 2011; 5(Suppl 1): P80.
Published online 2011 Jan 10.

PMCID: PMC3019510

Investigation of Antibody-Dependent Enhancement (ADE) of SARS coronavirus infection and its role in pathogenesis of SARS

Ming S Yip,[1] Chung Y Cheung,[2] Ping H Li,[1] Roberto Bruzzone,[1] JS Malik Peiris,[1,2] and Martial Jaume[1]

Author information Article notes Copyright and License information Disclaimer

Antibody-dependent enhancement (ADE) is a mechanism by which viruses, such as dengue, HIV and Ebola, gain entry into some target cells through the use of host antiviral humoral immune responses [1]. Here, we studied the ability of severe acute respiratory syndrome coronavirus (SARS-CoV) [2] to use ADE mechanisms to enhance its infectivity towards cells of the hematopoietic lineage.

We found that heat-inactivated immune serum from rodents vaccinated with recombinant native full-length Spike protein trimers [3] triggered infection of human immune cells (monocytic and B cell lines) by SARS-CoV Spike pseudotyped particle (SARS-CoVpp). **The occurrence of antibody-mediated infection of human Raji B cells was further investigated by using live SARS-CoV. Similarly to results obtained with the SARS-CoVpp, only anti-SARS-CoV Spike serum, but not mock immune-serum, induced a massive increase of SARS-CoV viral genes (ORF1b and Nucleocapsid) and viral proteins (Membrane and Nucleocapsid) in Raji B cells.** As revealed by immunostaining, only a relatively low, however significant percentage of the Raji cells get infected by antibody-mediated infection and did not allow direct assessment of productive replication by conventional cytopathic assays and TCID50 titration.

T**aken together, our data suggested that SARS-CoV is able to enter human immune cells via an antibody-mediated pathway and immunological consequences of such infection are under investigation (productive replication, cytokines secretion profile and cell death etc). Our data raise reasonable concerns regarding the use of SARS-CoV vaccine in humans and pave the way to further studies focusing on the role of immune-mediated infection phenomenon during SARS pathogenesis.**

Go to:

References

- Takada A, Kawaoka Y. Antibody-dependent enhancement of viral infection: molecular mechanisms and in vivo implications. Rev Med Virol. 2003;13:387–398. doi: 10.1002/rmv.405. [PubMed] [CrossRef] [Google Scholar]
- Du L, He Y, Zhou Y, Liu S, Zheng BJ, Jiang S. The spike protein of SARS-CoV--a target for vaccine and therapeutic development. Nat Rev Microbiol. 2009;3:226–236. doi: 10.1038/nrmicro2090. [PMC free article] [PubMed] [CrossRef] [Google Scholar]
- Kam YW, Kien F, Roberts A, Cheung YC, Lamirande EW, Vogel L, Chu SL, Tse J, Guarner J, Zaki SR, Subbarao K, Peiris M, Nal B, Altmeyer R. Antibodies against trimeric S glycoprotein protect hamsters against SARS-CoV challenge despite their capacity to mediate FcgammaRII-dependent entry into B cells in vitro. Vaccine. 2007;25:729–740. doi: 10.1016/j.vaccine.2006.08.011. [PubMed] [CrossRef] [Google Scholar]

Risk by ethnic background

A comparison between eight individual samples demonstrated that the Asian male one has an extremely large number of ACE2-expressing cells in the lung. This is based on an unfinished study by Yu Zhao, Zixian Zhao, Yujia Wang, Yueqing Zhou, Yu Ma, Wei Zuo and published by Bio Rxiv :
https://www.eturbonews.com/542533/coronavirus-risk-for-asians-africans-caucasians-revealed/

A second study investigates how and why the virus will enter the human body, by Michael Letko, Vincent Munster
Apparently the coronavirus enters a human body through some connection with something called the ACE2 receptor. East Asians and men have more than say white Europeans and women. Being a white woman seems to be the way to have much lesser risk.

According to this study and based on the assumption in this study and in regards to the receptor, Angiotensin-converting enzyme 2, human populations where samples were available were categorized by risk in obtaining a dangerous version of the virus. Most ill may not feel more than a common cold, for others Coronavirus can be fatal.
According to this preliminary study the risk of obtaining the virus:
High risk 90%-99%
Japanese in Tokyo, Japan
Southern Han Chinese
Kinh in Ho Chi Minh City, Vietnam
Han Chinese in Bejing, China
Chinese Dai in Xishuangbanna, China
Moderate Risk: 80-89%
Not found
Medium to Moderate Risk: 70-79%
Peruvians from Lima, Peru
Bengali from Bangladesh
Sri Lankan Tamil from the UK
Indian Telgu from the UK
Mexican Ancestry from Los Angeles, USA
South Asians (general average)

Medium Risk: 60-69%
Gujarati Indians from Houston, TX
Admixed Americans
Americans of African Ancestry in SW USA
Punjabi from Lahore, Pakistan
African Caribbeans in Barbados
Luhya in Webuye, Kenya
Mende in Sierra Leona
Africans (general average)
Esan in Nigeria
British in U.K.
Gambians in Western Division in The Gambia
Puerto Ricans
Low to Medium Risk: 50-59%
Colombians from Medellin
Yoruba in Ibadan, Nigeria
Finnish in Finland
Iberian Population in Spain
Europeans (in General)
Utah Residence (Caucasians)
Toscani, Italy

Populations at risk

Average of six genetic variants associated with higher ratios of ACE2 cells: rs233575 (A), rs714205 (G), rs1978124 (C), rs879922 (G), rs2048683 (G), rs1877752 (C)

Code	Population	%
JPT	Japanese in Tokyo, Japan	92%
CHS	Southern Han Chinese	92%
EAS	*East Asian*	91%
KHV	Kinh in Ho Chi Minh City, Vietnam	91%
CHB	Han Chinese in Beijing, China	90%
CDX	Chinese Dai in Xishuangbanna, China	90%
PEL	Peruvians from Lima, Peru	78%
BEB	Bengali from Bangladesh	77%
STU	Sri Lankan Tamil from the UK	75%
ITU	Indian Telugu from the UK	74%
MXL	Mexican Ancestry from Los Angeles USA	72%
SAS	*South Asian*	72%
GIH	Gujarati Indian from Houston, Texas	68%
AMR	*Admixed American*	66%
ASW	Americans of African Ancestry in SW USA	66%
PJL	Punjabi from Lahore, Pakistan	65%
ACB	African Caribbeans in Barbados	64%
LWK	Luhya in Webuye, Kenya	63%
MSL	Mende in Sierra Leone	62%
AFR	*African*	62%
ESN	Esan in Nigeria	62%
GBR	British in England and Scotland	61%
GWD	Gambian in Western Divisions in the Gambia	61%
PUR	Puerto Ricans from Puerto Rico	60%
CLM	Colombians from Medellin, Colombia	59%
YRI	Yoruba in Ibadan, Nigeria	57%
FIN	Finnish in Finland	57%
IBS	Iberian Population in Spain	56%
EUR	*European*	56%
CEU	Utah Residents with Northern and Western European Ancestry	53%
TSI	Toscani in Italia	51%

1000 Genomes Project

risk for Coronavirus

a

	AGE	SEX	RACE	Smoking Status	Single Cell Number
Donor1	63	F	African American	Never	5370
Donor2	55	M	Asian	Former	3813
Donor3	29	F	African American	Never	5150
Donor4	57	F	African American	Never	5142
Donor5	49	F	White	Active	5275
Donor6	22	F	African American	Never	4208
Donor7	47	F	White	Active	7446

b

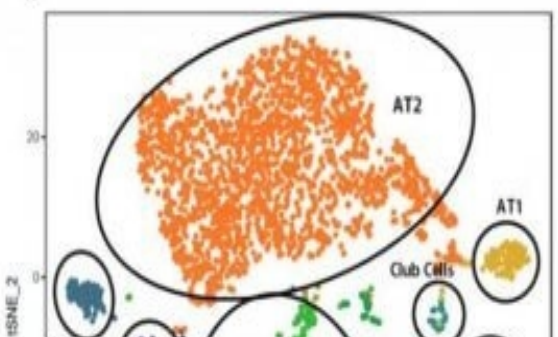

Summary

The 2019-nCoV virus spike protein has infinity for the ACE2 receptor and Females from prior studies are less at risk from nCoV-2019 due to the enhancing nature of Estrogen's effect on ACE2 pre-menopause.

We can consider those most at risk of nCoV-2019 spike protein as people with low ACE2 or inhibited receptors such as the elderly / smokers and those in high air pollution areas.

The reduction in the ACE2 receptors, would as the included data indicates mean that the NcoV-2019 has a more dramatic effect.

While the general population are liable to have symptoms akin to common cold comprising 200 virus strains of Rhinovirus or one of the 4 types of flu virus.

Air quality and smoking amplify infection effects and worsen outcomes in otherwise outwardly healthy people.

Acute Patients are going to require full scale medical intervention and a small percentage will not recover either in the first wave or if caught with ADE in following waves.

ADE forms an important concern on recurrent infection and vaccine initiatives- this explanes the lengths Chinese government liable to go to.

A strong positive correlation was found between ACE2 activity and concentration level in both male and female EH patients making both elderly and those with existing conditions at great risk of fatal outcomes first or second wave

Vaccines are liable to need multi path coverage, repeated shots to acquire immunity and a persentage of necrosis from animal studies.

Antibody-dependent enhancement (ADE) means that governments working basis that for for example economic shocks can be minimised and lets use figures :-

First wave per 100 cases

15 acute requiring intensive hospital care

1-3 die

This hasn't taken into account waves as with Spanish flu

https://www.cdc.gov/flu/pandemic-resources/1918-commemoration/three-waves.htm

During 1918, the U.S. was engaged in WWI. Hundreds and thousands of U.S. soldiers traveled across the Atlantic to deploy for war. The mass troop movement contributed to the global spread of flu.

More people died during the 1918 pandemic than the total number of military and civilian deaths that resulted from World War I.

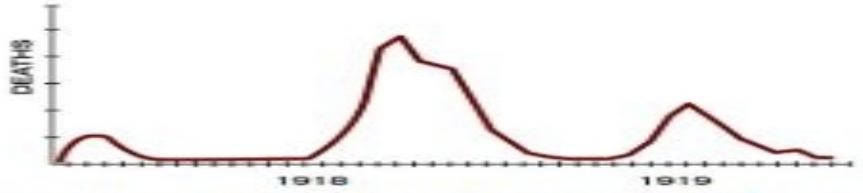

There were 3 different waves of illness during the pandemic, starting in March 1918 and subsiding by summer of 1919. The pandemic peaked in the U.S. during the second wave, in the fall of 1918. This highly fatal second wave was responsible for most of the U.S. deaths attributed to the pandemic.

A third wave of illness occurred during the winter and spring of 1919, adding to the pandemic death toll. The third wave of the pandemic subsided during the summer of 1919.

An estimated 1/3 of the world's population was infected with the 1918 flu virus – resulting in at least 50 million deaths worldwide.

The Data being the best I had available and aware of and Remembering Larry Tesler King of cut and paste, I did the best I could !

I invite discussion, criticism and debate- to be human is to be flawed and I appreciate data sets published. Hope for the best and plan for the worst lumsdenad@gmail.com